SEISMIC ANALYSES AND INSTRUMENTATION OF THE PATILLAS EARTH DAM

By

EDGARDO RUIZ MATEO

A thesis submitted in partial fulfillment of
the requirements for the degree of

MASTER OF SCIENCE

CIVIL ENGINEERING

UNIVERSITY OF PUERTO RICO
MAYAGÜEZ CAMPUS

MAY 2009

Approved by:

_____	_____
José A. Martínez Cruzado, Ph.D. Member Graduate Committee	Date
_____	_____
Luis E. Suárez Colche, Ph.D. Member Graduate Committee	Date
_____	_____
Miguel A. Pando, Ph.D. President Graduate Committee	Date
_____	_____
Mario Rivera Borrero, Ph.D. Representative of the Graduate School	Date
_____	_____
Ismael Pagán Trinidad, M.S. Chair of the Civil Engineering and Surveying Department	Date

Abstract

This thesis presents the results of seismic analyses performed for an earth dam located in Patillas, Puerto Rico. This embankment dam was built using hydraulic filling between 1912 and 1914. The dam geometry and material properties were estimated based on an exhaustive review of existing records and reports for this dam. The seismic evaluation of the dam consisted of static and pseudo-static limit equilibrium analyses, dynamic 2D finite element analyses with equivalent-linear models to account for soil non-linearity, and Newmark-type sliding block analyses to estimate expected deformation levels. The analyses considered different levels of seismic excitation based on return periods of 2,500 and 10,000 years. From the studies performed in this thesis the Patillas Dam is considered reasonably well suited to withstand large earthquake events. However, liquefaction assessment was not included in the scope of this research. In addition to the seismic evaluation, this thesis included instrumentation layout and installation for the dam. The thesis also presents results from ambient vibration tests which yield predominant periods for the dam similar to those obtained in the seismic analyses carried out for this thesis.

Acknowledgments

First of all I would like to thank my family for all of their love and support they always provide. To my sisters for making me want be the best I can to provide an example for them, and especially to my parents for all of their sacrifices and for laying the foundation for me to develop into who I am now. Your love is all I'll ever need.

I would also like to thank the members of my committee: Dr. José Martínez-Cruzado and Dr. Luis E. Suárez for all their help and guidance. Special thanks to my advisor and president of my graduate committee Dr. Miguel A. Pando for all his help through out all this process and for bearing with me, I greatly appreciate all your efforts to help me get where I am.

Thanks to Mauricio Upegui Botero for all of his work with the environmental vibration tests.

I would also like to thank the administrative personnel and the technicians of the Department of Civil Engineering of the University of Puerto Rico – Mayagüez, especially to Mr. Jaime Ramirez for always being there helping us out with all our lab work through the years.

Most of all I would like to thank my friends Henry Diaz, Omar Esquilín, Omar Flores, Carmen Y. Lugo, Mariely Mejías, Victor Negrón, and Wilmel Varela among many others. I would like to give special thanks to Alesandra Morales for being my delegate while I was away from Puerto Rico, Arleen Reyes for being my study partner for as long as I can remember, and especially Yaurel Guadalupe Torres for helping me with literally everything he could. All of your love and support is the key to my success.

TABLE OF CONTENTS

LIST OF FIGURES

LIST OF TABLES

Chapter 1

Introduction

1.1. General Description

This investigation was undertaken to determine the suitability of Patillas Dam to withstand the event of a large earthquake. Patillas Dam is an earth dam located on the southeastern part of the island of Puerto Rico. There is very little documentation regarding the materials used for the construction of the dam. Because of this limited information, this project required the determination of geotechnical properties of the dam materials. Using these properties a series of finite element analyses was performed for various ground motions.

1.2. Justification

Puerto Rico is located in a zone where there is very high seismic activity, and therefore essential structures such as dams must be able to withstand the events of a large earthquake. When evaluating Patillas Dam's characteristics and its location, it was found that the seismic vulnerability for this structure is classified as high to extreme risk level. For this reason an analysis to determine the seismic stability and level of deformation for the dam is needed to verify the dam's adequacy to withstand the event of a large earthquake.

1.3. Objectives

The main purpose of this study is to determine the adequacy of Patillas Dam to withstand the event of a large earthquake. The evaluation will be made using different ground motions. More specific objectives for this study are to:

- Install seismic instrumentation on the dam site.
- Determine the expected deformation of Patillas Dam in the event of a large earthquake.
- Obtain the dynamic response of several points of interest in the dam.
- Determine geotechnical earthquake engineering properties for the dam materials.

1.4. Thesis Organization

This document is organized into nine chapters and three appendixes. Chapter 1 provides a general description of the problem, a justification for this study, and its objectives. Chapter 2 presents the description of the geometry, geology, seismicity, construction, observations during the years, and reports for the dam. Chapter 3 discusses the seismic instrumentation installed on the dam. Chapter 4 describes the different methods used to perform the seismic analyses for the dam. Chapter 5 discusses the determination of the material properties used for the analyses. Chapter 6 includes the different ground motions to be used for the different analyses methods and a discussion of their selection. Chapter 7 presents the results from the seismic analyses and their discussion. The conclusions and recommendations are presented in Chapter 8. The list of references used for this work is found in Chapter 9.

Chapter 2

Earth dam Description

This chapter provides background information and a general description of the Patillas Dam located in Patillas, Puerto Rico. The chapter is divided in sections which include a general description, general geology, construction history, and dam performance and observations.

2.1. General Description

The Patillas Dam is an earthfill dam located on the southeastern part of the island of Puerto Rico. Figure 2-1 shows the general location of the dam.

Figure 2-1. General Location of Patillas Dam

The dam has a height of 147 ft measured from the toe to its crest and a length of 1,067 ft along the 15 ft wide crest (Hamilton and Román, 1988). Its crest is located at en elevation of 238.8 ft and the normal pool elevation of the dam is

222 ft with a maximum storage capacity of 17,073 acre-ft. A generalized cross section of the dam is shown in Figure 2-2. As shown in this figure, the dam is a zoned earth dam divided into two different zones: 1) The outer shells consisting of coarse material; and 2) an internal core that consists of fine grained material. The upstream face of the dam has a slope of 2H:1V from the crest down to elevation 212 ft and a 3H:1V slope below that elevation down to the original ground surface. Similarly, as shown in Figure 2-2, the downstream face has a slope of 1.5H:1V from the crest down to elevation 212 ft, and below this elevation the downstream slope is inclined at 2H:1V. The core of the dam was constructed by hydraulic fill methods with a 1H:1V upstream slope and 0.5H:1V downstream slope (Hamilton and Román, 1988).

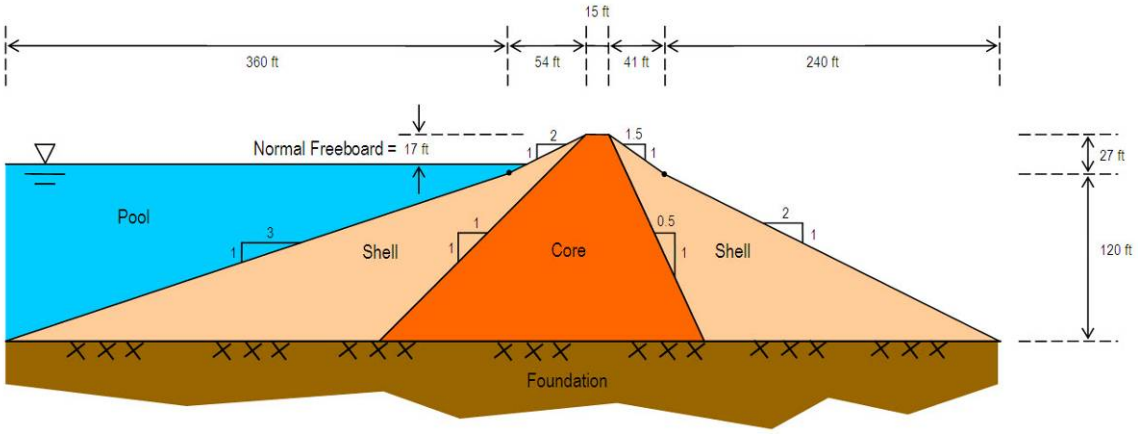

Figure 2-2. Generalized Cross Section of the Patillas Dam

2.2. General Geology

The location of the Patillas Dam is shown in Figure 2-3. This figure was taken from a general geology map of Puerto Rico (Briggs, 1964). The Patillas Dam

area is mostly on the undifferentiated lower tertiary and cretaceous formation (TKp). This formation is described as a predominantly plutonic rock. Downstream from the dam alluvial deposits (Qa) can be found. This is mainly sand, silt, clay and gravel floodplain and terrace deposits.

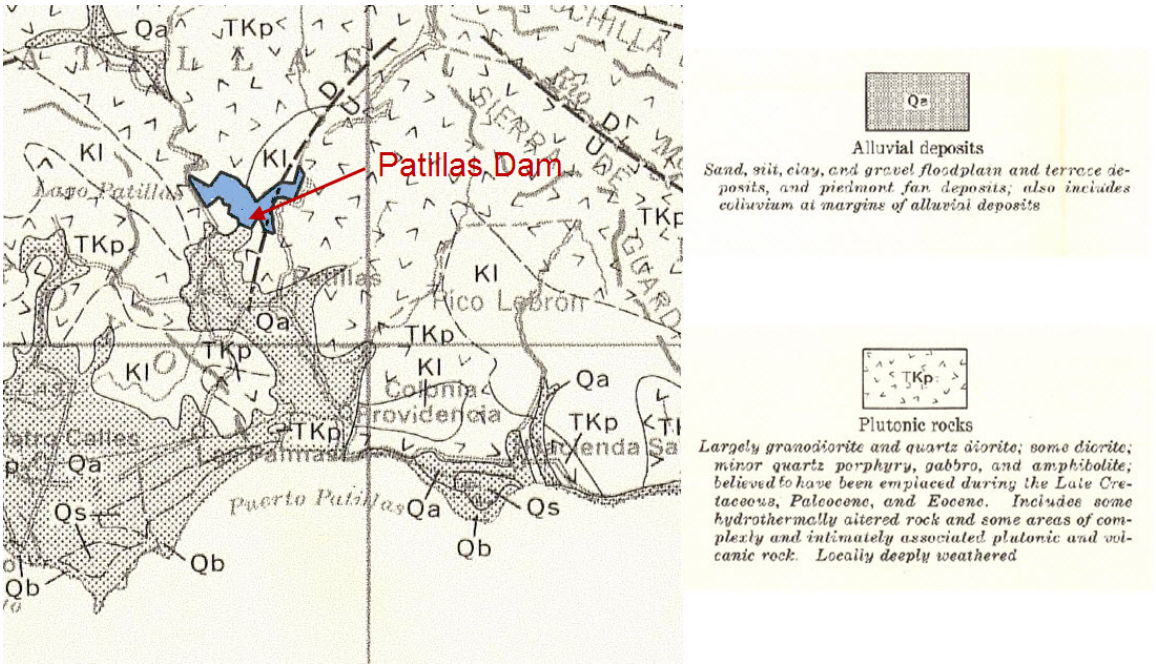

Figure 2-3. General Geology Map of the Patillas Dam Site (adapted from Briggs, 1964)

2.3. General Seismicity

Puerto Rico is located near the northeastern corner of the Caribbean plate. Frequent movement between the Caribbean and the North American plates generate high seismic activity in the island. When compared to the rest of the United States, the estimated Peak Ground Accelerations (PGA) for Puerto Rico is close to the largest values for the rest of the United States.

The last major earthquake to strike Puerto Rico (M = 7.3) occurred in 1918. Due to the lack of a major event since the 1918 earthquake, the expected long term seismic activity of the island represents a high level of seismic hazard (McCann, 1985). Figure 2-4 shows a map with the potential magnitudes (outer values of figure) for the different zones near Puerto Rico based on the elapsed time since the last large earthquake.

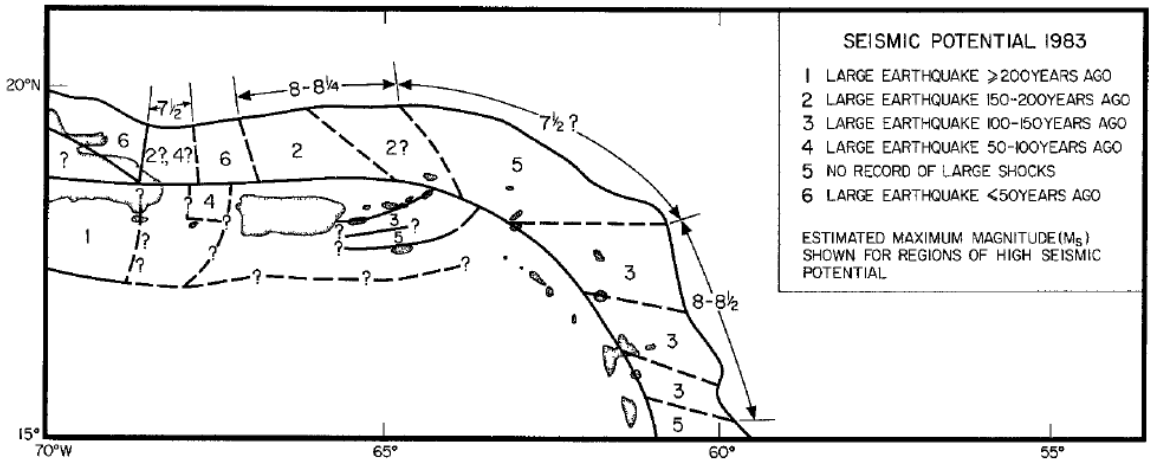

Figure 2-4. Estimate of Seismic Potential of Puerto Rico (from McCann, 1985)

The potential risk of a major earthquake striking the island of Puerto Rico creates a great concern regarding the stability of essential structures such as dams. For this reason it is necessary to ensure that such critical structures can withstand the event of a large earthquake. Chapter 5 discusses in detail the expected levels of ground motion for the Patillas Dam.

2.4. Construction History

The original construction of the Patillas Dam is described in the Report of the Commissioner of the Interior to the Governor of Puerto Rico (Commissioner of

the Interior, 1913). Construction of the Patillas Dam was commissioned by the Government of Puerto Rico primarily for irrigation purposes. Its construction began in 1912 and was finished in 1914 using hydraulic fill methods. The material used in the dam came from the spillway excavation.

During construction, the upstream and downstream shells served as dikes. Material was dumped along the inside edges of the shell dikes, and then jetted by high pressure hoses so that the finer materials would accumulate in the center of the dam. For the first 50 ft of dam height, the materials were carted using trestles and rails built at both ends of the dam. Construction above 50 ft used only rails that were located on top of the shell dikes. As the embankment increased in height, the rails were raised every few feet until completed. The inner core was built using a “puddle” construction which consisted in a hydraulic fill operation where the core was semi-liquid initially as the material settled and consolidated.

As shown in Figure 2-5, a cutoff trench was built beneath the upstream half of the core. The trench was approximately 33 ft deep and 10 ft wide at the base of the dam. A concrete wall was also constructed within the trench (Engemoen and Shaffner, 2002). This wall was founded in rock as shown in Figure 2-5.

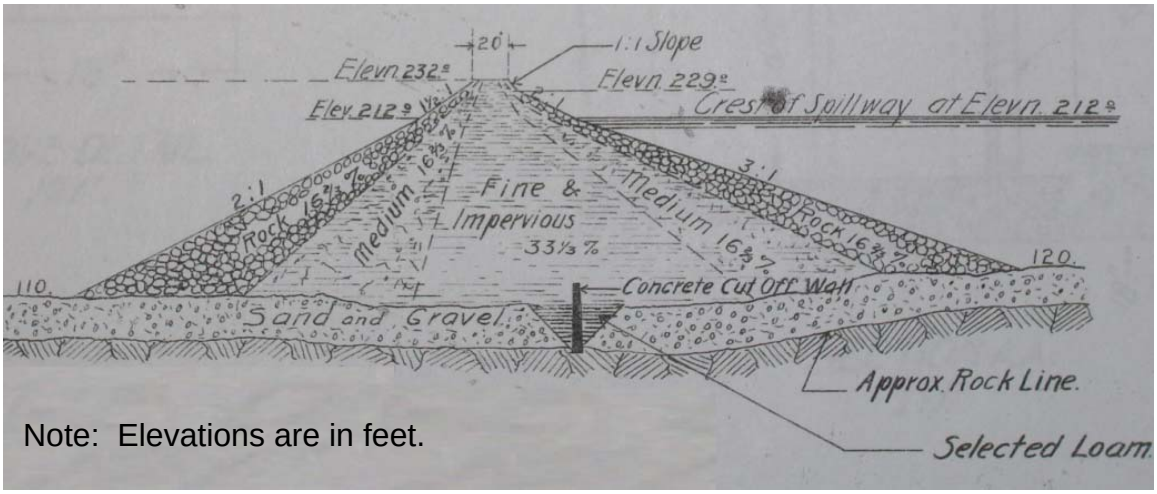

Figure 2-5. Material Zones and Foundation of the Patillas Dam

Everson (1969) states in an inspection report that in 1967 a survey of the dam was performed. This inspection report indicated that in 1987 the crest of the dam had a varying elevation ranging from 236.3 ft to 238.6 ft. In order to create a more uniform crest elevation, a cutoff concrete wall was constructed along the crest. This wall was built with a constant top elevation of 238.8 ft. The concrete wall had approximate dimensions of 1 ft wide and 8 ft deep. During this work, some test pits were excavated from which material information was obtained.

2.4.1. Core, Shells, and Foundation of the Dam

In 1967, some test pits were excavated at the crest of the dam, as well as on the downstream areas. These test pits indicated that the hydraulic fill core of the dam consisted of silty sand, with less than 25 percent gravel. This material was found to be generally dry of optimum (reference does not specify any details) and reasonably firm. A few in-place density tests were taken, which yielded a range in density of 76 to 100 percent of laboratory maximum density. Test pits in the

downstream area indicated the soils were shallow, suggesting not much overburden. These materials were described as silty to clayey sands while the shells were comprised of boulders and gravel (Everson, 1969).

Records of the materials at the spillway site (Engemoen and Shaffner, 2002) show that the soil foundation beneath the upstream and downstream shells consists primarily of fine grained alluvial materials. Figure 2-6 shows an aerial photo of Patillas Lake in which the earth dam and the spillway are visible.

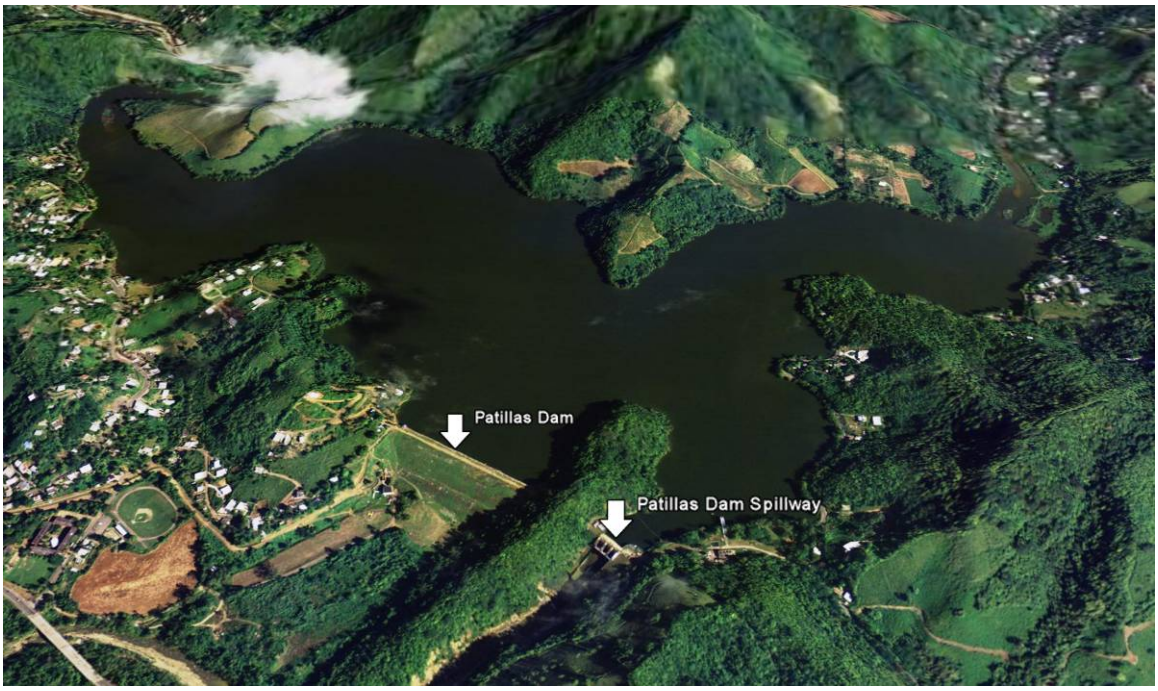

Figure 2-6. Aerial View of Patillas Dam and Spillway

Plan drawings of the original construction show a foundation consisting of what is described as “Sand and Gravel” as seen in Figure 2-5. From these same drawings it is determined that the rock line is approximately 30 ft below the toe of the dam.

2.4.2. Bedrock of the Dam

The left abutment is the ridge of rocks that separates the spillway from the dam. Engemoen and Shaffner (2002) report the rock at the spillway area as consisting of meta-volcanic tuff. From this information and the original drawings of the dam it is reasonable to assume that bedrock is located at a relatively shallow depth. The cross-section by Jacobs, Hall and Giles (1909) shows the bedrock at a depth of approximately 30 feet.

2.5. Dam Performance and Observations Reports

The Patillas Dam has been inspected and evaluated in several occasions since its construction. This section summarizes all of the inspection reports which were available for this study.

Portela and Alvarado (1969) reported that a topographic survey was performed in 1967 and it revealed that the elevation of the center of the crest of the dam was 238.6 feet above sea level. This was over 2 feet higher than both abutments. This report recommended leveling of the crest of the dam to ensure an uniform elevation along the centerline of the earth structure.

Consequently in 1969 the leveling of the crest was undertaken. During this work several investigation trenches were excavated. Handwritten notes from Everson (1969, 1970) discuss the findings from these trenches. Everson (1969 and 1970)

indicates that the core of the dam was comprised of a silty to clayey sand puddle core. No trenches were reported for the shell materials.

Hamilton and Román (1988) report results of an inspection conducted in 1987. The authors report a few irregularities such as unexpected settlements and sinkholes which were noticed in the downstream section of the dam. The sinkholes were reported to be located near elevation 165 feet.

In 1997, an investigation was performed by a geotechnical engineer from GeoConsult (Crumley, 1996). The report of this investigation concluded that the sinkholes were related to a trestle which was constructed at this location. The trestle was not fully removed, which is not unusual for earth dams constructed using hydraulic fill methods. To remediate this problem, the sinkholes were filled. In addition to the geotechnical investigation, GeoConsult (Crumley, 1996) installed six piezometers on the downstream slope. In their report, GeoConsult included a drawing with the location of each piezometer, the depth of each, and some readings taken for a few months. Even though there are drawings of the instrument locations, no coordinates were available to interpret the readings.

The United States Bureau of Reclamations (USBR) conducted a site inspection in 2002. Besides the previously discussed irregularities, visual observations indicated satisfactory behavior. No abnormalities or areas of concern were noted during the most recent site inspection (Engemoen and Shaffner, 2002). Table 2-

1 presents a list of all the references available for the Patillas Dam. A more detailed summary of the references is presented in Appendix A.

Table 2-1. List of References for Patillas Dam

Author	Year	Reference Title
Jacobs, J., Hall, B.M. and Giles, J.M.	1909	Patillas Dam: Plan, Profile and Sections of Dam. (Construction Drawings)
Commissioner of the Interior	1913	Report of the Commissioner of the Interior to the Governor of Puerto Rico.
Portela, E.A. and Alvarado, L.	1969	Report on the Condition of Patillas Dam.
Everson, M.	1969	Investigation Relative to Leveling of Patillas Dam. (Hand Written Notes)
Everson, M.	1970	Investigation Relative to Leveling of Patillas Dam. (Hand Written Notes)
Portela, E.A. and Alvarado, L.	1972	Report on the Condition of Patillas Dam.
Hamilton, R.R. and Román, P.A.	1988	Patillas Dam Phase I – Inspection Report.
Román, P.A.	1995	Patillas Dam Phase I – Inspection Report.
Crumley, A.R.	1996	Informe Geotécnico sobre las Causas de unos Sumideros en la Represa de Patillas. (In Spanish)
Román, P.A.	1998	Patillas Dam Phase I – Inspection Report.
Engemoen, W.O. and Shaffner, P.	2002	Evaluation of Geotechnical Issues.
Graham, W.J.	2002	Loss of Life Due to Dam Failure.
LaForge, R.	2002	Probabilistic Seismic Hazard Analysis for the Patillas Dam, Puerto Rico.
Farrar, J.	2003	Field Exploration Request.
Fiedler, W.R. and Trojanowski, J.	2003	Flood Routing Study
Engemoen, W.O. and Fiedler, W.R.	2003	Risk Analysis Report

Chapter 3

Installation of Seismic Instrumentation

The installation of seismic instrumentation of the dam took place from January and March of 2008. This was done by the Puerto Rico Strong Motion Program (PRSMP). This chapter describes the instrumentation used, the installation process, and the location of the instrumentation.

3.1. Instrumentation Used

The seismic instrumentation for the Patillas Dam consisted of a series of sensors along the center profile of the downstream slope. Figure 3-1 shows the instruments placed.

Figure 3-1. Instruments Used in Patillas Dam

A triaxial sensor (ES-T) was placed on the base of the downstream slope. Another triaxial sensor is located on the crest of the dam. Three pairs of uniaxial sensors (ES-U2) were placed in the inner section of the profile aligned with the triaxial sensors. These measure vertical and transverse movements. Each set of sensors has a spacing of 62.5 feet between one and the other. Two digital recorders (MAKALU) were placed at the crest of the dam to gather all the data from the sensors. Figure 3-2 shows a profile view of the downstream slope with the location of the seismic sensors.

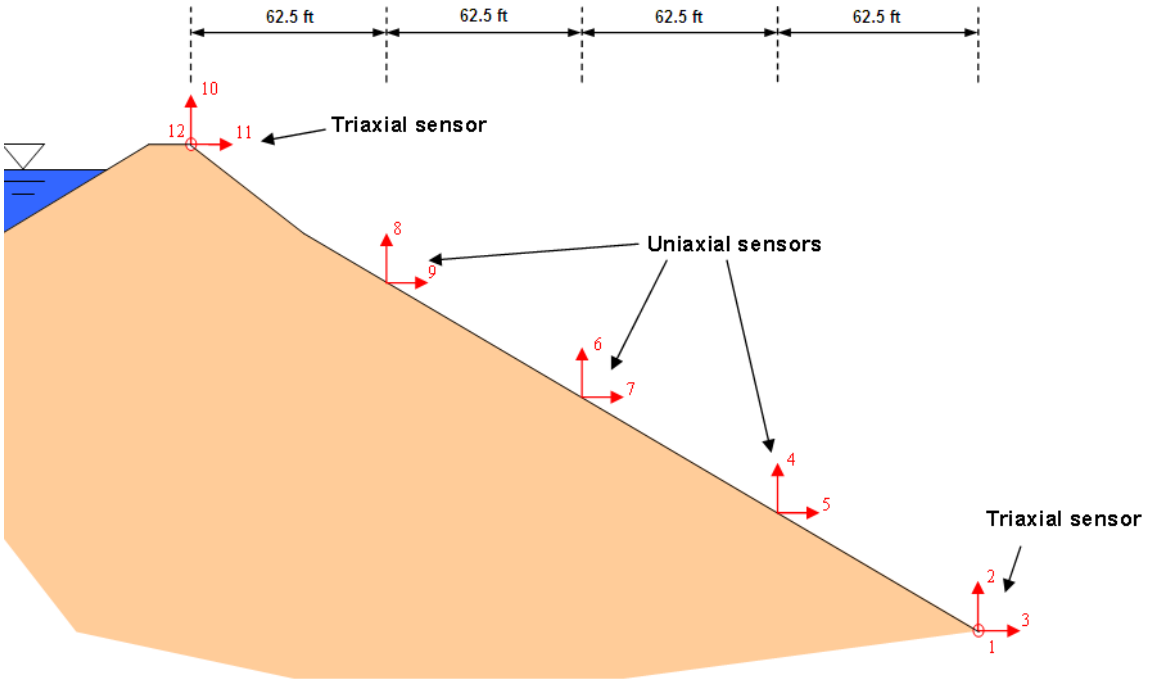

Figure 3-2. Location of Instruments along Downstream Slope

An additional station was placed on the left abutment of the dam to serve as free-field data. At this station a digital recorder with a triaxial sensor (ETNA) was placed. All the instruments discussed in the previous paragraph are from a company called Kinemetrics.

Both the MAKALU and ETNA digital recorders are equipped with a Global Positioning System (GPS) to provide the location of the seismic stations and the exact time. By doing this, these stations are in accordance with the specifications of the stations installed by the PRSMP. Also equipment will be placed to provide Internet connection to the recorders.

With this type of instrumentation it is possible to study in detail the seismic amplification that occurs from the base of the dam to the crest. The data obtained can be used to compare with the seismic analyses previously discussed in this document. This way the integrity of the dam can be evaluated and recommendations to enhance its performance can be made.

3.2. Installation of Instruments

The installation of the instruments consisted of various stages: 1) Site preparation, 2) wiring of the site, and 3) placement of instruments. In order to install the instruments it was necessary to prepare the site. To ensure a stable and leveled placing of the sensors and recorders, concrete pads were

constructed on each location. Simple concrete pads such as the one showed in Figure 3-3 were used for the sensors located on the slope.

Figure 3-3. Example of Concrete Pad for Sensors on Slope

For the locations at the crest were the MAKALU and ETNA recorders were placed, a concrete box such as the one showed in Figure 3-4 was constructed. These would be buried with their top at the same height of the crest surface.

Figure 3-4. Concrete Box for Digital Recorders at the Crest

Once all the concrete pads and boxes were constructed, the placing of electrical piping was installed. PREPA had a series of specific requests in regards to the electrical piping. These were made mainly to prevent vandalism of the system. These requests were:

1) **Underground Pipes along the Crest.** The use of underground pipes for the power lines that ran along the crest of the dam. These pipes would be made of PVC and placed against the upstream face of the concrete wall located beneath the crest surface. Figure 3-5 presents a picture taken during the installation of these pipes.

Figure 3-5. Picture of Underground Pipes

In order to pass the power lines to the downstream side of the crest, holes were drilled through the concrete wall. Once on the other side of the wall, small excavations were made to continue the underground pipes to the instrument locations.

2) **Rigid Pipes for Exposed Piping.** Steel pipes were used in the areas were piping would be exposed. This would mainly be used along the downstream slope of the dam. Due to the type of material (rock boulders), and the length and large inclination of the slope it is very difficult for heavy machinery to operate. This made underground piping along the full length of the slope an unviable option. The steel pipes would be placed underground in two benches along the downstream slope. The excavations for these benches were made by hand. Figure 3-6 presents an example of the steel piping used.

Figure 3-6. Example of Exposed Piping Used in Patillas Dam

After the pipes were placed, electrical wiring was passed through all the pipes. The power was taken from a small structure near the right abutment of the dam. The power source was tested and the instruments were installed as previously described. Figure 3-7, 3-8, and 3-9 show the triaxial sensor at the toe, one of the pairs of uniaxial sensors located along the slope, and the station at the crest with a triaxial sensor and the two MAKALU recorders.

Figure 3-7. Triaxial Sensor at the Toe of the Dam

Figure 3-8. Pair of Uniaxial Sensors on the Slope

Figure 3-9. Triaxial Sensor and MAKALU Digital Recorders on the Crest

Once the instruments were placed at their corresponding location, it was necessary to level each instrument and complete the software setup. This was performed by technicians from the PRSMP from the University of Puerto Rico–Mayagüez.

Chapter 4

Methodology for Seismic Analyses

This chapter describes the analytical procedures used to evaluate the seismic stability of the Patillas Dam. The objectives of these analyses were twofold: 1) evaluate the seismic stability of the dam; and 2) estimate ground motion levels at the location of the proposed instrumentations. The following sections describe the approach taken to achieve fulfill these objectives.

4.1. Seismic Stability Evaluation

The seismic stability of the dam was evaluated using pseudo-static slope stability analyses and the Newmark-type sliding block analysis. The ground motion levels were estimated using 2-D finite element analyses. The following sections provide details regarding the methodology used. Both sets of analyses were only carried out for the cross-section where the seismic instrumentation was installed (see Chapter 2). The results of these analyses together with the details regarding geometry, material properties, and input ground motions used are presented in Chapter 5.

4.1.1. Pseudo-Static Slope Stability Analysis

As a first approximation, the seismic stability of the dam was evaluated using a pseudo-static analysis using the general procedure summarized by Kramer (1996). In essence this methodology consists in analyzing the slope stability of a

selected cross-section of the earth dam using limit equilibrium analyses. The earthquake loading is considered by including in each slice of the sliding mass an additional set of pseudo-static forces applied at the center of gravity of each slice. These pseudo-static forces approximately represent the effects of the earthquake. Depending on the limit equilibrium method selected for the slope stability analyses, the method will satisfy different equilibrium conditions. For example, most methods satisfy global moment equilibrium and therefore the sum of moments must include the moments generated by each pseudo-static force acting at each slice. The pseudo-static forces acting at a slice "i" are as follows:

$$F_{h_i} = \frac{a_h W_i}{g} = k_h W_i \qquad (4\text{-}1)$$

$$F_{v_i} = \frac{a_v W_i}{g} = k_v W_i \qquad (4\text{-}2)$$

Where a_h and a_v are the horizontal and vertical design accelerations, k_h and k_v are dimensionless horizontal and vertical pseudo-static coefficients (a_h and a_v normalized with respect to the acceleration of gravity, g) and W_i is the weight of the slice "i" within the assumed failure mass. The selection of the pseudo-static coefficients for this type of analyses depends mainly on the seismicity of the area of the dam and the level of seismic risk selected for the design.

The pseudo-static analyses carried out for this thesis were performed using the computer program SLOPE/W (GEO-SLOPE, 2004). This computer software has incorporated several slope limit equilibrium analysis methods. The pseudo-static slope stability analyses carried out for this study included the limit equilibrium

methods, Bishop's modified method (BMM), and Janbu's method. More specific details of these analyses including material properties and layering, pseudo-static coefficients, and results are presented in Chapters 5 and 6.

4.1.2. Sliding Block Analysis

To estimate the permanent deformations of the dam after an earthquake a sliding block analysis was performed. This method is also known as Newmark's sliding block method. The method consists in determining the acceleration required to cause the hypothesized failure mass to move or slide. The method assumes the soil mass behaves as a rigid body and its displacement history is calculated by double integrating the sections of the horizontal acceleration time history that exceed a previously computed yield acceleration (also know as critical acceleration). The Newmark procedure is shown schematically in Figure 4-1.

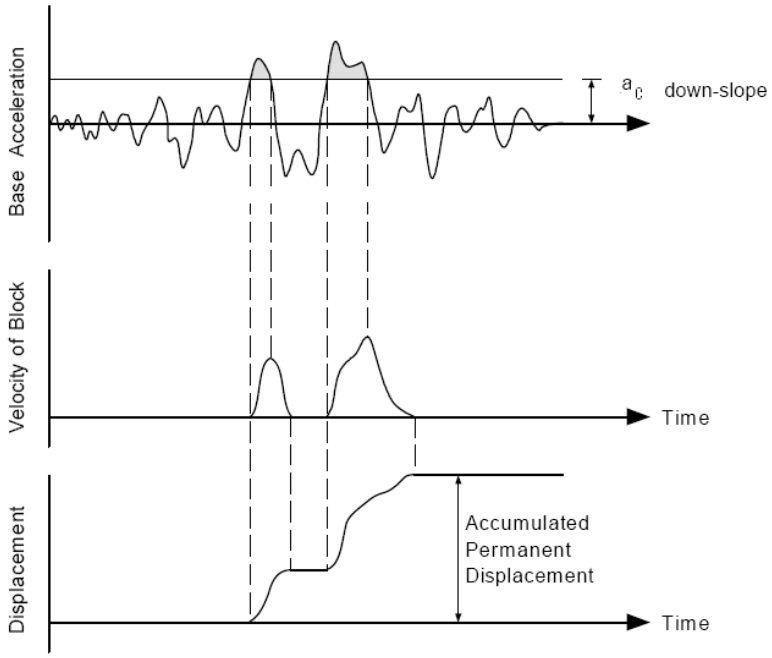

Figure 4-1. Displacement History Calculation Using the Sliding Block Method

For this set of analyses it is necessary to compute the yield acceleration for a given trial failure surface. This is done by first computing the slope stability factor of safety using a limit equilibrium method (see Section 4.1.1). The factor of safety against slope stability is computed using a pseudo-static analysis as described before. The factor of safety is computed for different levels of horizontal acceleration as shown schematically in Figure 4-2.

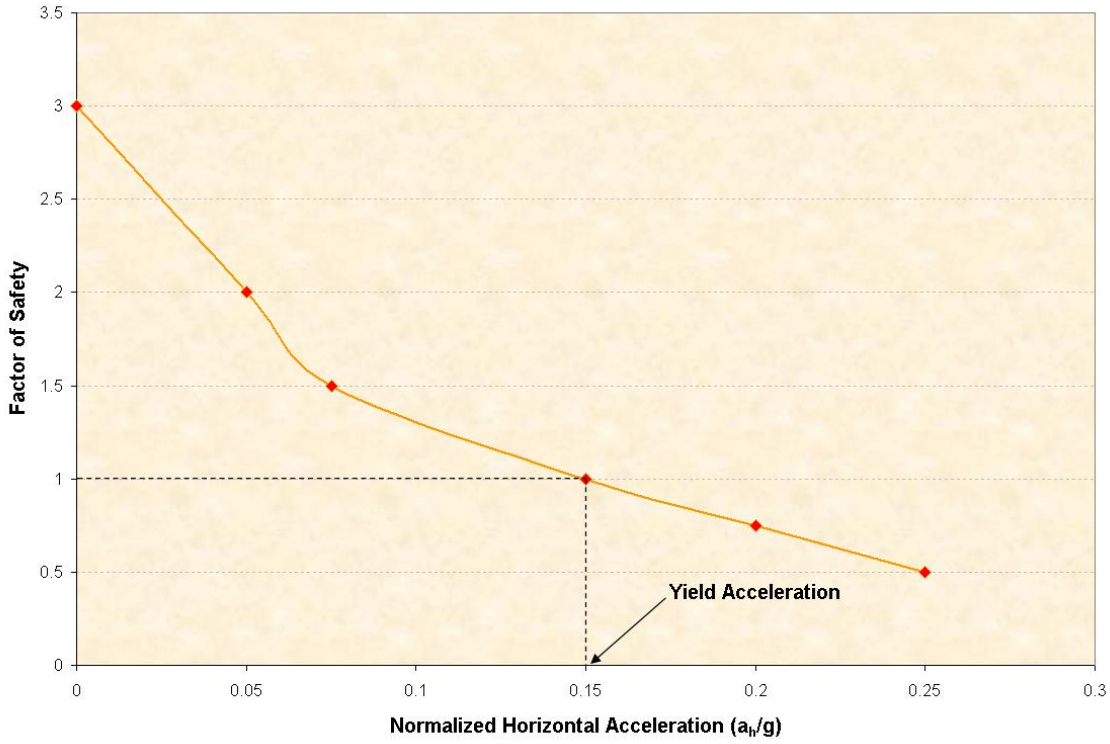

Figure 4-2. Schematic of Yield Acceleration

4.2. 2-D Dynamic Finite Element Analysis

The seismic performance of the Patillas Dam, including levels of ground motion, was evaluated using two-dimensional dynamic finite element analyses using the computer program QUAKE/W (GeoSlope, 2004).

The two-dimensional dynamic finite element analyses involved preparing finite element meshes of the instrumented cross-section of Patillas Dam. The models involved plane strain four node quadrilateral and three node triangular finite elements. A mesh sensitivity analysis was carried out prior to selecting the final mesh configuration. The first step of the analytical procedure, once the finite element mesh was defined, was the computation of the in-situ stresses within the dam. This was done by carrying out a switch-on gravity type of analysis. This procedure results in realistic stresses of the earth structure but deformations are not adequate. The resulting stress values represent the initial condition of the dam prior to earthquake excitation. Figure 4-3 shows a contour plot of the finite element model with the corresponding initial vertical stress condition. The initial stresses are then used to define the stress-dependant properties of the different materials within the dam.

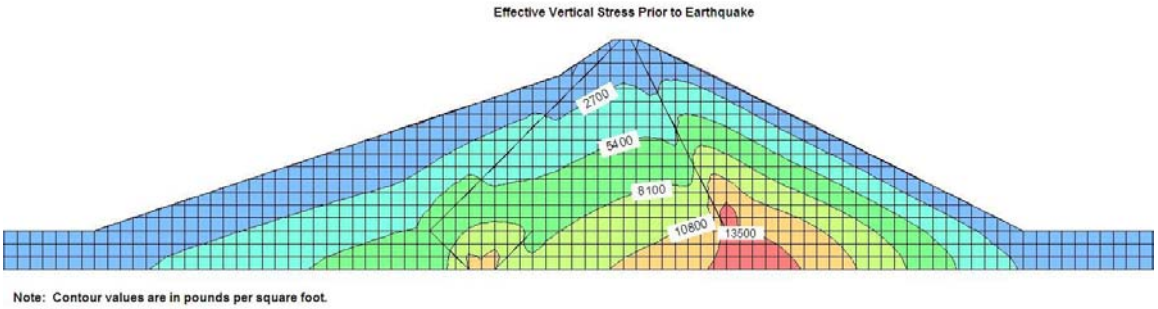

Figure 4-3. In-Situ Vertical stress Condition of Patillas Dam Prior to Earthquake Excitation

The second stage of the analytical procedure consisted in carrying out the dynamic analyses per se. QUAKE/W carries out an explicit solution of the problem and uses an equivalent-linear model to incorporate the material non-linearity. This procedure is well documented and has been used successfully in dynamic analyses of earth structures. The method uses an iterative procedure to assign shear modulus and damping ratio for each element as a function of the shear strain level. This type of analysis was carried out for different levels of ground motion.

Chapter 5

Material Properties for Analyses

This chapter discusses the determination of the properties for the dam materials and its foundation. The criterion to determine these is described for each of the methods to be used to perform the analyses: pseudo-static, dynamic finite element, and sliding block methods. In addition to the material properties, the natural vibration period of the dam was determined to compare with the results of an environmental vibration test performed in the dam.

5.1. Pseudo-static Analysis

There is limited information regarding the embankment and foundation materials. Because of this it is necessary to perform the analyses using a range of values. The properties needed to perform a limit equilibrium analysis are the unit weight (γ), cohesion (c), and angle of friction (ϕ) of the soil materials which dictate their resistance. Tree sets of properties were chosen: 1) a lower boundary that uses the most conservative values, 2) an upper boundary with the most optimistic values, and 3) a set of values that is assumed to generate the most probable response. Table 5-1 presents the values determined for the different sets of properties. These values were based on the material descriptions available from the references discussed in Chapter 2.

Table 5-1. Material Properties for Pseudo-Static Analyses

Material	γ (pcf)	ϕ (degrees)			c (psf)		
		Lower Boundary	Most Probable	Upper Boundary	Lower Boundary	Most Probable	Upper Boundary
Upstream Shell	130	34	36	38	0	0	0
Downstream Shell	130	34	36	38	0	0	0
Core	130	30	32	32	0	0	200
Foundation	125	28	30	32	0	0	0

To perform a seismic analysis it is necessary to use total stresses. This is due to the fact that seismic loading occurs rapidly and changes in pore pressure are very difficult to estimate, therefore an analysis using effective soil properties will yield unreliable estimates. For this reason it is necessary to adapt the properties from Table 5-1 to equivalent material properties to perform a total stress analysis. To convert the material properties, the model for the dam was divided into different zones as shown in Figure 5-1.

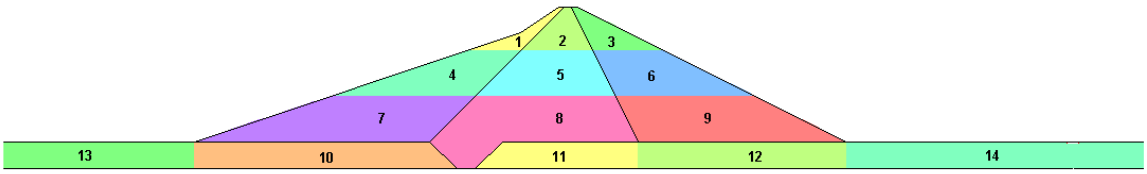

Figure 5-1. Zones for Total Stress Material Properties.

After the model was divided into zones, the equivalent material properties for the total stress analyses were determined by calculating the shear resistance of the soil mass for the average initial stress of each zone. This was done using the following equation:

$$S_u = \sigma \tan\varphi + c \qquad (5\text{-}1)$$

where S_u is the undrained shear strength of the material, and σ is the average initial stress for each zone. Table 5-2 presents the equivalent strength parameters to be used in the pseudo-static analyses.

Table 5-2. Equivalent Material Properties for Total Stress Analyses

Zone	Equivalent S_u (psf)		
	Lower Boundary	Most Probable	Upper Boundary
1	632	667	703
2	1083	1148	1348
3	1361	1436	1514
4	1458	1539	1622
5	2122	2251	2451
6	2624	2770	2920
7	1749	1847	1947
8	3897	4134	4334
9	3887	4104	4326
10	1628	1732	1837
11	4232	4503	4777
12	3743	3984	4226
13	382	407	431
14	382	407	431

These equivalent properties will be used to perform the pseudo-static slope stability analyses because changes in pore pressures do not affect the soil resistance.

5.2. Dynamic finite element Analysis

To determine the maximum shear modulus for the dam it was necessary to divide the structure into different zones. Figure 5-2 shows how the model was divided.

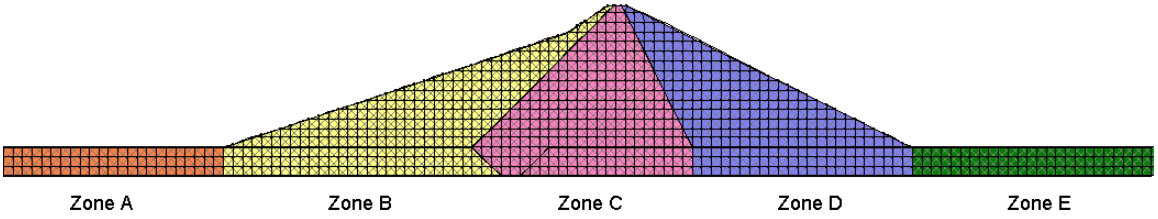

Figure 5-2. Division of Patillas Dam in Zones for Dynamic finite element Analysis

Based on the available information about the dam cross-section presented in Chapter 2, for the analyses the shells were modeled as gravel, while the core and foundation were modeled as sand. In 1986, Seed et al. performed a series of studies from which an expression to determine the maximum shear modulus of sands and gravels was developed. The expression is dependant on the void ratio (e) and the mean effective stresses (σ'_m) of the soil.

$$G_{\max} = 1000 K_{2,\max} (\sigma'_m)^{0.5} \qquad (5\text{-}2)$$

The $K_{2,\max}$ variable associates a constant value for different void ratios of sands, while σ'_m is the mathematical average of the vertical and horizontal stresses the soil is subjected to. The $K_{2,\max}$ values for sand for the different void ratios are

displayed in Table 4-3, while $K_{2,\max}$ for gravel is in the range of 80 to 180 (Seed et al. 1980).

Table 5-3. Values of K2,max for Sand (from Kramer, 1996)

e	$K_{2,\max}$
0.4	70
0.5	60
0.6	51
0.7	44
0.8	39
0.9	34

Basing engineering judgment on the available information about the dam construction, the void ratio for the sandy material in the dam is expected to be between 0.4 to 0.8 with 0.6 as the most probable value, while the $K_{2,\max}$ for the shells is between 180 to 100 with 140 as the most probable value.

To obtain the values of σ'_m an initial insitu stress analysis was performed using SIGMA/W. These results, in combination with the values of $K_{2,\max}$ discussed in the previous paragraph, were used to determine a range of values for G_{max} for the different zones. Once the shear modulus was obtained, it was possible to calculate the shear wave velocity (v_s) of the different zones as well. This was done to verify that the values of G_{max} were within a credible range. The Figures 5-3 to 5-7 show the range of G_{max} and v_s for each of the zones with the most

probable value represented with a dashed line. Depths in these figures are determined using the crest of the dam as reference.

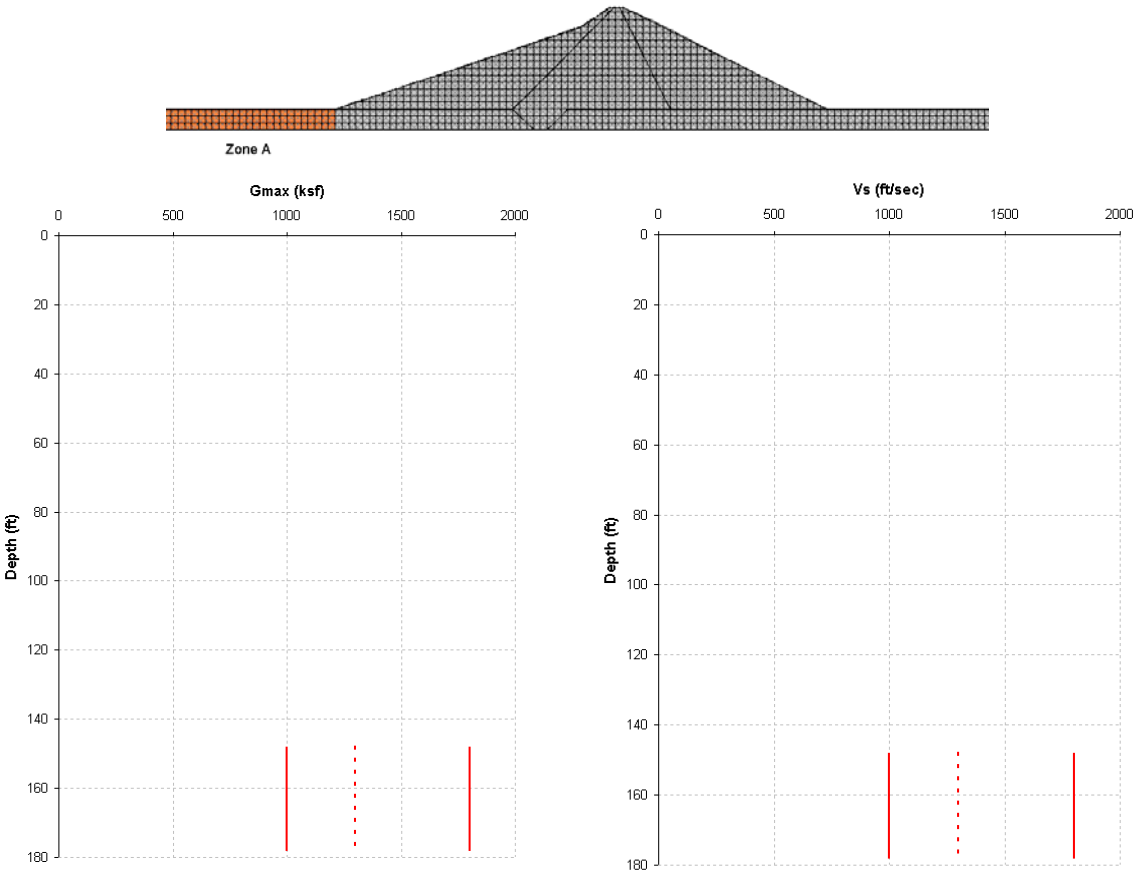

Figure 5-3. Gmax and Vs for Zone A

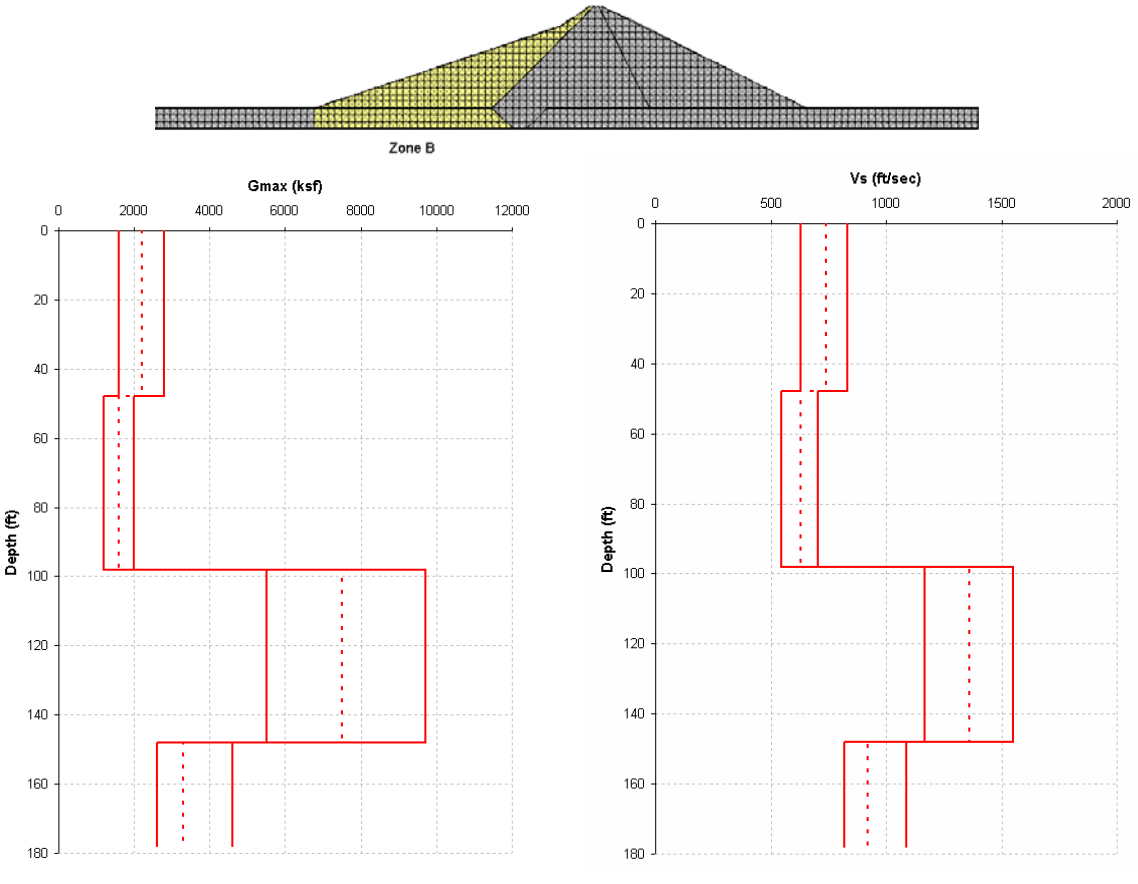

Figure 5-4. Gmax and Vs for Zone B

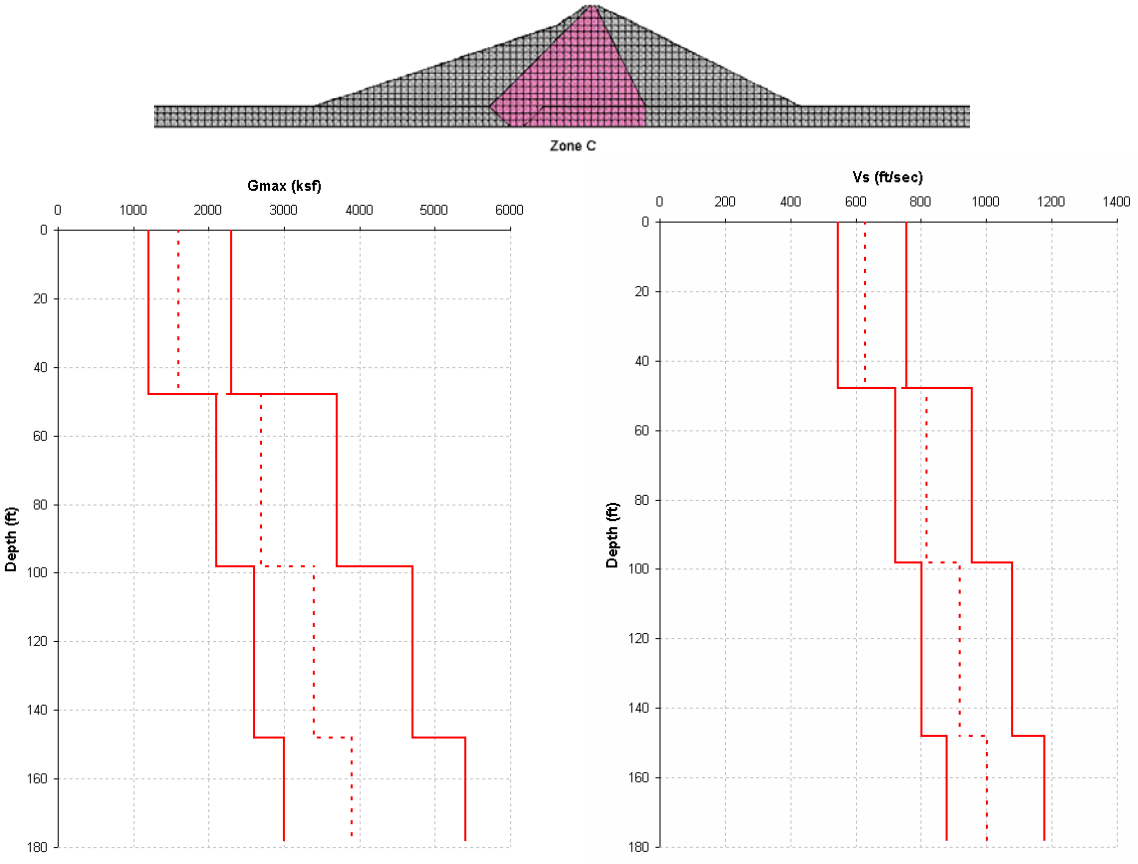

Figure 5-5. Gmax and Vs for Zone C

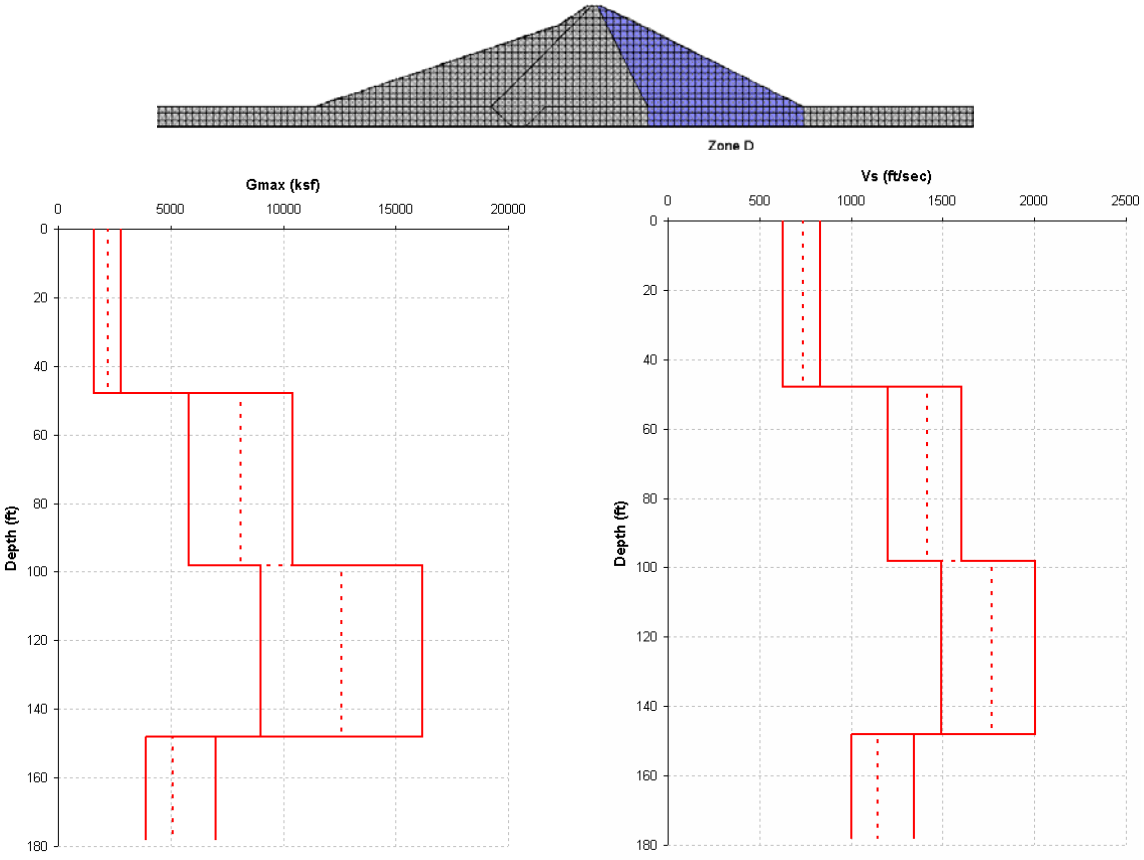

Figure 5-6. Gmax and Vs for Zone D

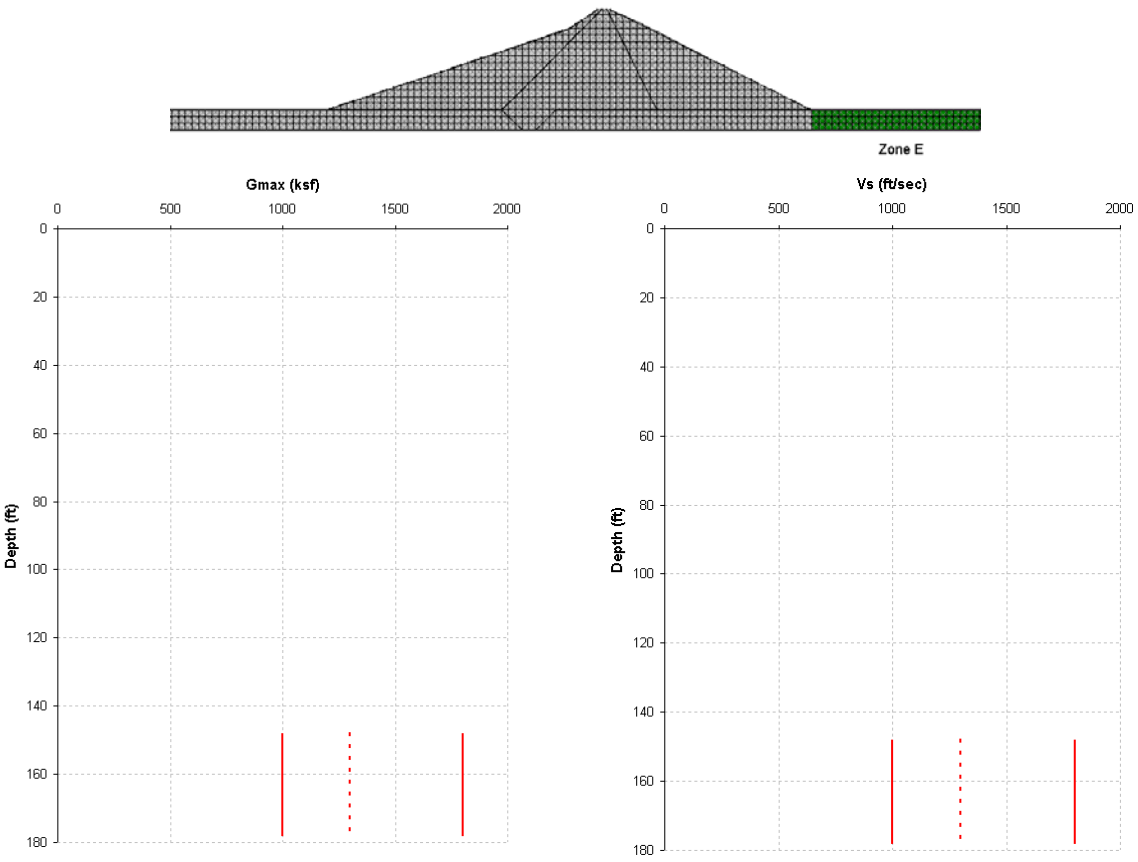

Figure 5-7. Gmax and Vs for Zone E

After determining the maximum shear modulus for the dam, we proceeded to assign the modulus reduction and damping variation curves for the different soil types. These curves have been generated from experimental analyses on different soil types and are widely used in geotechnical earthquake engineering. Seed and Idriss (1970) prepared a report for the Earthquake Engineering Research Center of the University of California-Berkeley that suggests a series of modulus reduction and damping variation curves for sands. For gravels, another reference was consulted (Seed et al, 1986). The curves for the sandy material were used for the core and foundation of the dam, while the curves for gravels were used for the shells. Figures 5-8 and 5-9 present these curves.

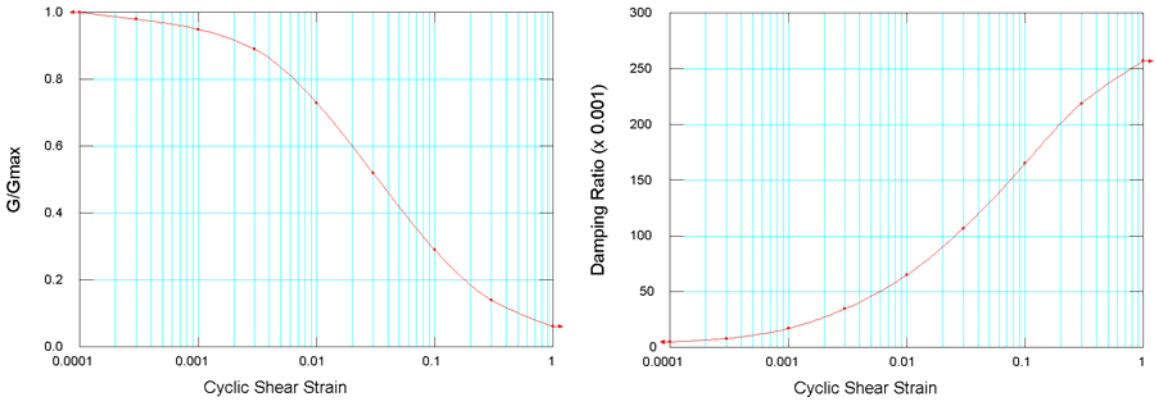

Figure 5-8. Modulus Reduction and Damping Variation Curves for Sands

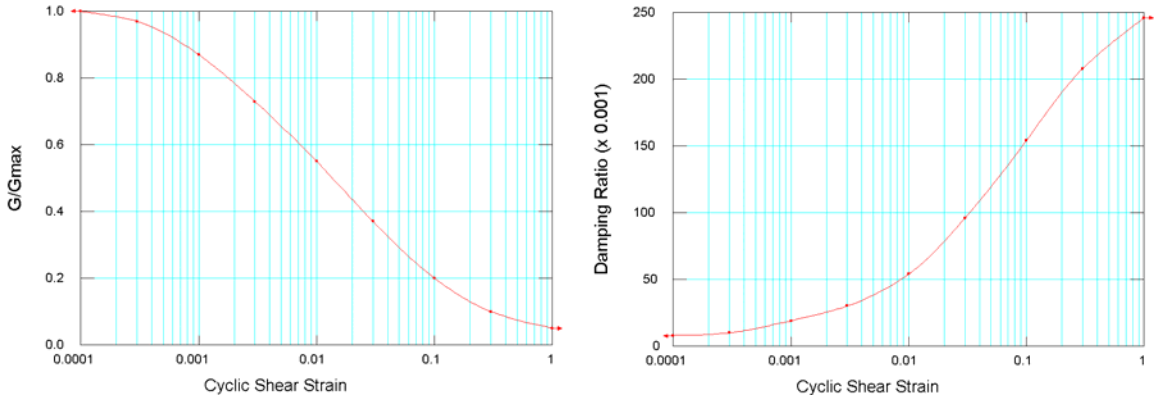

Figure 5-9. Modulus Reduction and Damping Variation for Gravels

In addition to the G_{max} and behavior curves, an initial value of damping ratio was needed. As mentioned earlier, a typical initial value of 5% was used for the analyses. With this information and the ground motions that will be discussed in the following chapter, it is possible to conduct an dynamic finite element analysis using an equivalent-linear model.

5.3. Sliding Block Analysis

The sliding block analyses that will be carried out will use the results from the pseudo-static and dynamic finite element analyses. For this reason the sliding block analyses will have the same material properties as those from Table 5-2 to describe the material shear resistance. It will also take into account the same shear modulus and damping ratio as for the equivalent-linear models since the sliding block analyses are dependant from the results of the dynamic finite element analyses.

5.4. Natural Vibration Period of Patillas Dam

Using the shear modulus values determined in Section 5.2, the natural vibration period of the dam was determined by performing a modal analysis for each set of properties. Table 5-4 presents the dam periods obtained for each set of properties.

Table 5-4. Natural Vibration Periods for Patillas Dam

Set of Properties	Period, T (sec)
Lower Boundary	0.564
Most Probable	0.489
Upper Boundary	0.422

In 2008 the Puerto Rico Strong Motion Program (PRSMP) installed a series of instruments to monitor the behavior of Patillas Dam (see Chapter 3). These instruments were then used to perform an environmental vibration test in which the natural vibration period of the dam was determined. The results from these tests showed that the predominant period for Patillas dam was between 0.43 and 0.45 seconds. When comparing these results with the periods calculated from the different set of properties, it was found that the actual dam period falls within the range of the ones estimated and is very close to the upper boundary set which was the most optimistic set of properties. This confirms that the estimated properties for the analyses are reliable.

Chapter 6

Seismicity of the Patillas Dam and Selection of Seismic Excitation for Analyses

When conducting a seismic analysis it is essential to choose the appropriate excitation for the model. A previous study performed by the U.S. Bureau of Reclamations (LaForge, 2002) determined a specific ground motion that was recommended for the Patillas Dam site. This chapter describes the method used by this study as well as the criteria used to determine other input motions for the analyses.

To determine the appropriate excitation for a seismic analysis there are several options. For pseudo-static analyses the effect of an earthquake is represented as an additional constant force that is determined by the peak ground acceleration (PGA) expected for the site which can be easily determined from seismic hazard maps. For dynamic finite element and sliding block analyses a seismic record is required. There are several ways to determine the appropriate seismic record for a specific site. LaForge (2002) conducted a probabilistic seismic hazard analysis (PSHA) for Patillas Dam.

A PSHA provides framework in which uncertainties such as size, location, rate of recurrence and variations in ground motion characteristics can be identified, quantified, and combined in order to provide a better understanding of a seismic

hazard (Kramer, 1996). The PSHA can be described in a series of four steps (Kramer, 1996):

1) Identification and characterization of earthquake sources. For a PSHA it is also necessary to characterize the probability distribution of potential rupture locations within the source. Usually a normal distribution is assigned for each zone, implying that earthquakes are equally probable to occur at any point within the source.
2) The seismic recurrence must be characterized. A recurrence relationship (such as Gutenberg-Richter, 1944) is used to specify the average rate at which an earthquake of some size will be exceeded.
3) The ground motion produced at the site by earthquakes of any possible size occurring at any possible point in each zone must be determined with the use of predictive relationships.
4) The uncertainties in earthquake location, size, and ground motion parameter prediction are combined to obtain the probability that the ground motion parameter will be exceeded during a particular time period.

The following sections describe the determination of the seismic input for the models. The pseudo-static analysis will use the PGA for the site, while the dynamic finite element and sliding block analyses will use several acceleration-time histories.

6.1. Pseudo-static Analysis

To determine the seismic forces to be applied for the model it was necessary to obtain the PGA for the Patillas Dam site. The USGS provides contour maps of the expected PGA for the island of Puerto Rico. Figure 6-1 shows an example of one of these maps. From this map it is determined that the PGA at the Patillas Dam site is in the range of 0.35 to 0.40g for a ground motion with a 2% probability of exceedance in 50 years (equivalent to a 2,500 year return period).

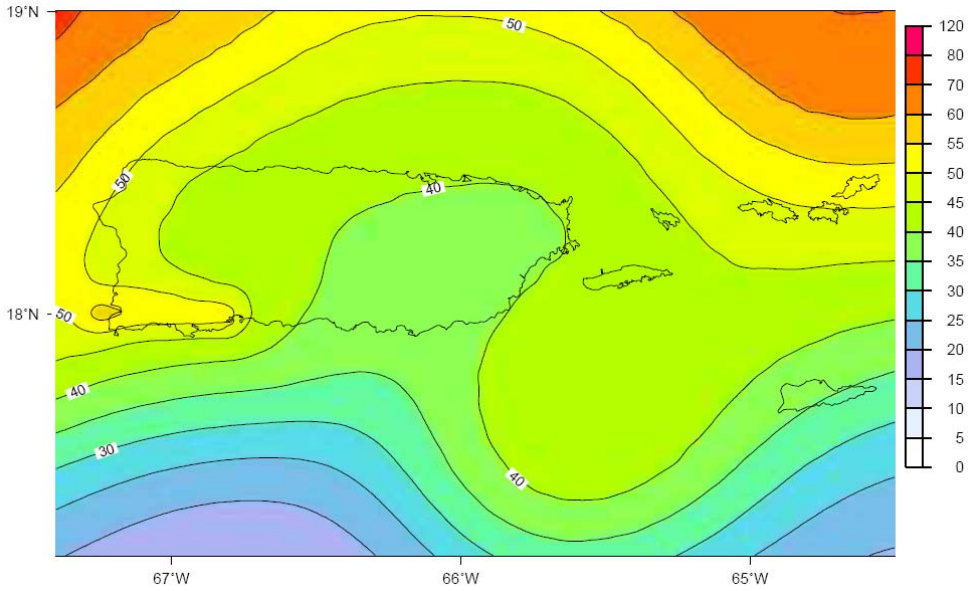

Figure 6-1. PGA for 2% Exceedance in 50 Years (Mueller et al., 2003)

These types of maps only provide a general idea of the PGA for the site. In addition to the contour maps available, other studies have been performed (Mueller et al., 2003) in which a series of curves was developed to determine the PGA for a given return period. This study was done for the cities of San Juan, Ponce, and Mayagüez (Figure 6-2, Figure 6-3, and Figure 6-4, respectively).

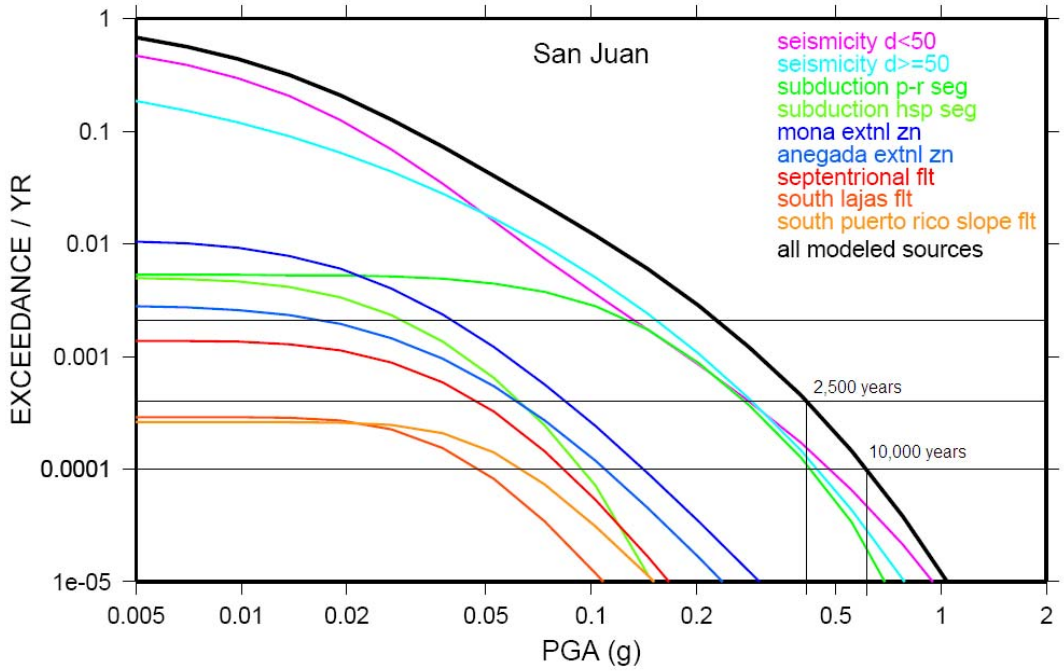

Figure 6-2. PGA Curve for San Juan (Mueller et al., 2003)

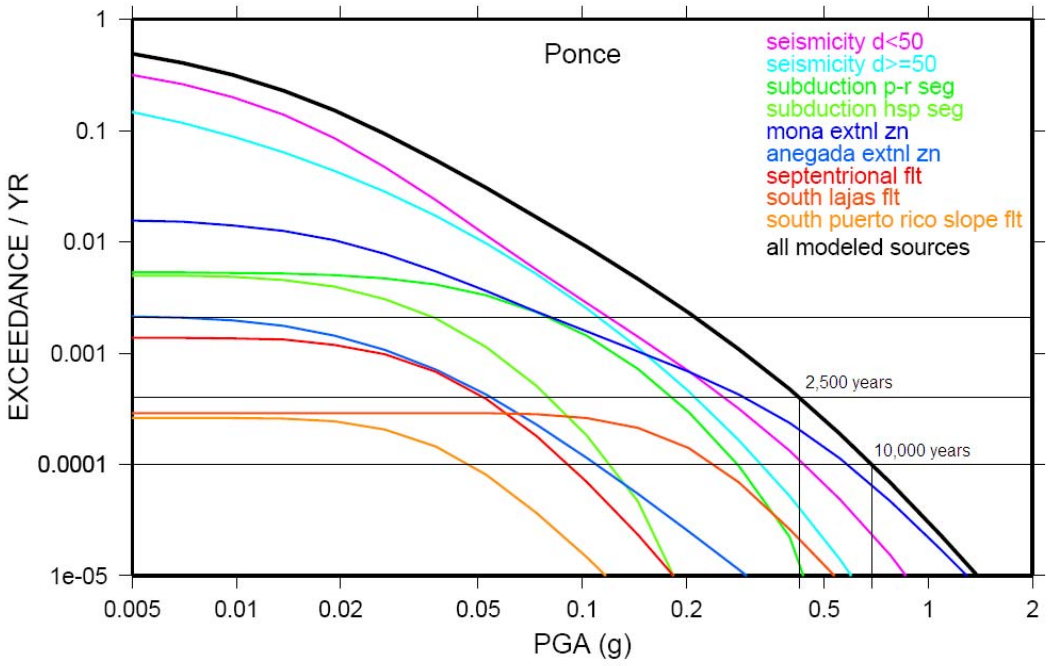

Figure 6-3. PGA Curve for Ponce (Mueller et al., 2003)

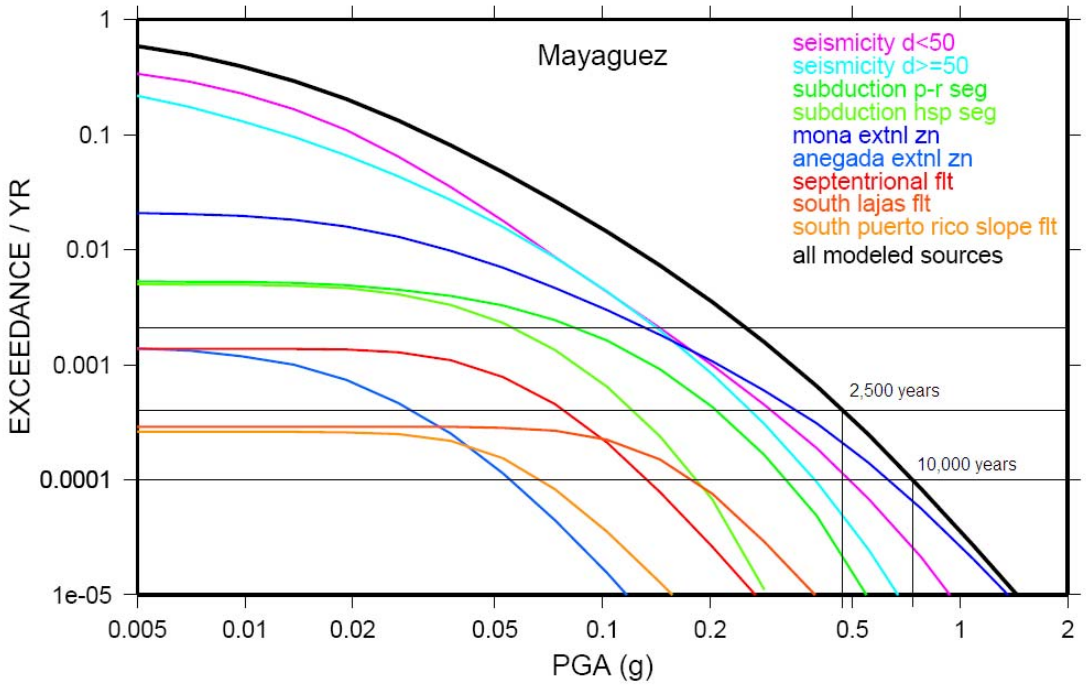

Figure 6-4. PGA Curve for Mayagüez (Mueller et al., 2003)

For the analyses return periods of 2,500 and 10,000 years will be considered. These return periods were chosen because the International Building Code (ICC, 2006) utilizes a return period of 2,500 years, while the International Commission of Large Dams (ICOLD, 2001) recommends a ground motion with a 10,000 year return period. To determine the PGA for the Patillas Dam the values obtained for these return periods were determined for the cities of San Juan, Ponce, and Mayagüez, and then extrapolated to the dam site. The resulting PGA values for the 2,500 and 10,000 year return periods were 0.37g and 0.64g, respectively.

These PGA values correspond to the bedrock surface; therefore it was necessary to determine the amplification of the PGA due to the soil foundation.

This was performed by modeling the foundation using the computer program SHAKE2000. Table 6-1 presents the amplified PGA for Patillas Dam.

Table 6-1. Results of PGA Amplification

Set of Properties	Amplified PGA (g)	
	2,500 yrs	10,000 yrs
Lower	0.474	0.674
Most Probable	0.586	0.776
Upper	0.583	0.969

After amplifying the PGA for the different set of properties, the horizontal seismic coefficient (k_h from Eq. 4-1) is calculated to account for the seismic force on the failure slope. To determine this coefficient, the values from Table 6-1 need to be correlated to the seismic coefficient, k_h. Kramer (1996) mentions in his book a 1984 reference of Hynes-Griffin and Franklin (1984) that specifies the following correlation for embankment dams:

$$k_h = \frac{0.5 a_{\max}}{g} \tag{5-1}$$

where $a_{\max}$ is the PGA at the ground surface. Using this equation and the amplified PGA values, the seismic coefficient value for each set of properties was determined. Table 6-2 shows the results of these calculations.

Table 6-2. Seismic Coefficients for Pseudo-Static Analyses

Set of Properties	Seismic Coefficient, k_h	
	2,500 yrs	10,000 yrs
Lower	0.237	0.337
Most Probable	0.293	0.388
Upper	0.291	0.484

The material properties discussed in Section 5.1 and the values from Table 6-2 will be used as the input parameters for SLOPE/W to perform the pseudo-static analyses.

6.2. Dynamic Finite Element and Sliding Block Analyses

To perform a dynamic finite element analysis it is necessary to apply an actual acceleration-time history to the model. The same is the case for the sliding block analysis. For the analyses three ground motions will be applied to the model: 1) a record from the Michoacán earthquake of 1985, 2) a record from the San Salvador earthquake of 1985, and 3) an artificial ground motion generated to fit the 1996 Uniform Building Code (UBC) design spectrum for the site. The following subsections discuss the criteria used in the selection of the ground motions.

6.2.1. Michoacán Earthquake of 1985

In 2002 the USBR (LaForge, 2002) conducted a PSHA for the Patillas Dam site. In this study it was determined that the Muertos Subduction Zone represented the most dangerous seismic source for the Patillas Dam for recurrence periods above 1,000 years. The largest magnitudes that can be generated in this zone are in the range of 7.5 to 8 (LaForge, 2002). A search was performed for seismic records that matched this magnitude located at a distance of 50 km or less. A recurrence period of 10,000 years was determined for the dam. No explanation for this is given in the report, but the International Commission of Large Dams (ICOLD, 2001) recommends this recurrence period for dams. Taking this into consideration, LaForge (2002) recommended that the Zacatula (state of Guerrero)records of the September 19, 1985 earthquake of Michoacán, Mexico (Figure 6-5) be used specifically for the dam since it would approximate the 10,000 year uniform hazard acceleration response spectra. Figure 6-6 shows the response acceleration spectra for this ground motion record.

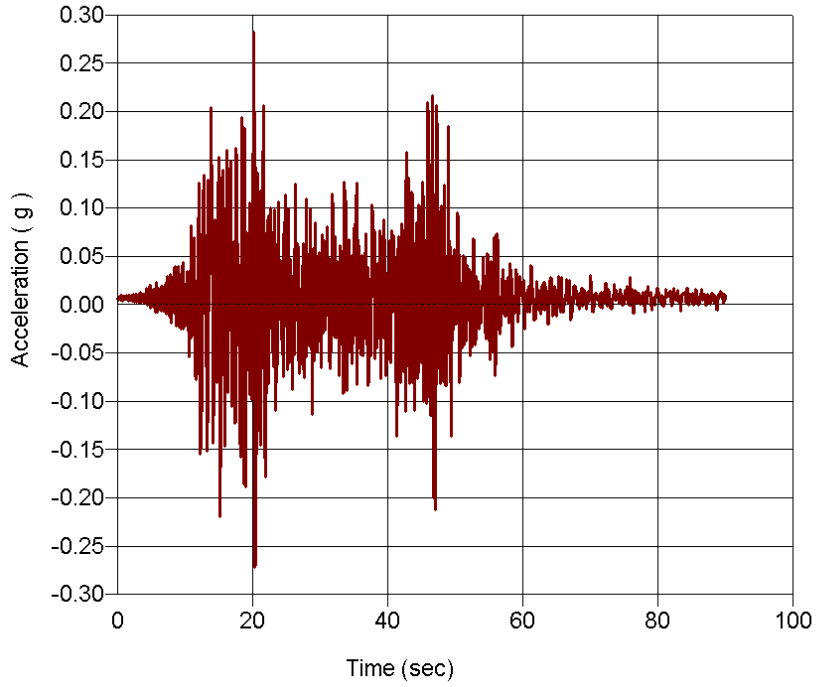

Figure 6-5. Seismic Record of Michoacán, Mexico Earthquake on September 19, 1985

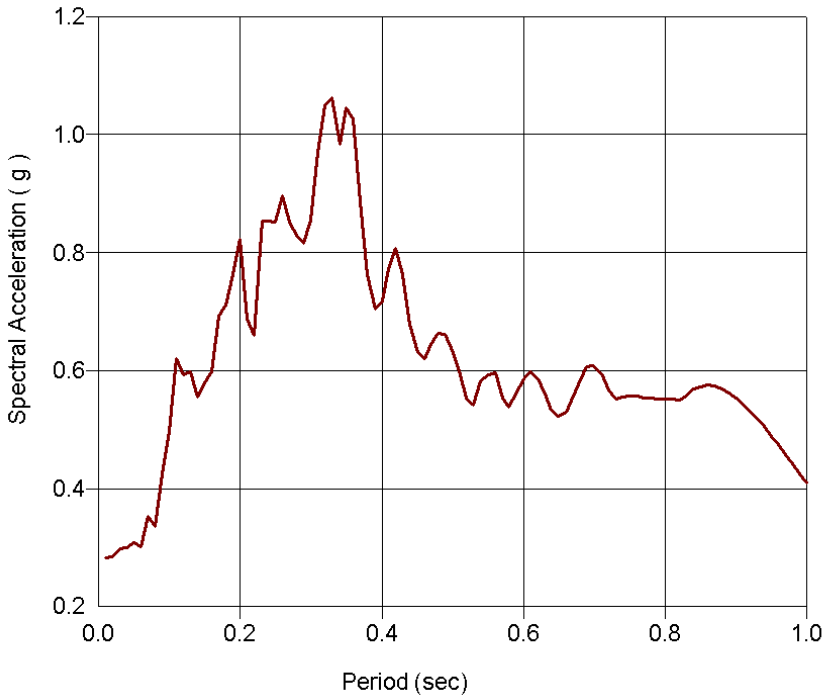

Figure 6-6. Spectral Acceleration of the Michoacán Ground Motion

6.2.2. San Salvador Earthquake of 1986

As part of a thesis investigation performed in the University of Puerto Rico-Mayagüez (Irizarry, 1999), smooth design spectra were developed for the cities of San Juan, Mayagüez, and Ponce. These were developed using the 1997 National Earthquake Hazard Reduction Program Provisions which consider strong motions with 2% of occurrence in a 50 year period (equivalent to a 2,500 year recurrence). Due to its vicinity, the results from the Ponce area will be considered. The 1986 San Salvador earthquake was chosen from these studies. This earthquake had a moderate magnitude of 5.4, but since it was a shallow earthquake at a short distance it caused a great amount of damage. By choosing this earthquake and the one from Michoacán (from the previous section), both a lesser magnitude at shorter distance and a greater magnitude at a larger distance events are considered for the analyses. Figure 6-7 presents the San Salvador earthquake record to be used, while Figure 6-8 shows the response acceleration spectra for the ground motion.

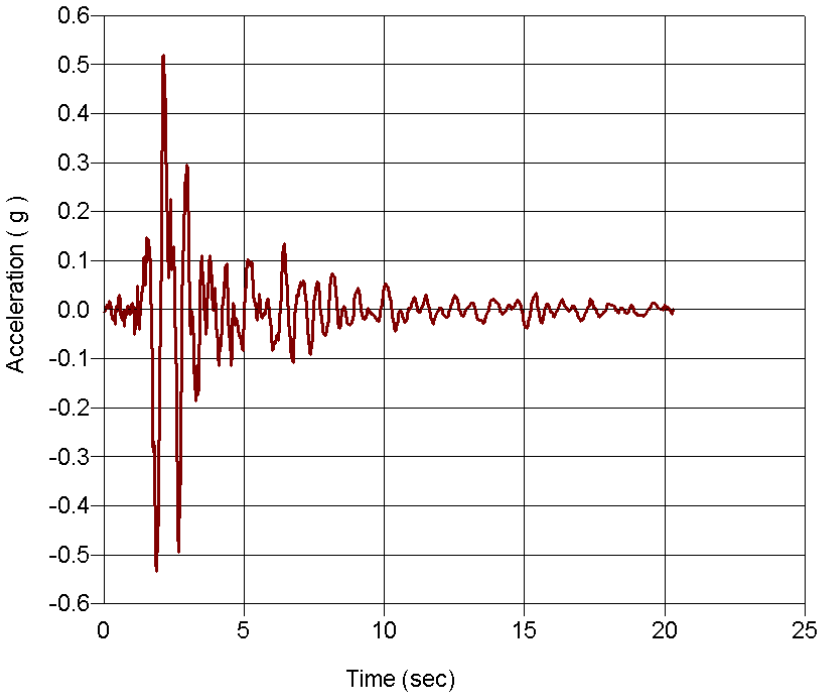

Figure 6-7. Seismic Record of 1986 San Salvador Earthquake

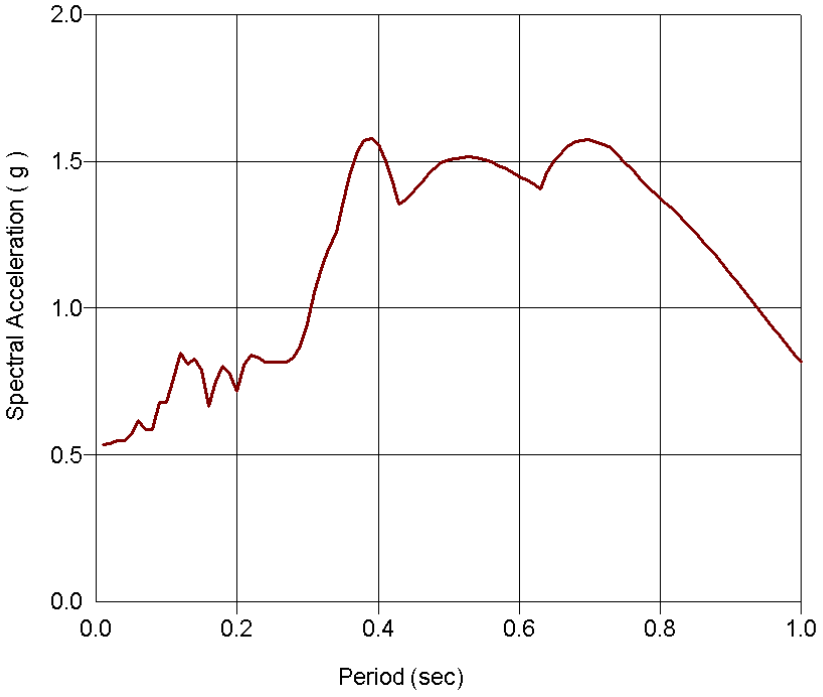

Figure 6-8. Spectral Acceleration of the 1986 San Salvador Ground Motion

6.2.3. Artificial Ground Motion Record

Besides from the Michoacán and San Salvador input motions, an additional ground motion record will be used for the analyses. This will be an artificial record constructed to approximately fit the Uniform Building Code (UBC) design spectra. As of this reference Puerto Rico is located in a seismic zone Z = 3. The foundation of the site is classified as a soil type D since its estimated average shear wave velocity is in the range of 600 to 1200 ft/sec as seen in the previous chapters. The resulting record developed will take this into consideration as well as the foundation soil type. This will be done with the aid of a MATLAB routine ArtifQuakeLet.m developed by Montejo and rez (2004). The resulting ground motion can be seen in Figure 6-9, while the corresponding response acceleration spectrum is shown in Figure 6-10.

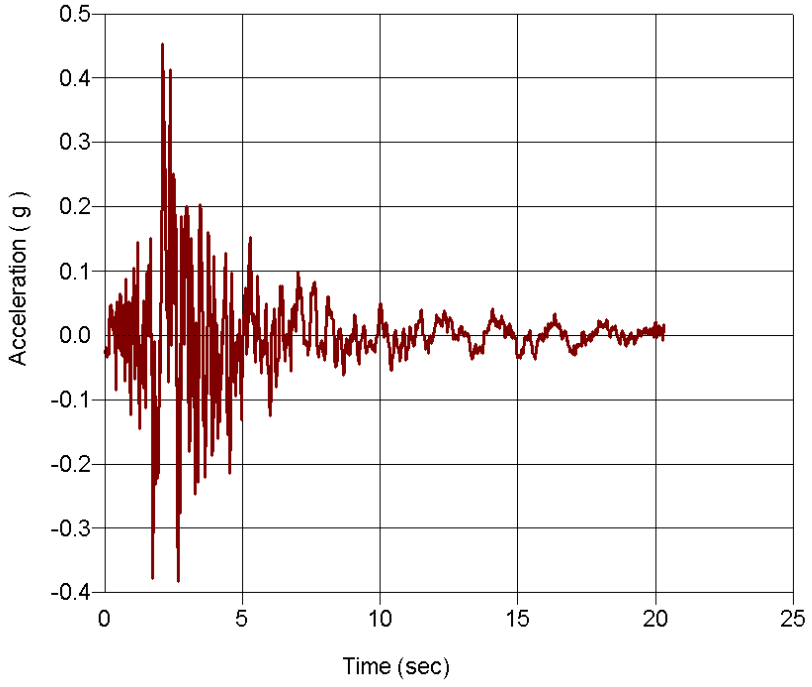

Figure 6-9. Artificial Ground Motion Compatible with UBC Spectra

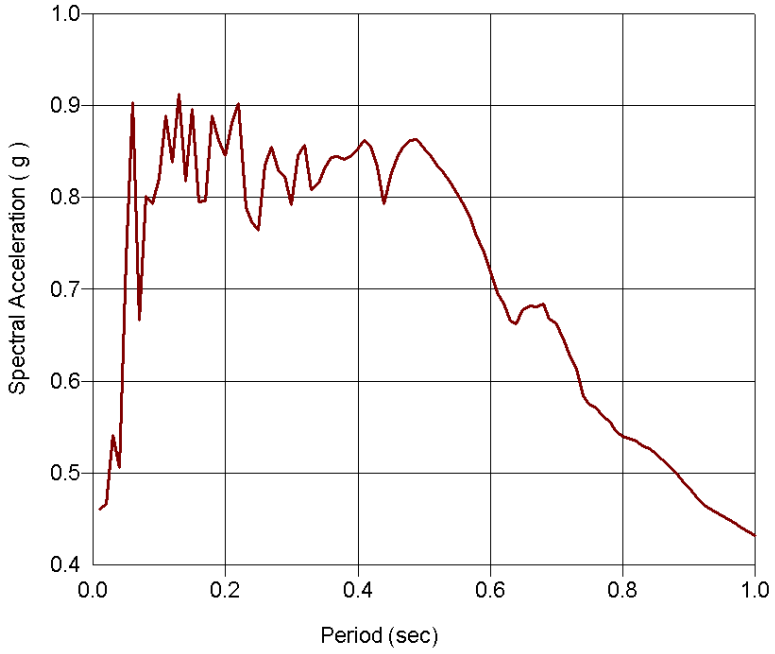

Figure 6-10. Spectral Acceleration of the Resulting Artificial Ground Motion

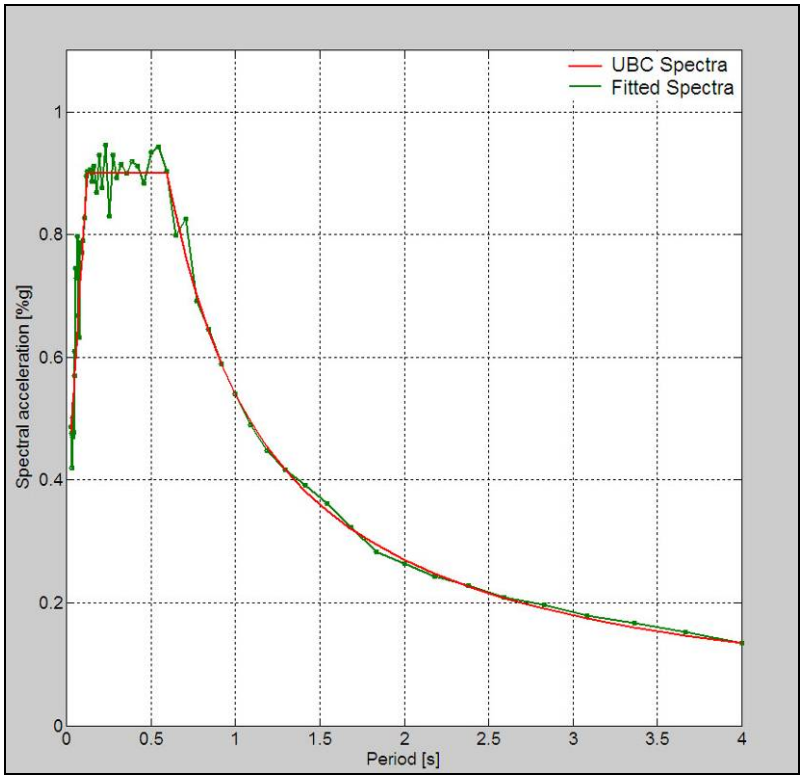

Figure 6-11. Comparison of Spectra of Artificial Ground Motion with the UBC Spectra

Figure 6-11 presents a comparison of the UBC design spectra with the resulting spectra from the artificial ground motion. The red curve represents the UBC design spectra while the green line represents the response spectra for the artificial ground motion. From this figure it is evident that the artificial ground motion is an accurate representation of the UBC design spectra.

Having chosen the ground motions for the Patillas Dam site and with the material properties already determined, it is now possible to perform the seismic analyses.

6.3. Seismic Vulnerability of Patillas Dam

The seismic vulnerability of Patillas Dam was determined using the procedure described by G.J. Bureau (2003). The procedure consists of determining a series of factors that take into account several characteristics of the dam and combining them to determine a total risk factor (TRF) in case of an earthquake. The total risk factor (TRF) is determined as shown in Equation 6-2.

$$TRF = [(CRF+HRF+ARF) + DHF] \times PDF \qquad (6\text{-}2)$$

The dam structure influence is represented by the sum (CRF+HRF+ARF) of capacity, height, and age factors. The downstream hazard factor (DHF) is based on population (Patillas has a population 21,183) and property at risk (Bureau, 2003). The seismic hazard and performance of similar dams is also taken into

consideration and represented by the predicted damage factor (PDF). Table 6-3 shows the dam risk class depending on the TRF value calculated.

Table 6-3. Dam Risk Class (from Bureau, 2003)

Total Risk Factor (TRF)	Dam Risk Class
2 to 25	I (low)
25 to 125	II (moderate)
125 to 250	III (high)
> 250	IV (extreme)

Using the available information for Patillas Dam and considering the Michoacán earthquake described in Section 6.2 of this document, the following factors were determined for the site (Table 6-4). These factors were determined using guideline tables from Bureau (2003).

Table 6-4. Factors Calculated for Patillas Dam

Factor Considered	Value Obtained
CRF	4
HRF	6
ARF	6
DHF	12 to 20
PDF	7.5

Using these factors, Patillas Dam has a TRF in the range of 210 to 270. This would make Patillas Dam fall under a classification of high to extreme risk in the event of an earthquake.

Chapter 7

Results for Seismic Analyses of Patillas Dam

This chapter discusses the results obtained from the pseudo-static, dynamic finite element, and sliding block analyses for Patillas Dam. All the results are based on the material properties and seismic information described in the previous chapters. In addition to the seismic analyses, the static stability analyses will also be discussed.

7.1. Static Stability Analyses

As part of the studies a static stability analysis was performed. For this analysis the computer program SLOPE/W was used. The analyses were performed for the same material properties as those used in the pseudo-static analyses (see Chapter 4). Table 7-1 shows the factor of safety (FoS) results for these analyses.

Table 7-1. Results from Static Stability Analyses

Set of Properties	Factor of Safety
Lower Boundary	1.145
Most Probable	1.216
Upper Boundary	1.292

These results represent the failure surfaces for the minimum factor of safety obtained for each set of properties (Appendix C). These failure surfaces will be used for the sliding block analyses to calculate an estimate of the total deformation for the failure masses.

7.2. Pseudo-Static Analyses

The pseudo-static analyses were performed using SLOPE/W. The models were constructed using the material properties discussed in Chapter 5, while the seismic force coefficients are discussed in Chapter 6. Using these values the pseudo-static minimum factor of safety was calculated. Table 7-2 presents a summary of these results.

Table 7-2. Results of Pseudo-Static Analyses

Set of Properties	Factor of Safety	
	2,500 yr. Return Period	10,000 yr. Return Period
Lower Boundary	0.705	N/A*
Most Probable	0.679	N/A*
Upper Boundary	0.721	N/A*

* No minimum FoS was determined. Entire dam moves in these cases.

From these results it can be said that the pseudo-static stability of Patillas Dam is not acceptable because all the factors of safety are below unity. For the seismic forces due to the earthquake with 2,500 year return period, it was possible to establish a minimum factor of safety with defined failure surfaces (Appendix C). This was not the case for the seismic forces associated with the 10,000 year

return period. These analyses never converged on a failure surface even after using extremely large radiuses for the failure mass. In these cases the entire dam will move for the PGA's associated with this return period. Even though the pseudo-static approach shows instability of the dam while subjected to a seismic event, this method typically serves as a screening evaluation to determine if more rigorous analyses are required.

7.3. 2-D Dynamic Finite Element Analyses

QUAKE/W was used to perform the analyses. The purpose of the dynamic finite element analyses is to estimate the accelerations and amplifications at certain points of interest within the dam. These estimates can be used as a base of comparison with the seismic instrumentation installed in the dam to aid in the determination of a possible response in case of an earthquake. Figure 7-1 shows the location of the points of interest measured in the analyses. Nodes 1 to 4 are located at the central profile of the dam. Nodes 5 to 9 are located along the downstream slope where the seismic instruments were installed, and node 10 is located apart from the dam to serve as a "free-field" station.

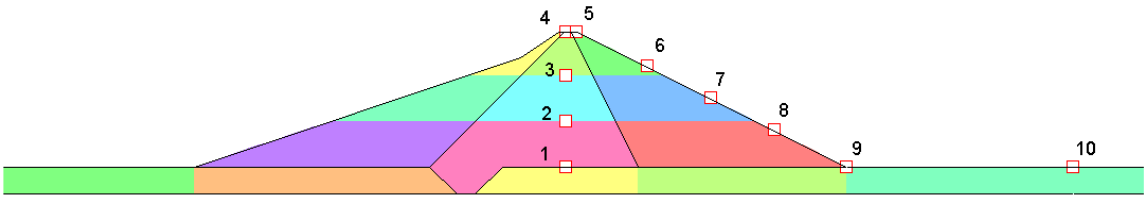

Figure 7-1. Location of Measurement Points

For each of the points mentioned, spectral acceleration responses were determined. To help interpret the analyses responses, the amplification of the maximum acceleration from the input ground motions will be used as the base of comparison. We determined this amplification ratio by using the following equation:

$$Amplification\ Ratio = \frac{Maximum\ acceleration\ \ from\ analysis\ result}{Maximum\ acceleration\ \ from\ input\ motion} \qquad (7\text{-}1)$$

The PGA's of the Michoacán, San Salvador and the UBC-Compatible ground motions are 0.283g, 0.535g and 0.452g, respectively. Tables 7-3, 7-4, and 7-5 present a summary of the amplification ratios obtained using the different ground motions.

Table 7-3. Amplification Ratios for the Michoacán Record

Node	Amplification Ratio		
	Lower Boundary	Most Probable	Upper Boundary
1	1.81	1.60	1.72
2	3.21	2.90	3.18
3	4.52	5.37	6.21
4	8.11	8.13	8.13
5	8.14	8.17	8.14
6	4.45	4.06	4.75
7	3.53	3.44	3.36
8	2.32	2.49	2.25
9	1.72	1.55	1.27
10	4.85	5.03	4.03

Table 7-4. Amplification Ratios for the San Salvador Record

Node	Amplification Ratio		
	Lower Boundary	Most Probable	Upper Boundary
1	1.51	1.49	1.47
2	2.68	2.74	2.53
3	4.38	4.33	4.07
4	6.31	5.41	5.13
5	6.32	5.46	5.18
6	3.70	3.49	3.46
7	2.31	2.18	2.15
8	1.73	1.55	1.61
9	1.40	1.25	1.27
10	1.58	1.75	1.60

Table 7-5. Amplification Ratios for the UBC-Compatible Ground Motion

Node	Amplification Ratio		
	Lower Boundary	Most Probable	Upper Boundary
1	1.04	1.23	1.24
2	1.62	2.00	2.39
3	2.86	3.08	4.03
4	4.17	3.86	5.69
5	4.19	3.94	5.72
6	2.21	2.52	3.63
7	1.81	1.81	2.30
8	1.23	1.36	1.51
9	1.03	1.09	1.20
10	2.24	2.51	2.18

From the results in these tables it is evident that the acceleration responses increase the farther the points are from the source of motion. The responses from the Michoacán ground motion yielded the highest amplifications even though this record has the lowest PGA. In addition to this, the response depending on the range of properties (Lower boundary, Most probable, and Upper boundary sets of properties) varies for the different ground motions. To better illustrate this, the Figures 7-2, 7-3, and 7-4 show how the accelerations are amplified along the center profile of the dam.

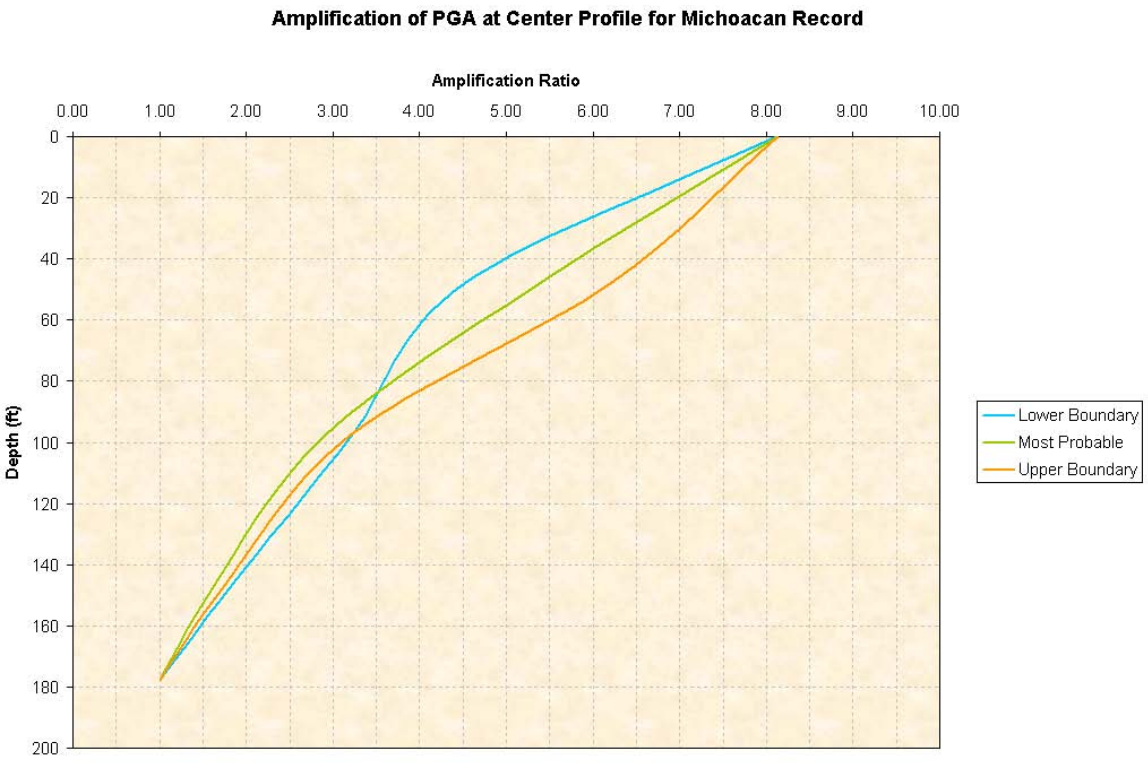

Figure 7-2. Amplification for Michoacán Record

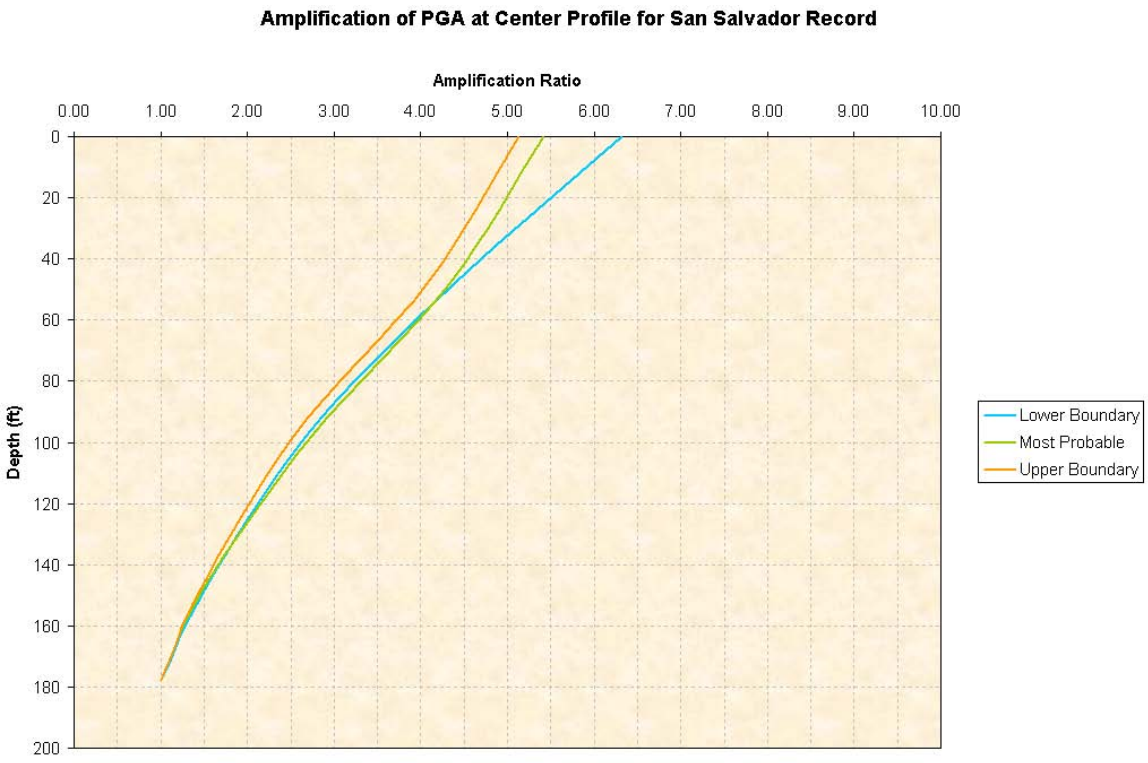

Figure 7-3. Amplification for San Salvador Record

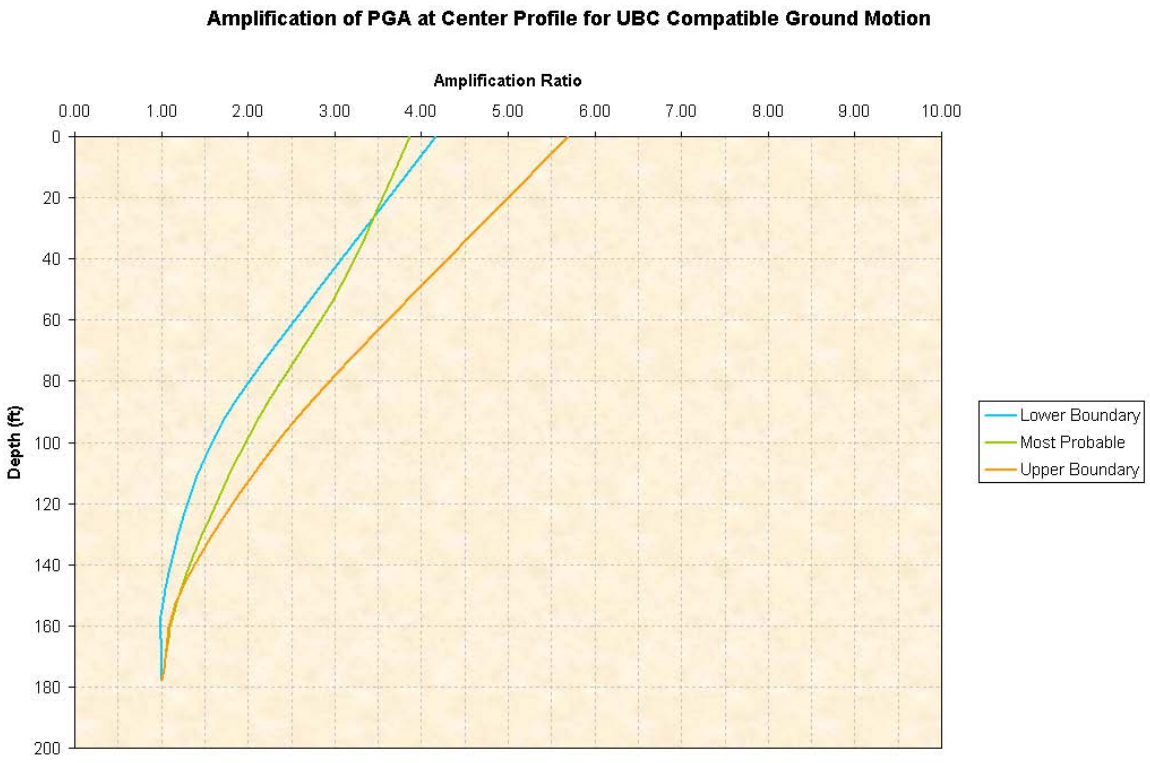

Figure 7-4. Amplification for UBC Compatible Ground Motion

The results of the QUAKE/W runs depend on the material stiffness. This makes the Lower Boundary set less rigid than the Upper Boundary with the Most Probable set somewhere in between. When reviewing these figures, each ground motion curve presented different behaviors as the soil properties vary. Logic tells us that accelerations should amplify more on less rigid soils than on stiffer materials, but this is not always the case. This variation in behavior is due to the fact that the response of a structure is dependant on material properties such as soil stiffness and unit weight which dictate its natural vibration period. When a ground motion and a structure period coincide, the structure response will be much more violent. In addition to these results, the response for all nodes can be found in Appendix C.

7.4. Sliding Block Analyses

To perform the sliding block analyses the program SLOPE/W was used. SLOPE/W has an option to perform finite element analysis in which stresses from a QUAKE/W analysis are used to determine the stability variations during an earthquake and estimate the resulting permanent deformations. This option was used to determine the deformations for the failure surfaces determined in the static stability analyses. The same range of strength parameters as in the pseudo-static analyses was used with their corresponding QUAKE/W result files from the dynamic finite element analyses. Deformations were estimated for the Michoacán, San Salvador, and the UBC compatible ground motions. Table 7-6 shows the yield acceleration (a_y) and deformation values obtained from the sliding block analyses.

Table 7-6. Results from Sliding Block Analyses

Set of Properties	Michoacán		San Salvador		UBC	
	a_y (g)	Def. (ft)	a_y (g)	Def. (ft)	a_y (g)	Def. (ft)
Lower	0.093	5.028	0.093	3.870	0.093	1.472
Most Probable	0.142	2.099	0.142	1.195	0.142	0.442
Upper	0.142	1.047	0.142	2.511	0.142	1.490

The sliding block analyses use the stresses from the QUAKE/W runs, therefore these analyses are dependant on the stiffness of the materials. This would make the Lower boundary the least rigid, the Upper boundary the stiffest, and the Most Probable set somewhere in between these. It would be expected that the least rigid model would have larger deformations, while the stiffest model would have

the lowest deformations. By observing the results from Table 6-6, this behavior is not always reflected. These variations occur because each model has a different natural vibration period and therefore have different responses for the different ground motions.

The Division of Safety of Dams from the California Department of Water Resources (Babbit and Verigin, 1996) considers deformations larger than 5 feet to be serious, and several factors should be taken into consideration in order to decide if structural modifications are required. The range of deformations obtained from the sliding block analyses goes from 0.442 ft to 5.028 ft, with eight of the nine total cases analyzed falling below the acceptable deformation of 5 ft. The only case in which the 5 ft deformation was exceeded was the lower boundary set of properties for the Michoacán ground motion. This case represents the analysis with the most conservative properties with the most severe seismic excitation considered in this document. Taking this in to consideration along with the fact that the 0.028 feet exceedance of the acceptable deformation of 5 ft represents an excess of 0.56% of this acceptable deformation, it can be argued that the dam falls within the criteria of the allowable deformation to withstand a seismic event.

Chapter 8

Conclusions and Recommendations

8.1. Summary and Conclusions

For this investigation a series of analyses were conducted to determine the suitability of Patillas Dam to withstand the occurrence of a large earthquake. Pseudo-Static, Dynamic Finite Element, and Sliding-Block analyses were used in conjunction with an equivalent-linear model, in order to determine the dam's adequacy. To provide a wide range of possibilities, different seismic inputs were used in the analyses.

There were no initial engineering properties for the dam materials in the available documentation for Patillas Dam. Using the descriptions given in these documents, some engineering judgment based on geotechnical literature and the performance of a rigorous analysis of the stress conditions in the dam, a range of geotechnical earthquake engineering properties was determined for the different sections of the dam. From the determined material properties, the vibration period of the dam was estimated to be in the range of 0.42 to 0.56 seconds.

Once the material properties were determined several analyses were performed to estimate the deformation expected for Patillas Dam. These analyses combined the previously determined range of material properties with the

different ground motions selected to account for different scenarios. The deformation results from these studies ranged from as low as 0.442 ft to as much as 5.028 ft.

In addition to the deformation estimates, spectral responses at various points of interests were determined for each of the cases analyzed. The measured points were taken along the center profile of the dam and along the downstream slope. The responses from the center profile of the dam were used to compare how the acceleration at the base amplifies as the wave travels from the base to the crest. From this it was observed that the wave propagation depends greatly on the combination of material properties and the applied ground motions. The locations of the responses along the downstream slope coincide with the seismic instrumentation installed at the site. Information from these points can be used as a reference to compare with the instrument readings at the site.

The Pseudo-Static analyses resulted in FoS values lower than 1, which by definition would indicate that the dam would fail in case of an earthquake. Nevertheless this type of analysis typically serves as a screening evaluation to determine if more rigorous methods of analysis need to be considered.

When evaluating the results from the Dynamic finite element and Sliding-Block analyses, Patillas Dam yielded deformation results within the accepted deformation values (≤ 5 ft) for all of the cases analyzed except for the case with

the least competent material properties subjected to the strongest ground motion considered in this thesis. This is by far the most conservative of all the analyses performed. With this in mind, the exceedance of this deformation was less than 1% the allowable value, which can be argued as a negligible difference and therefore complies with the accepted maximum deformation.

When taking into consideration the 94 years of service without any considerable problems and the results from the seismic analyses discussed in this document it was concluded that Patillas Dam is suited to withstand the events of a large earthquake.

8.2. Recommendations

Because of the uncertainties regarding the material properties of the dam and the foundation, it is recommended that field studies be performed to determine material properties such as shear wave velocity, permeability, material density, friction angle, and undrained shear strength among others. This can be performed by a subsurface exploration or geophysical methods. Once actual material properties for the site are obtained, similar analyses to the ones performed for this document should be carried out in order to obtain a more accurate response for the dam.

Chapter 9

References

1. Babbit, D.H. and Verigin, S.W. (1996). “General Approach to Seismic Stability Analysis of Earth Embankment Dams”. California Department of Water Resources, Division of Safety of Dams.
2. Briggs, R.P. (1964). “Provisional Geologic Map of Puerto Rico and Adjacent Islands”. U.S. Geological Survey (USGS), Miscellaneous Geologic Investigations Map I-392, scale 1:24000.
3. Bureau, G.J. (2003). “Earthquake Engineering Handbook”. Dams and Appurtenant Facilities, Chapter 26, CRC Press, New York.
4. Comissioner of the Interior (1913). “Report of the Commissioner of the Interior to the Governor of Puerto Rico”. Pp. 323-324.
5. Crumley, A.R. (1996). “Informe Geotécnico sobre las Causas de unos Sumideros en la Represa Patillas” (in Spanish). Geotechnical Report, GeoConsult, 1996.
6. Engemoen, W.O. and Fiedler, W.R. (2003). “Risk Analysis Report”. Dam Safety Studies for Patillas Dam Puerto Rico. U.S. Department of the Interior Bureau of Reclamation (USBR), Technical Service Center, Denver, Colorado, February 2003.
7. Engemoen, W.O. and Shaffner, P. (2002). “Evaluation of Geotechnical and Geologic Issues”. Dam Safety Studies for Patillas Dam Puerto Rico.

U.S. Department of the Interior Bureau of Reclamation (USBR), Technical Service Center, Denver, Colorado, December 2002.

8. Everson, M. (1969). “Investigations Relative to Leveling of Crest of Patillas Dam”. Handwritten Notes from M. Everson, September 24, 1969.
9. Everson, M. (1970). “Investigations Relative to Leveling of Crest of Patillas Dam”. Handwritten Notes from M. Everson, February 6, 1970.
10. Farrar, J. (2003). “Field Exploration Request”. Dam Safety Studies for Patillas Dam Puerto Rico. U.S. Department of the Interior Bureau of Reclamation (USBR), Technical Service Center, Denver, Colorado, February 2003.
11. Fiedler, W.R. and Trojanowski, J. (2003). “Flood Routing Study”. Dam Safety Studies for Patillas Dam Puerto Rico. Technical Memorandum No. PT-8130-SS-02-1, U.S. Department of the Interior Bureau of Reclamation (USBR), Technical Service Center, Denver, Colorado, March 2003.
12. GEO-SLOPE (2004). “User’s Guide”. SLOPE/W, QUAKE/W. GEO-SLOPE/W International Ltd, Calgary, Alberta, Canada.
13. Graham, W.J. (2002). “Loss of Life Due to Dam Failure”. Dam Safety Studies for Patillas Dam Puerto Rico. U.S. Department of the Interior Bureau of Reclamation (USBR), Technical Service Center, Denver, Colorado, June 2002.
14. Gutenberg, B. and Richter, C.F. (1944). “Frequency of Earthquakes in California”. Bulletin of the Seismological Society of America, Vol. 34, p. 185-188.

15. Hamilton, R.R. and Román, P.A. (1988). “Phase I Inspection Report – Patillas Dam”. Puerto Rico Electric Power Authority (PREPA), San Juan, Puerto Rico, May 1988.
16. Hynes-Griffin, M.E. and Franklin, A.G. (1984). “Rationalizing the Seismic Coefficient Method”. Miscellaneous paper GL-84-13, US Army Crops of Engineers Waterways Experimental Station, Vicksburg, Mississippi, 21pp.
17. ICC (2006). “International Building Codes 2006”. International Code Council (ICC), Country Club Hills, IL.
18. ICOB (1997). “1997 Uniform Building Code”. International Conference of Building Officials (ICBO), Whittier, CA.
19. ICOLD (2001). “Design Features of Dams to Effectively Resist Seismic Ground Motion”. International Commission of Large Dams (ICOLD), Bulletin 120, Committee on Seismic Aspects of Dam Design, ICOLD, Paris.
20. Irizarry, J. (1999). “Design Earthquakes and Design Spectra for Puerto Rico’s Main Cities Based on Worldwide Strong Motion Records”. MS Thesis, University of Puerto Rico-Mayagüez, Mayagüez, Puerto Rico.
21. Jacobs, J., Hall, B.M., and Giles, J.M. (1909). “Patillas Dam: Plan, Profile and Sections of Dam”. Construction drawings, August 1909.
22. Krahn, J. (2004). “Stability Modeling with SLOPE/W: An Engineering Methodology”. 1st Edition. GEO-SLOPE/W International Ltd, Calgary, Alberta, Canada.

23. Kramer, S.L. (1996). "Geotechnical Earthquake Engineering". Prentice Hall, Englewood Cliffs, NJ, p. 653.
24. LaForge, R. (2002). "Probabilistic Seismic Hazard Analysis for the Patillas Dam, Puerto Rico". Dam Safety Studies for Patillas Dam Puerto Rico. Technical Memorandum No. D8330-2002-08, U.S. Department of the Interior Bureau of Reclamation (USBR), Technical Service Center, Denver, Colorado, July 2002.
25. McCann, W.R. (1985). "On the Earthquake Hazards of Puerto Rico and the Virgin Islands". Bulletin of the Seismological Society of America, Vol. 75, No. 1, pp. 251-262, February 1985.
26. Mueller, C.S. et al. (2003). "Seismic Hazard Maps for Puerto Rico and the U.S. Virgin Islands". U.S. Geological Survey (USGS), Golden, CO.
27. Portela, E.A. and Alvarado, L. (1969). "Report on the Condition of Patillas Dam". Puerto Rico Electric Power Authority (PREPA), San Juan, Puerto Rico, April 1969.
28. Portela, E.A. and Alvarado, L. (1972). "Report on the Condition of Patillas Dam". Puerto Rico Electric Power Authority (PREPA), San Juan, Puerto Rico, 1972.
29. Román, P.A. (1995). "Phase I Inspection Report – Patillas Dam". Puerto Rico Electric Power Authority (PREPA), San Juan, Puerto Rico, September 1995.

30. Román, P.A. (1998). “Phase I Inspection Report – Patillas Dam”. Puerto Rico Electric Power Authority (PREPA), San Juan, Puerto Rico, February 1998.
31. Seed, H.B. and Idriss, I.M. (1970). “Soil Moduli and Damping Factors for Dynamic Response Analysis”. Report EERC 72-10, University of California, Berkeley, CA.
32. Seed, H.B. et al. (1986). “Moduli and Damping Factors for Dynamic Analyses of Cohesionless Soils”. Journal of Geotechnical Engineering, ASCE, 112(1): 1016-1032.
33. Terzaghi, K., Peck, R.B. and Mesri, G. (1996). “Soil Mechanics in Engineering Practice”. 3rd Edition. John Wiley & Sons Inc., New York, NY.
34. Wieland, M. (2005). “Review of Seismic Design Criteria of Large Concrete and Embankment Dams”. 73rd Annual Meeting of ICOLD, Paper No. 012-W4, Tehran, Iran, May 1-6, 2005.

Appendix A

Summary of Patillas Dam Information

The following table presents a summary of the most important information and quotes from different references such as PREPA, USBR, and GeoConsult with regards to materials description and the general behavior of Patillas Dam.

Table A-1. Summary of Patillas Dam Information

Reference	Description	Summary and Quotes
Commissioner of the Interior (1913)	Report of the Commissioner of the Interior to the Governor of Puerto Rico	• "a considerable quantity of clay excavated from the spillway has been sluiced into the dam" • "Clay from the spillway will be dumped on a platform at this point and washed into the dam through a 16 inch pipe." • "During the past year 348,677 m^3 of rock and clay were placed in the dam, amounting to 47.5% of the total quantity of dam embankment." • "The dam is built of earth and stone with an impervious sluiced clay center and has a concrete cut-off wall through the center extending down into impervious material and of sufficient height to form a good bon with the clay core of the dam." • Crest width = 20 ft; Downstream slope = 2:1; Upstream slope = 3:1 to 2:1 • "The dam was built 4 ft above the theoretical lines to allow for settlement." • "Material composed largely of boulders and gravel was used for the outer sections, while that containing about 25% clay was deposited on the inner sides of the embankments"

Table A-1 (continued). Summary of Patillas Dam Information

Reference	Description	Summary and Quotes
Portela, E.A. and Alvarado, L. (1969)	Report on the Condition of Patillas Dam	• A 1967 survey of the top of the dam showed that the highest elevation of 238.6 ft is found near the center of the crest. • It is over 2 ft lower near both abutments. • Leveling of crest is recommended.
M. Everson (1969-1970)	Investigation Relative to Leveling Crest of Patillas Dam (Hand written notes)	• Silty sand puddle core. • Dam is topped with cobbles and boulders sized to 15 inch in diameter. • Shallow excavation on downstream slope revealed silty sand to clayey sand. • Two trenches (10 ft deep) revealed cobbles and boulders to a depth of 6 ft. The material below 6 ft is described as silty sand (SM). • Field densities (% of max density) were taken at depths of 6, 7, 8, and 10 ft of those trenches. Results varied from 76 to 100%.
Portela, E.A. and Alvarado, L. (1972)	Report on the Condition of Patillas Dam	• A concrete wall has been constructed to level the crest at a constant elevation. • The wall is 12 inches wide, and buried 6 to 8 ft beneath the crest. This wall runs all along the crest.

Table A-1 (continued). Summary of Patillas Dam Information

Reference	Description	Summary and Quotes
Hamilton, R.R. and Román, P.A. (1988)	Patillas Dam Phase I – Inspection Report	• Crest elevation after leveling (construction of concrete wall) = 238.8 ft • Height = 147 ft; Crest width = 15 ft; Base width = 625 ft; Crest length = 1067 ft • Downstream slope = 1.5:1 to elevation 212 ft and 2:1 below this. • Upstream slope = 2:1 to elevation 212 ft and 3:1 below this. • "In 1917, 3 years after completion of initial construction, the crest of the dam was raised approximately 5 ft adjacent to the abutments to match construction camber provided at the center of the dam for settlement which did not take place."
Román, P.A. (1995)	Patillas Dam Phase I – Inspection Report	• Sinkholes were found in the downstream slope. • Recommendation to investigate these sinkholes is made.
Crumley, A.R. (1997)	Informe Geotécnico sobre las Causas de unos Sumideros en la Represa de Patillas (in Spanish)	• Report concluded that the sinkholes were related to a trestle constructed at this location that wasn't fully removed. • The sinkholes were filled with gravel. • Boreholes were made to install six piezometers on the downstream slope. • The material found in these boreholes is described as gravel and fine grained (sand, silt or clay). • There are some readings from the piezometers installed in this document.

Table A-1 (continued). Summary of Patillas Dam Information

Reference	Description	Summary and Quotes
Román, P.A. (1998)	Patillas Dam Phase I – Inspection Report	• Dam has continued to have good performance. • Previous sinkholes have not presented any problems.
W. Engemoen and P. Shaffner (2002)	Evaluation of Geotechnical and Geologic Issues	• Performed static stability analyses and a dynamic analysis of Patillas Dam. • Analyses were performed with very limited information and a large amount of the properties used were assumed. • From the analyses performed, the dam does not appear to be in any danger. • Recommendations to perform subsurface studies are made in order to have the necessary information to perform more reliable analyses and obtain an accurate assessment of the dam's condition.

Appendix B

Natural Vibration Period of Models

The natural vibration period for the models was determined in order to provide a better understanding of the dam's response to seismic excitation. To determine the period for the dam models, modal analyses were carried out using the computer code SAP2000 v.11. These were performed using the three sets of values (lower boundary, most probable, and upper boundary) discussed in Section 4.2. As an additional consideration, rotation of the elements was restircted. Table B-1 presents the results from these modal analyses.

Table B-1. Results from Modal Analyses

Set of Properties	Period, T (sec)
Lower Boundary	0.564
Most Probable	0.489
Upper Boundary	0.422

The values obtained present a behavior in which the least rigid model yield the highest vibration period, while the stiffest model results in the lowest vibration period.

Appendix C

Results from Seismic Analyses of Patillas Dam

This appendix contains additional figures from the seismic analyses described in this document. These figures include the failure surfaces for the limit equilibrium methods and spectral responses. The appendix will be divided in sections according to the analysis method, and in subsections when needed.

C.1. Static Stability Analyses

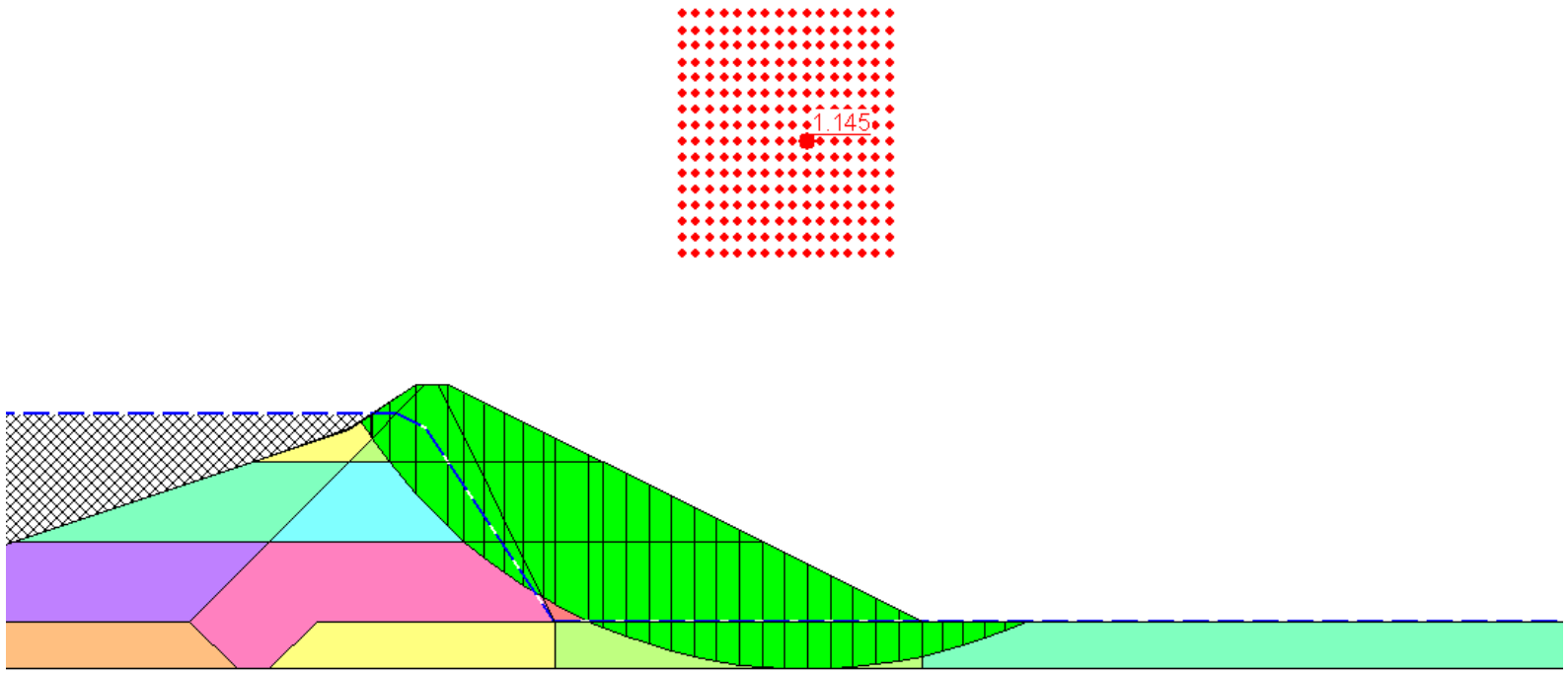

Figure C-1. Failure Surface of Static Stability Analysis of Lower Boundary Set of Properties

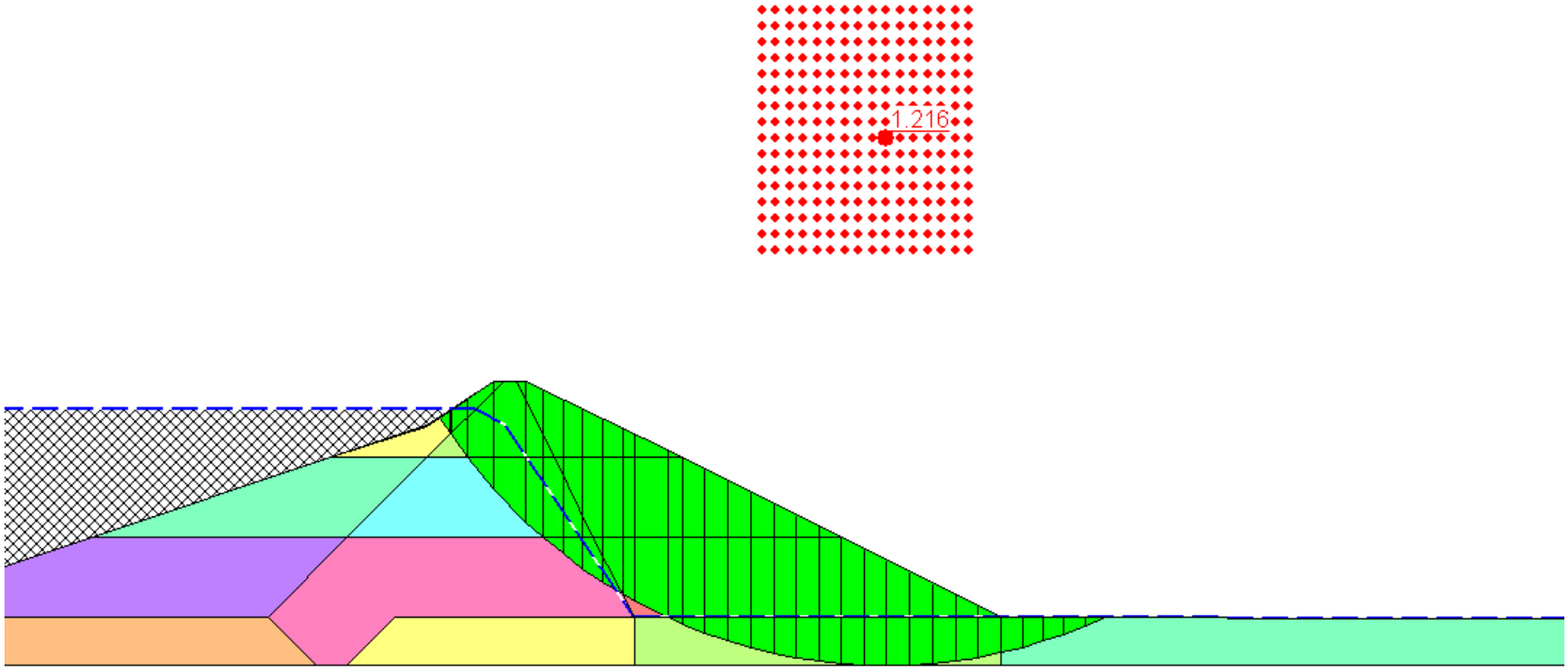

Figure C-2. Failure Surface of Static Stability Analysis of Most Probable Set of Properties

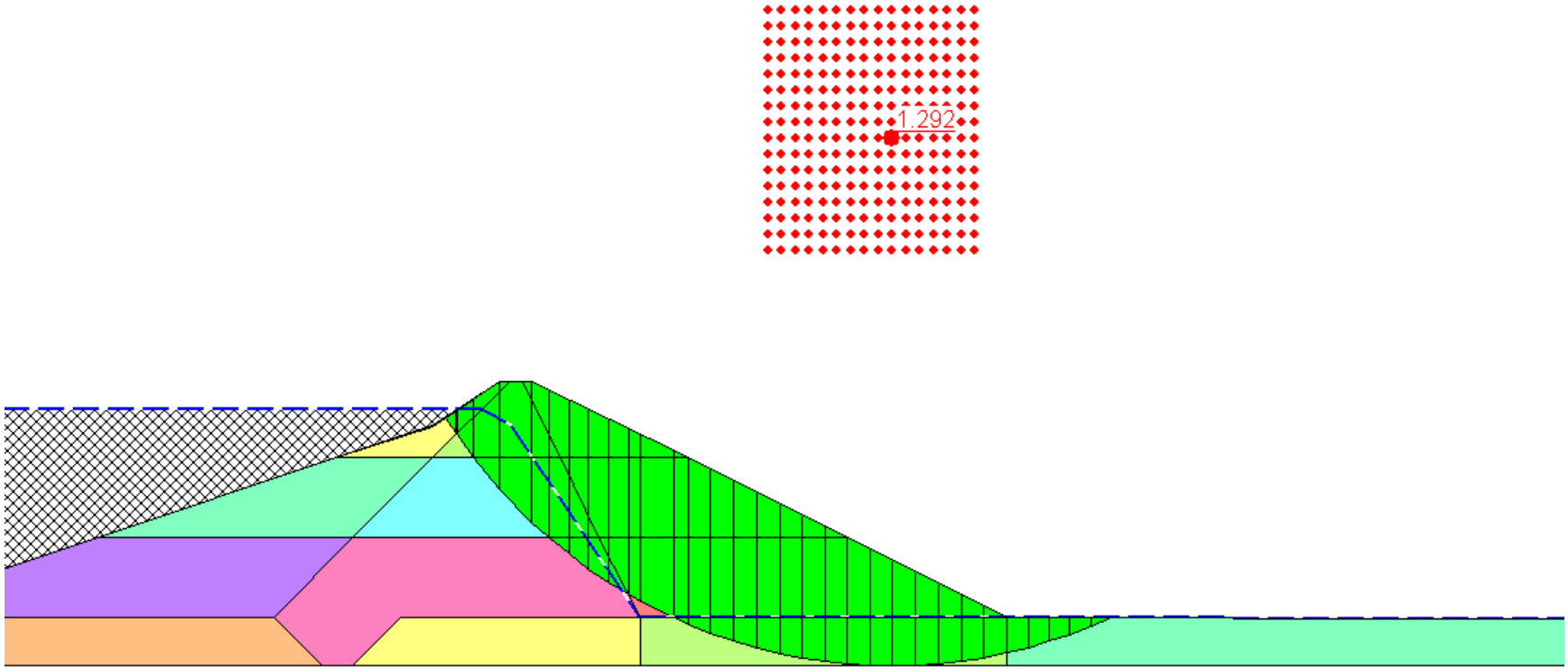

Figure C-3. Failure Surface of Static Stability Analysis of Upper Boundary Set of Properties

C.2. Pseudo-Static Analyses

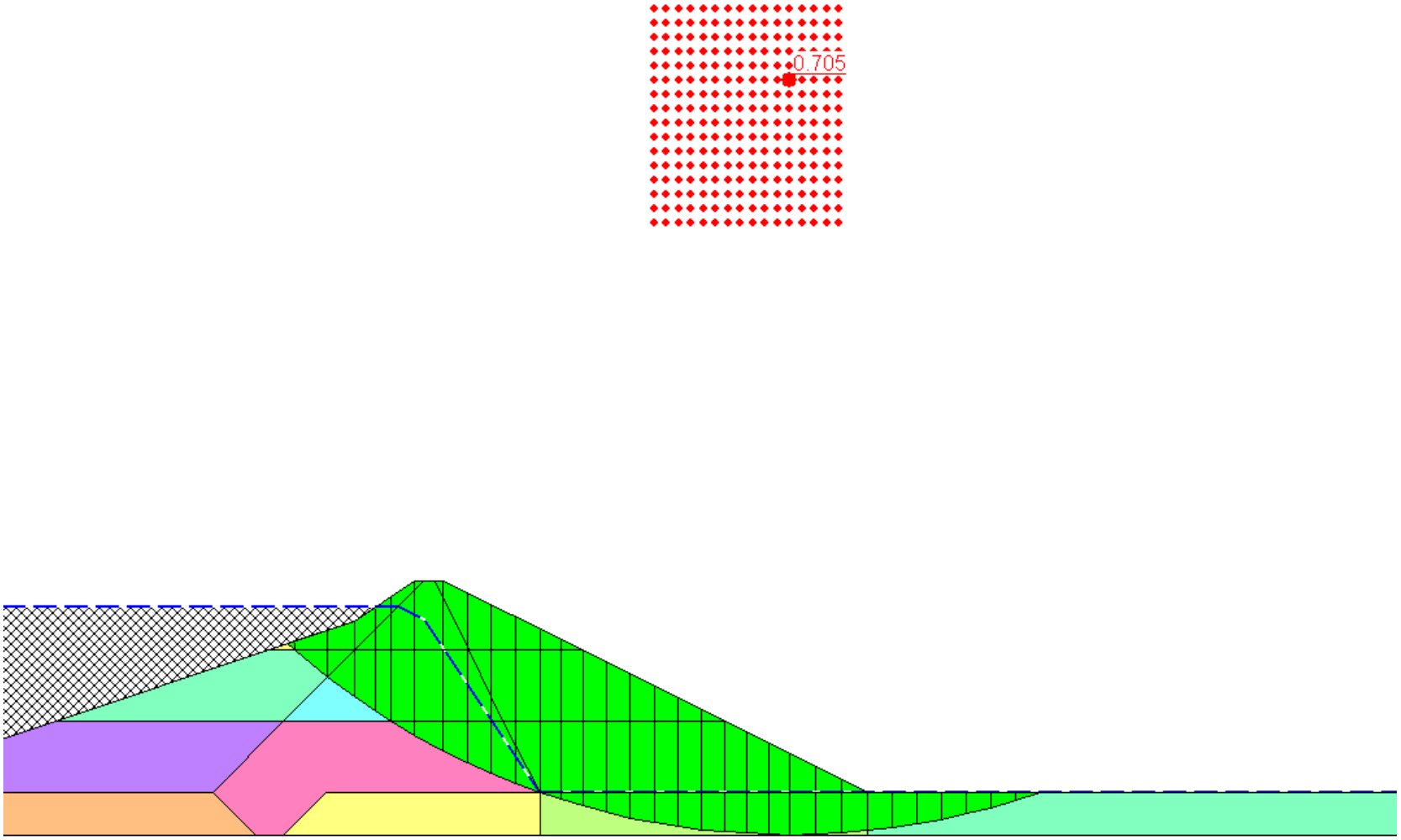

Figure C-4. Failure Surface of Pseudo-Static Stability Analysis of Lower Boundary Set of Properties

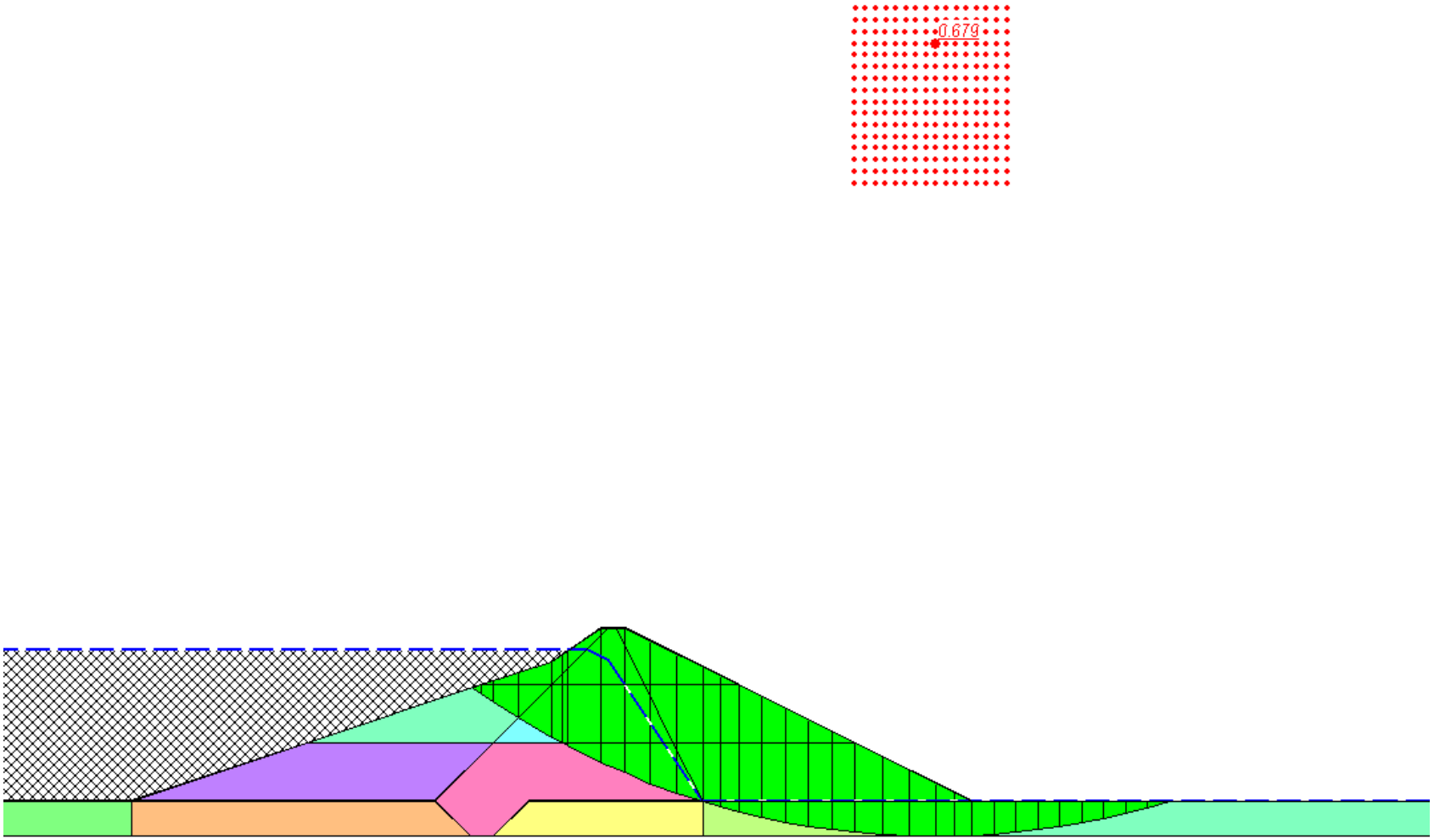

Figure C-5. Failure Surface of Pseudo-Static Stability Analysis of Most Probable Set of Properties

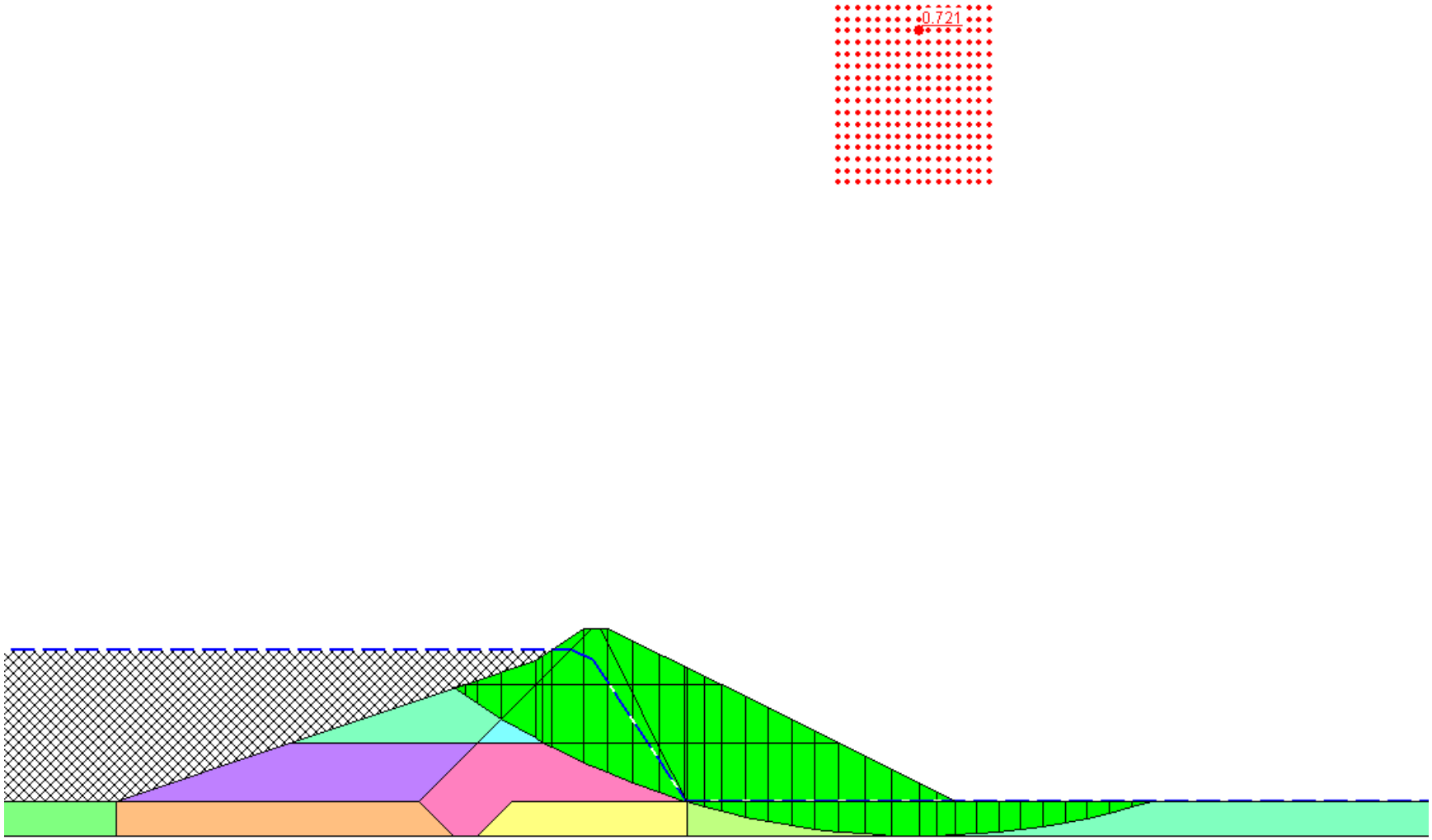

Figure C-6. Failure Surface of Pseudo-Static Stability Analysis of Upper Boundary Set of Properties

C.3. 2-D Dynamic Finite Element Analyses

This section contains the spectral acceleration response for different points in the model. This was done for each ground motion used in the analyses and for each set of material properties as previously discussed. Figure C-7 shows the location of the measurement points.

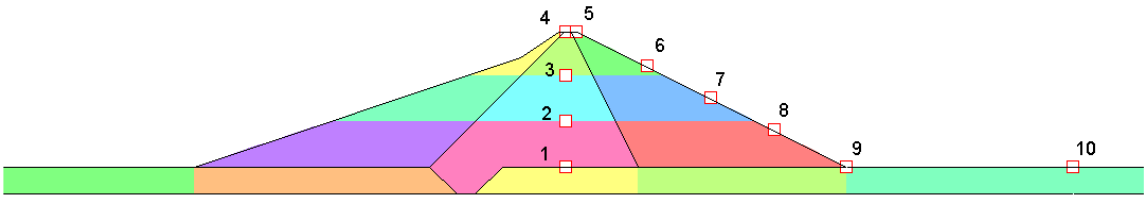

Figure C-7. Location of Measurement Points

C.3.1. Michoacán Ground Motion Responses

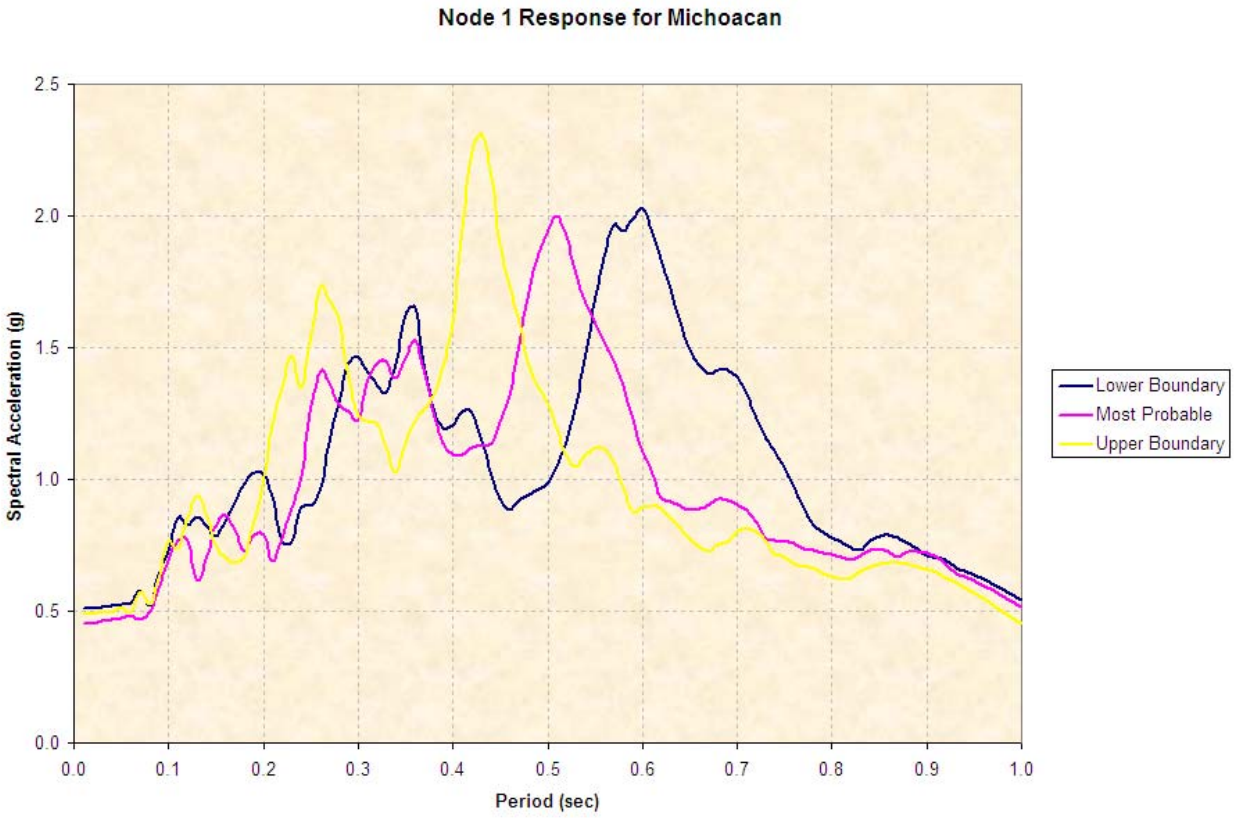

Figure C-8. Node 1 Response for Michoacán Ground Motion

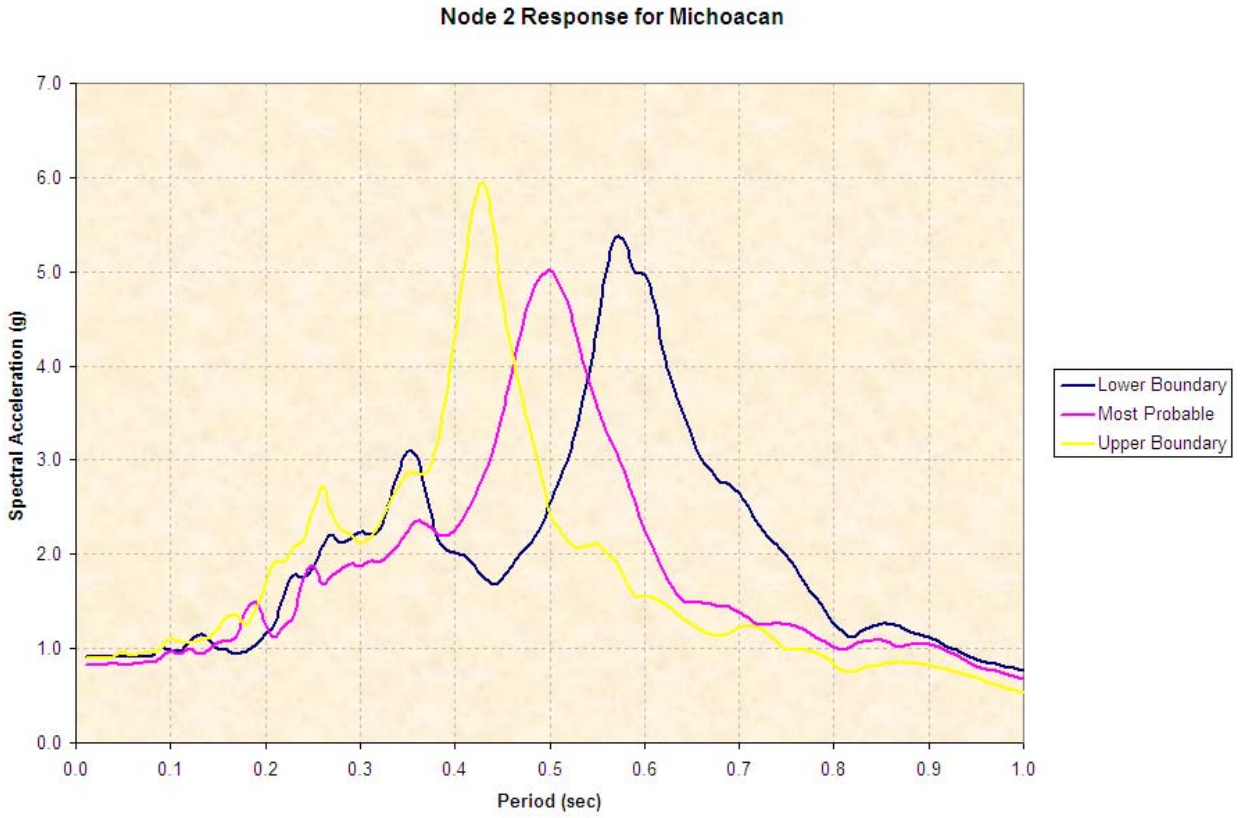

Figure C-9. Node 2 Response for Michoacán Ground Motion

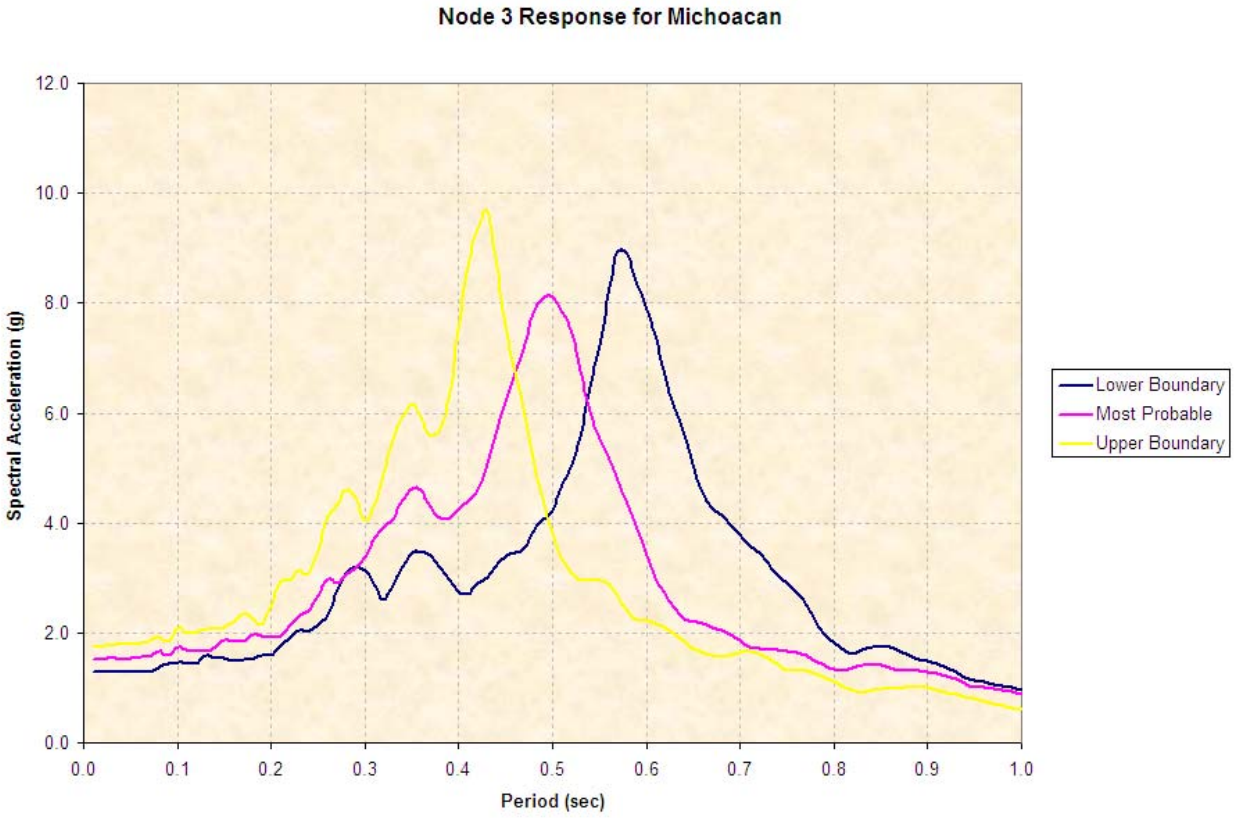

Figure C-10. Node 3 Response for Michoacán Ground Motion

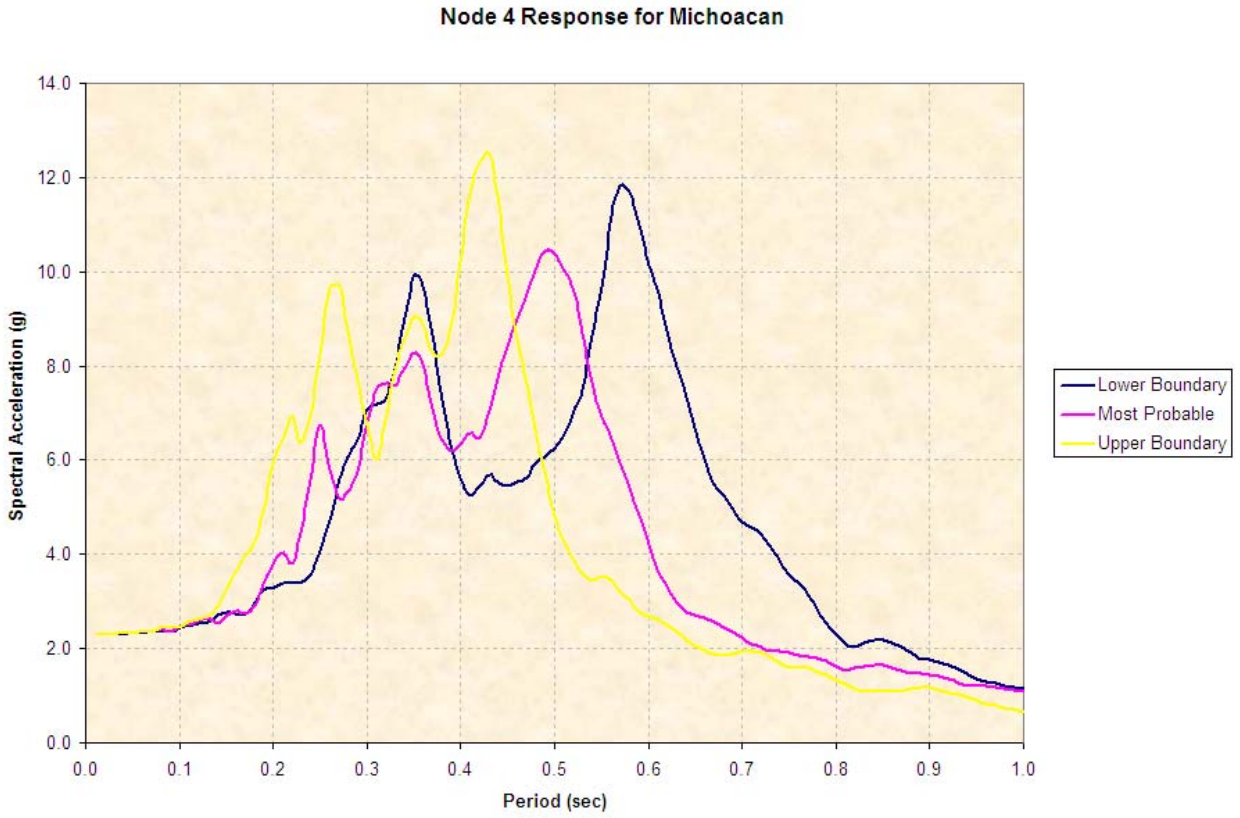

Figure C-11. Node 4 Response for Michoacán Ground Motion

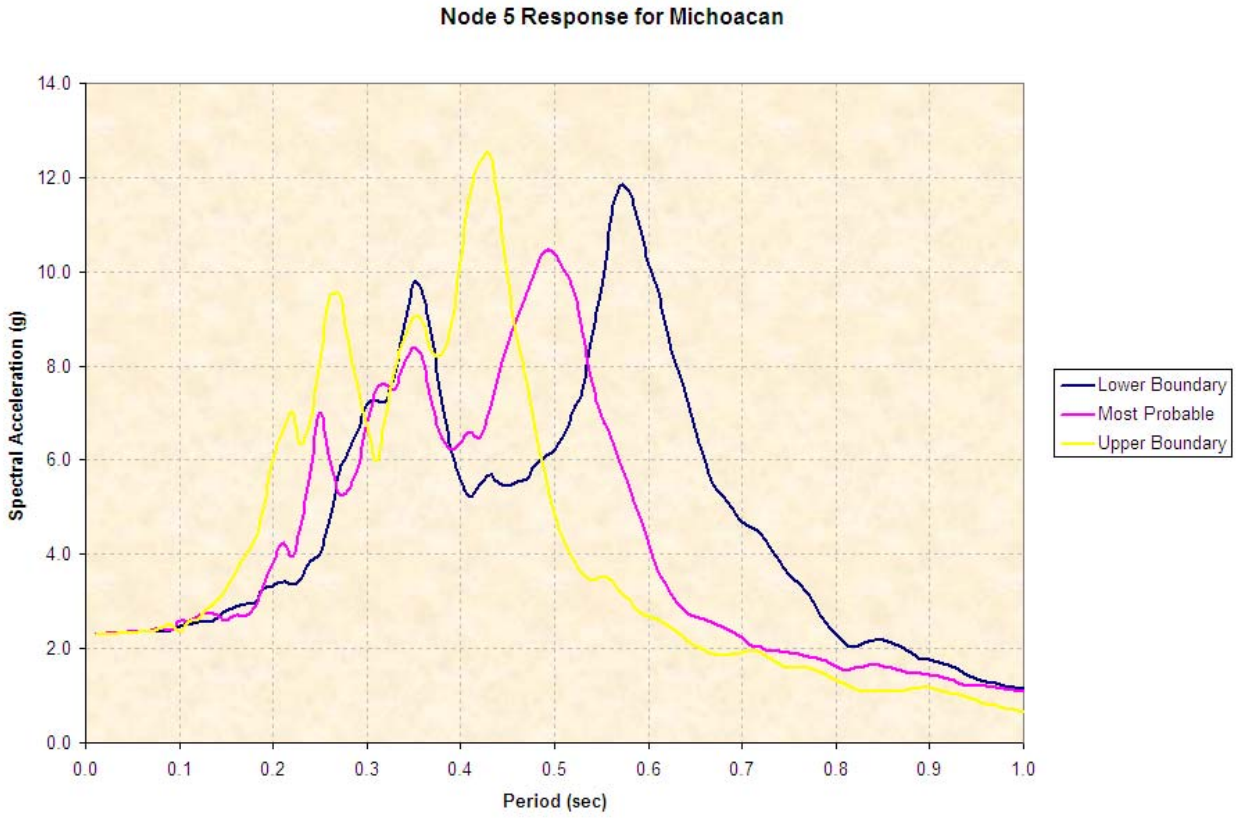

Figure C-12. Node 5 Response for Michoacán Ground Motion

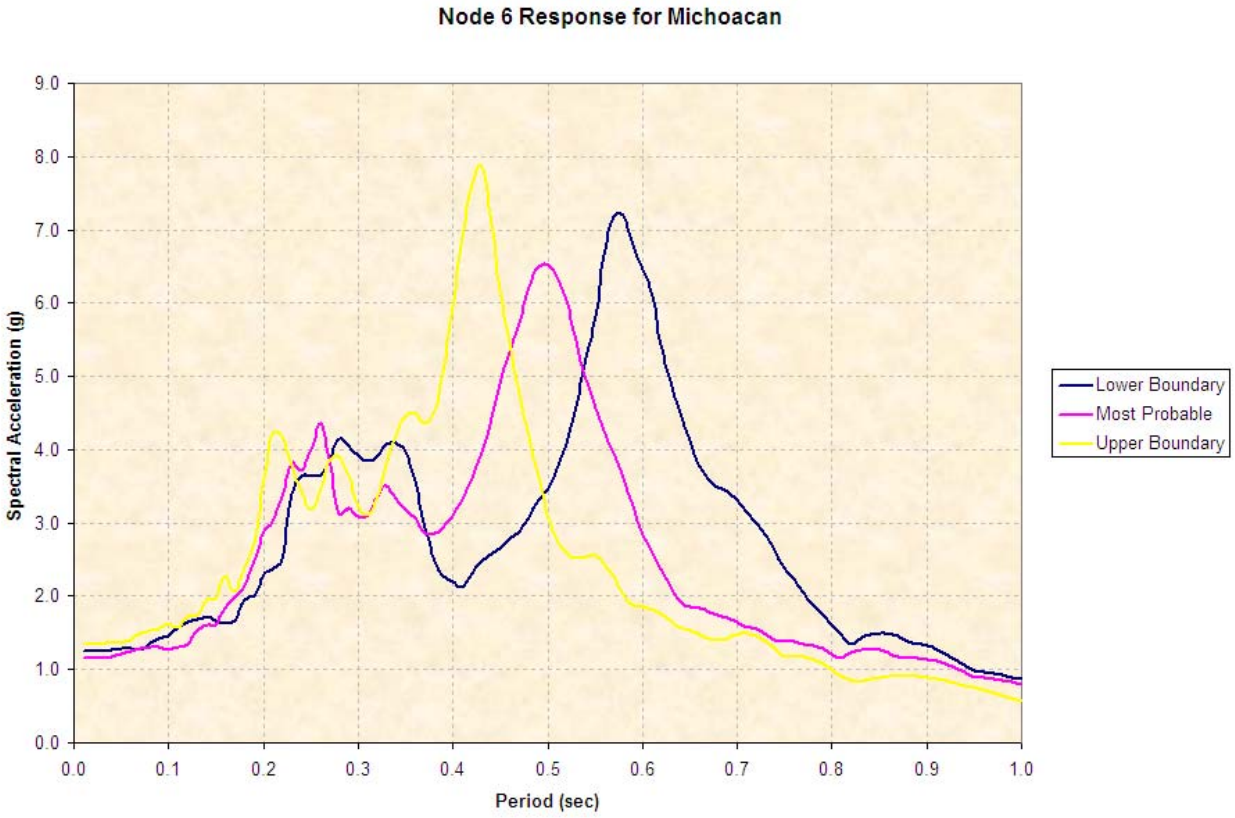

Figure C-13. Node 6 Response for Michoacán Ground Motion

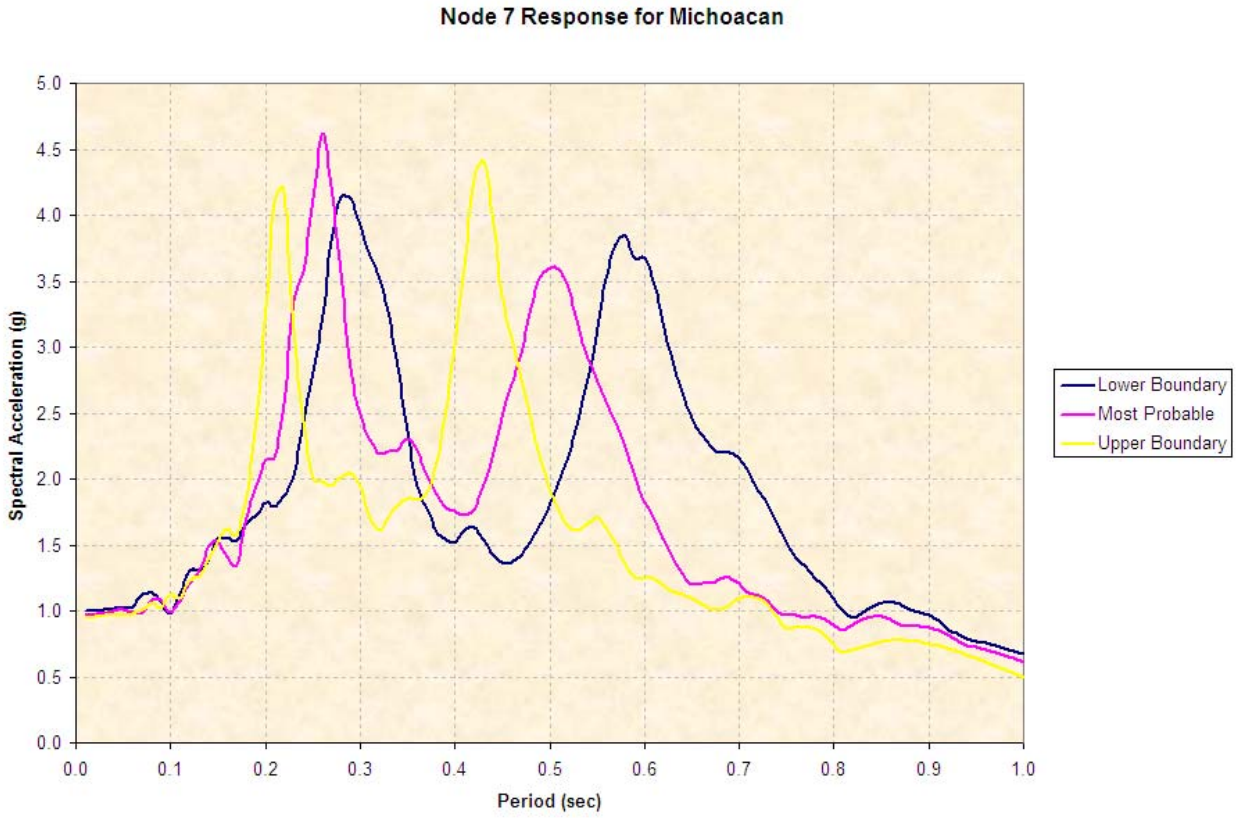

Figure C-14. Node 7 Response for Michoacán Ground Motion

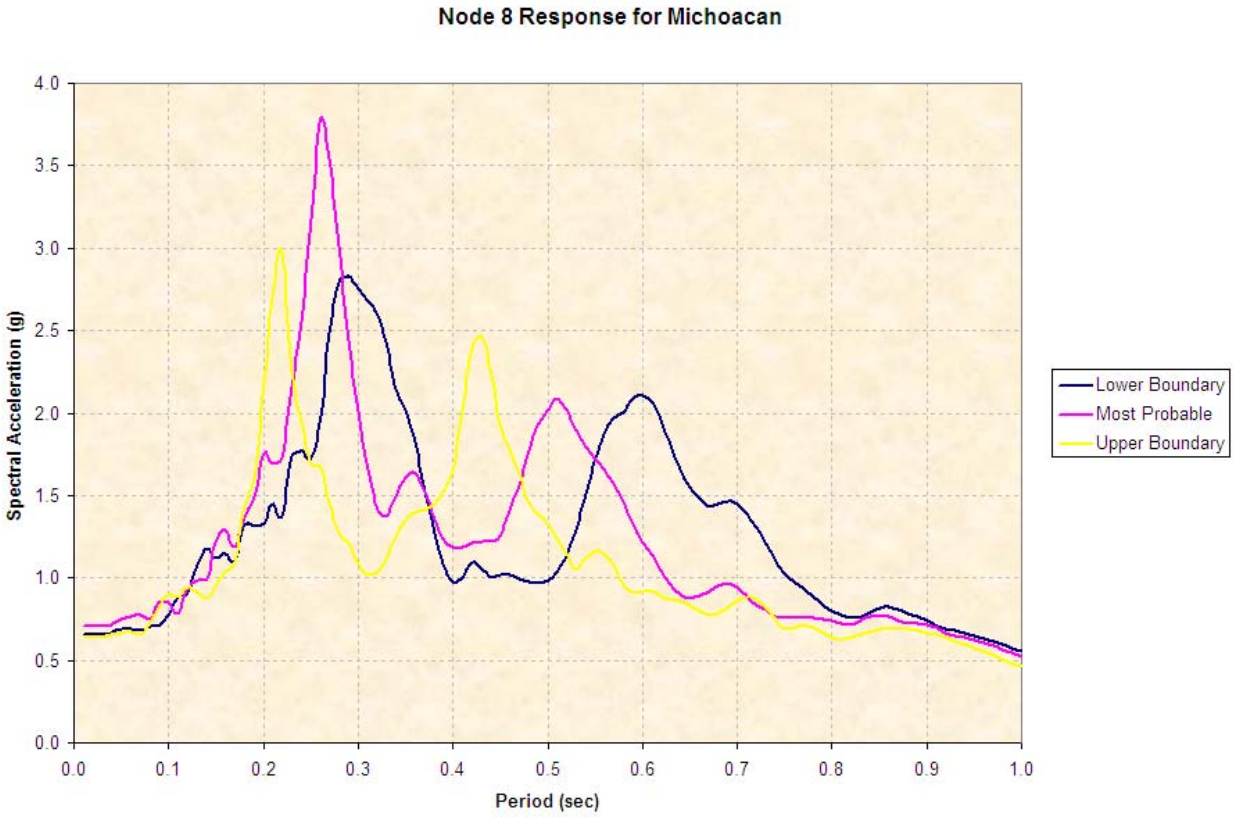

Figure C-15. Node 8 Response for Michoacán Ground Motion

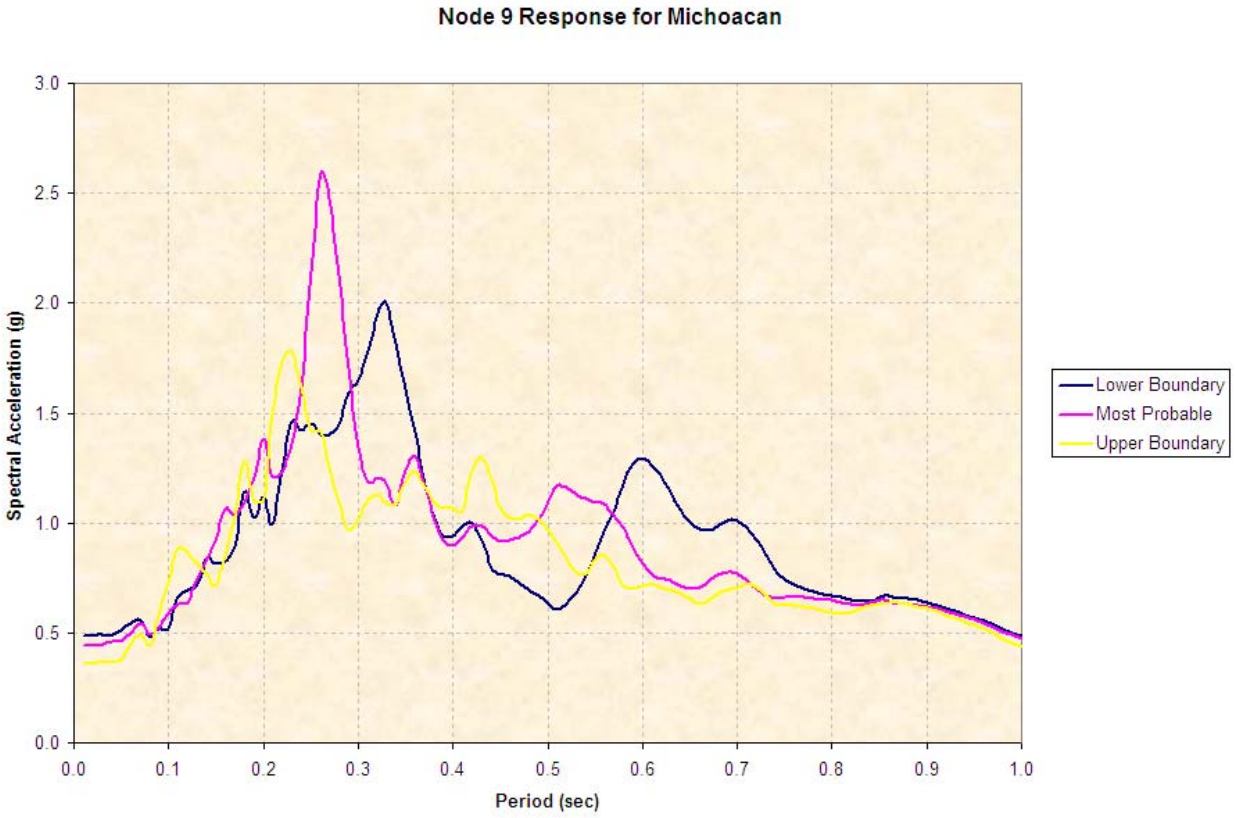

Figure C-16. Node 9 Response for Michoacán Ground Motion

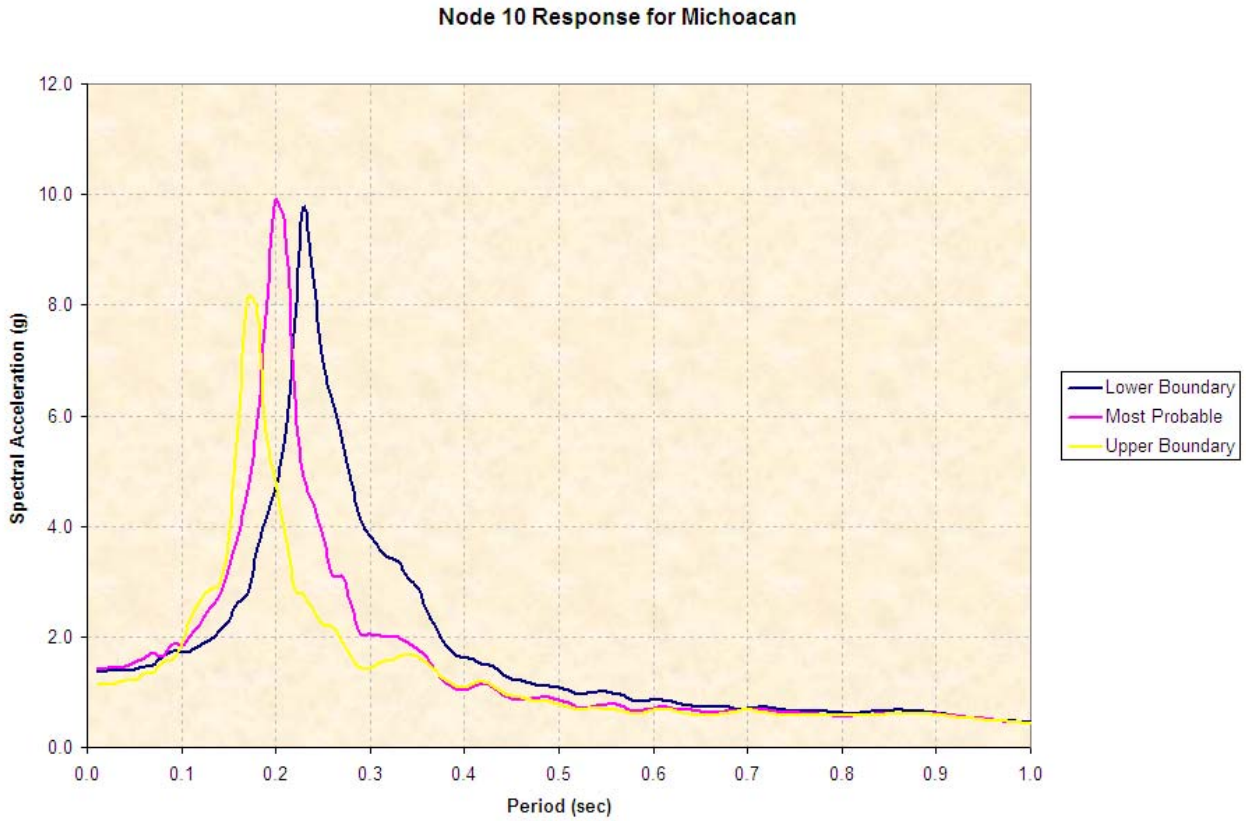

Figure C-17. Node 10 Response for Michoacán Ground Motion

C.3.2. San Salvador Ground Motion Responses

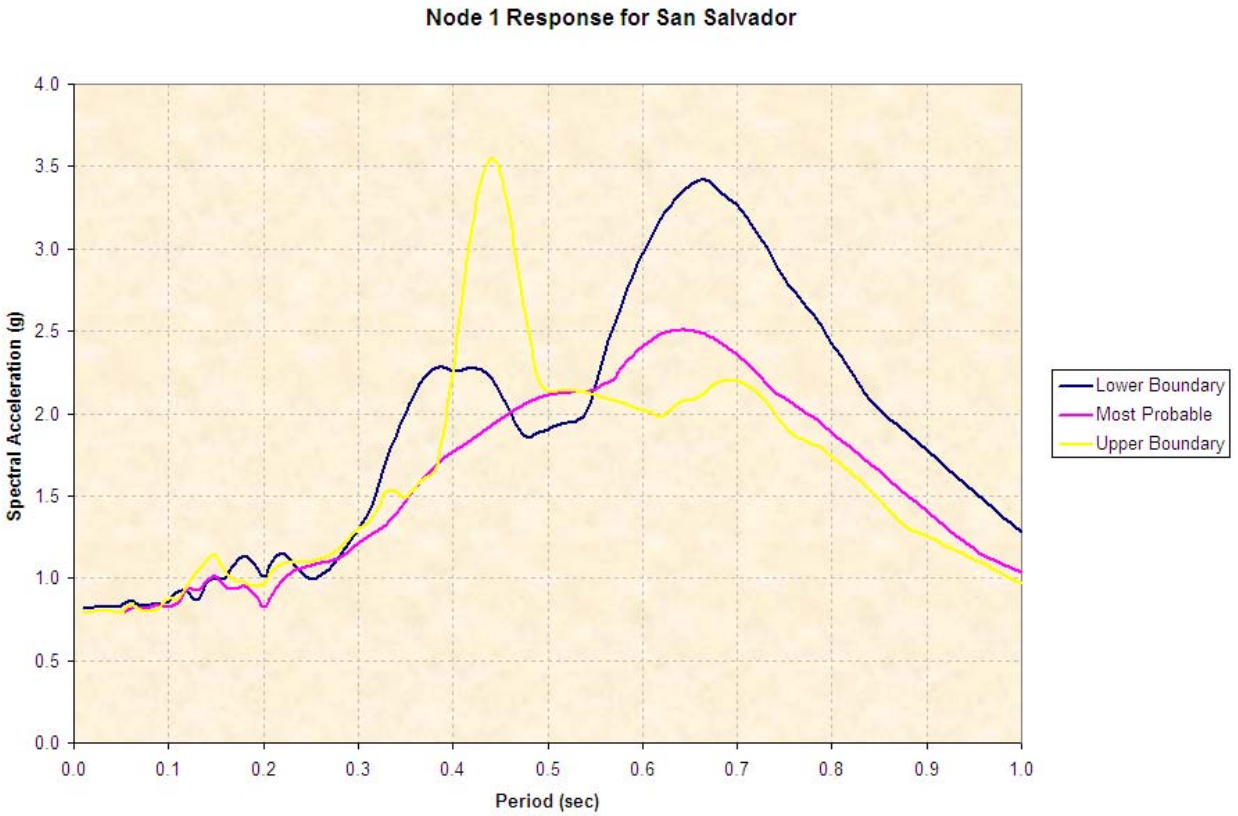

Figure C-18. Node 1 Response for San Salvador Ground Motion

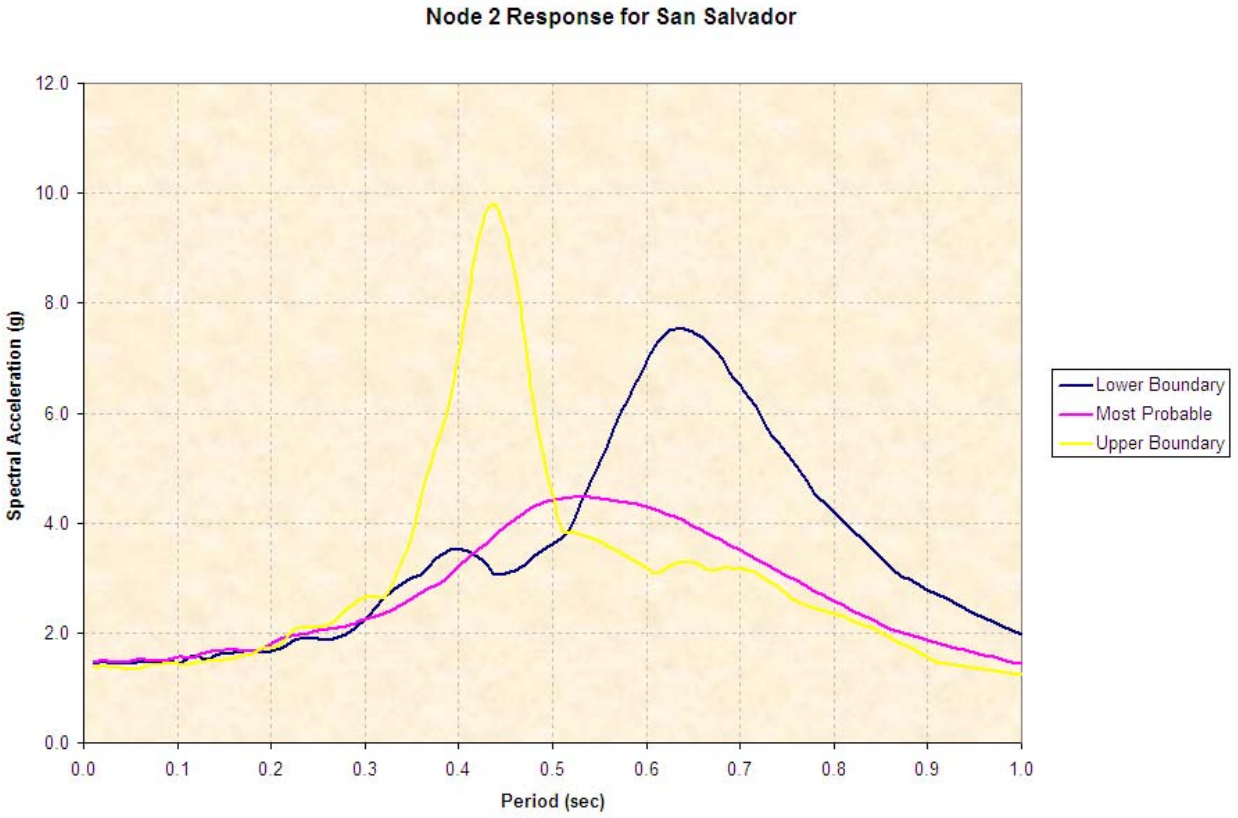

Figure C-19. Node 2 Response for San Salvador Ground Motion

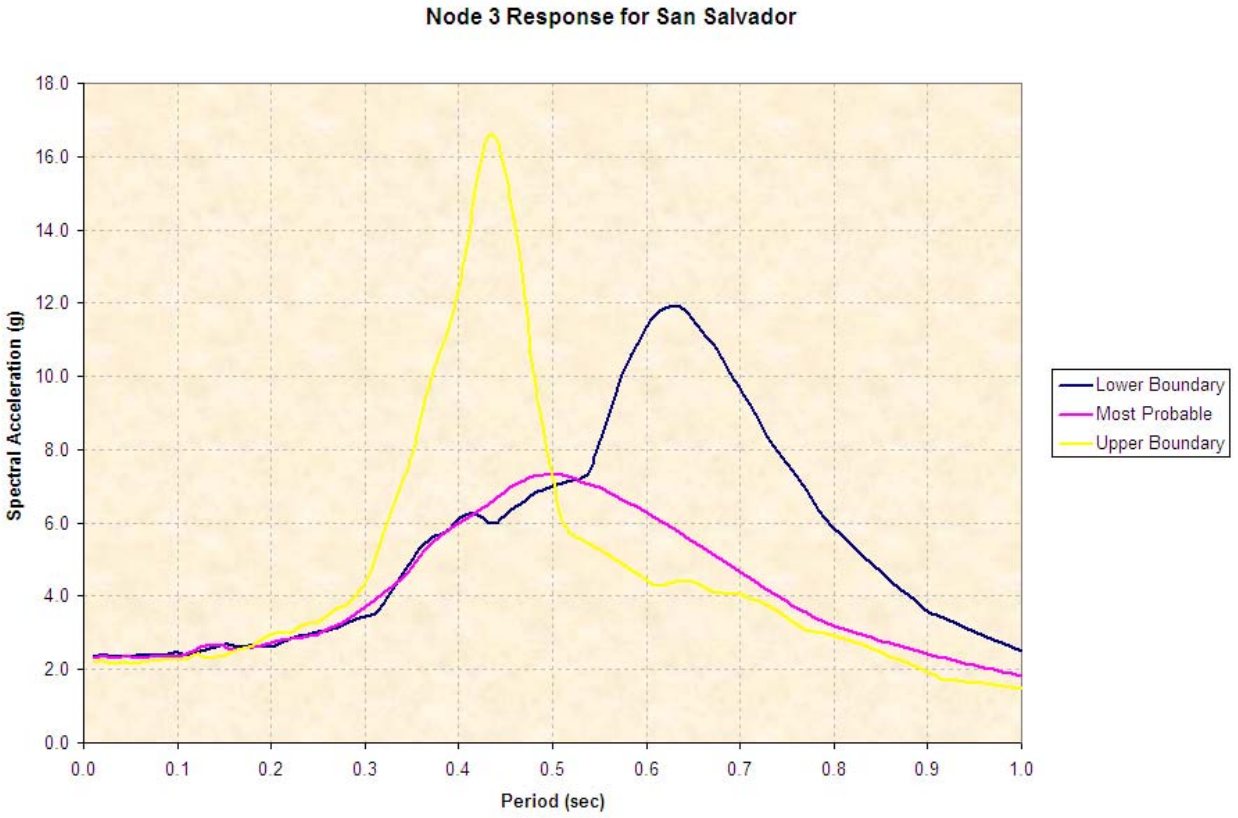

Figure C-20. Node 3 Response for San Salvador Ground Motion

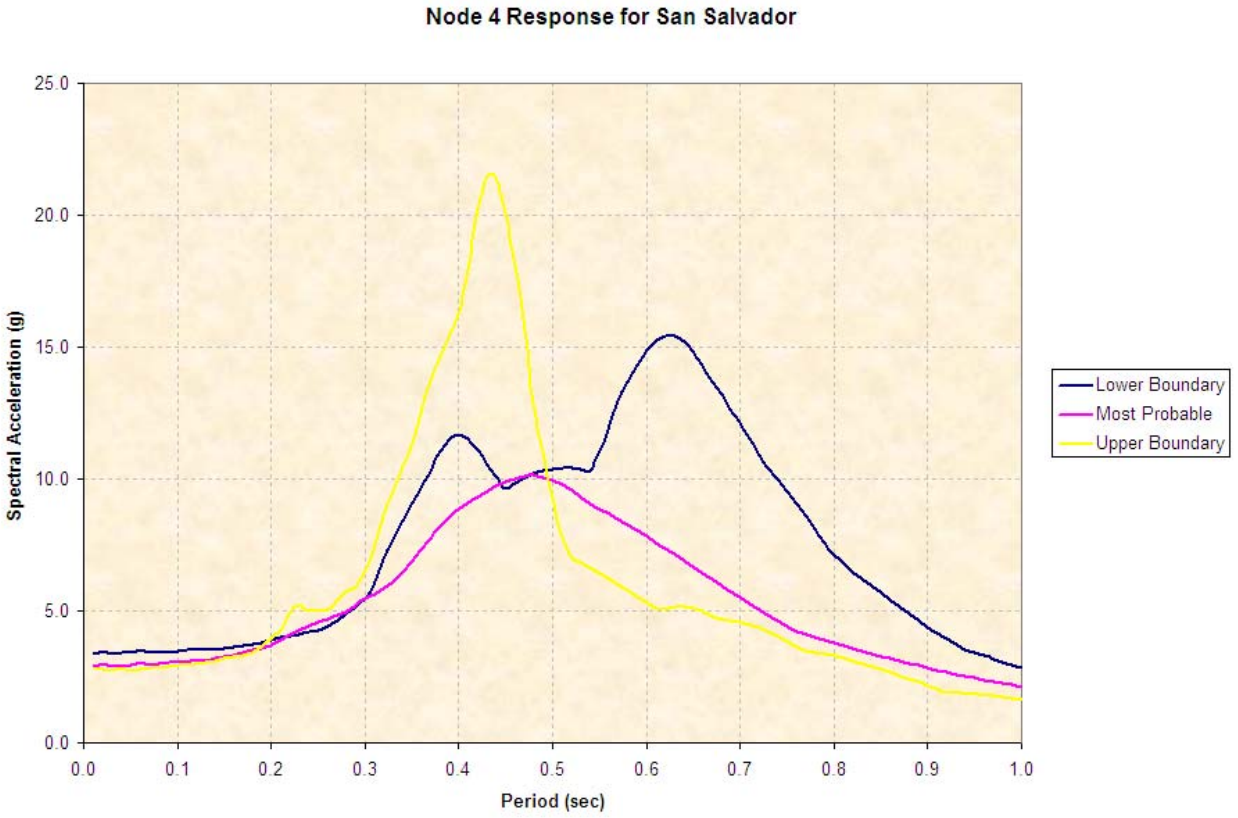

Figure C-21. Node 4 Response for San Salvador Ground Motion

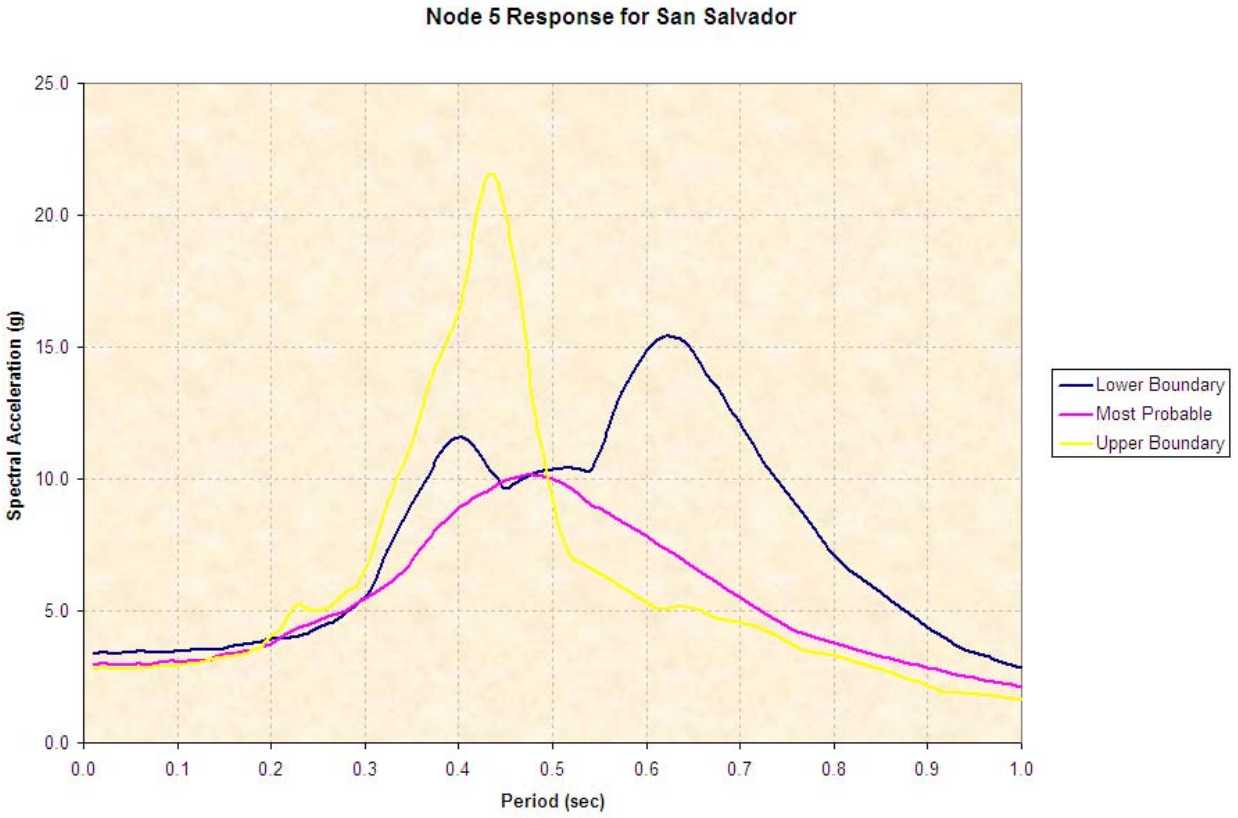

Figure C-22. Node 5 Response for San Salvador Ground Motion

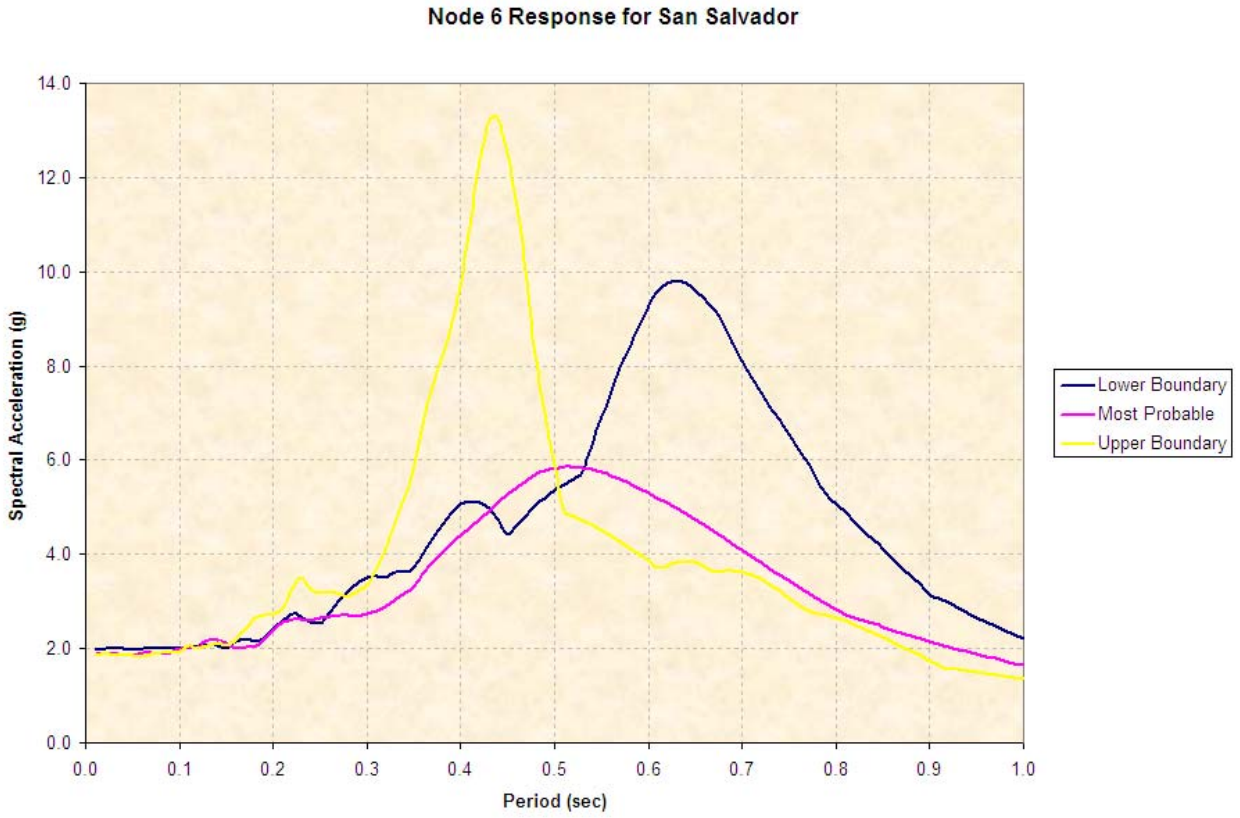

Figure C-23. Node 6 Response for San Salvador Ground Motion

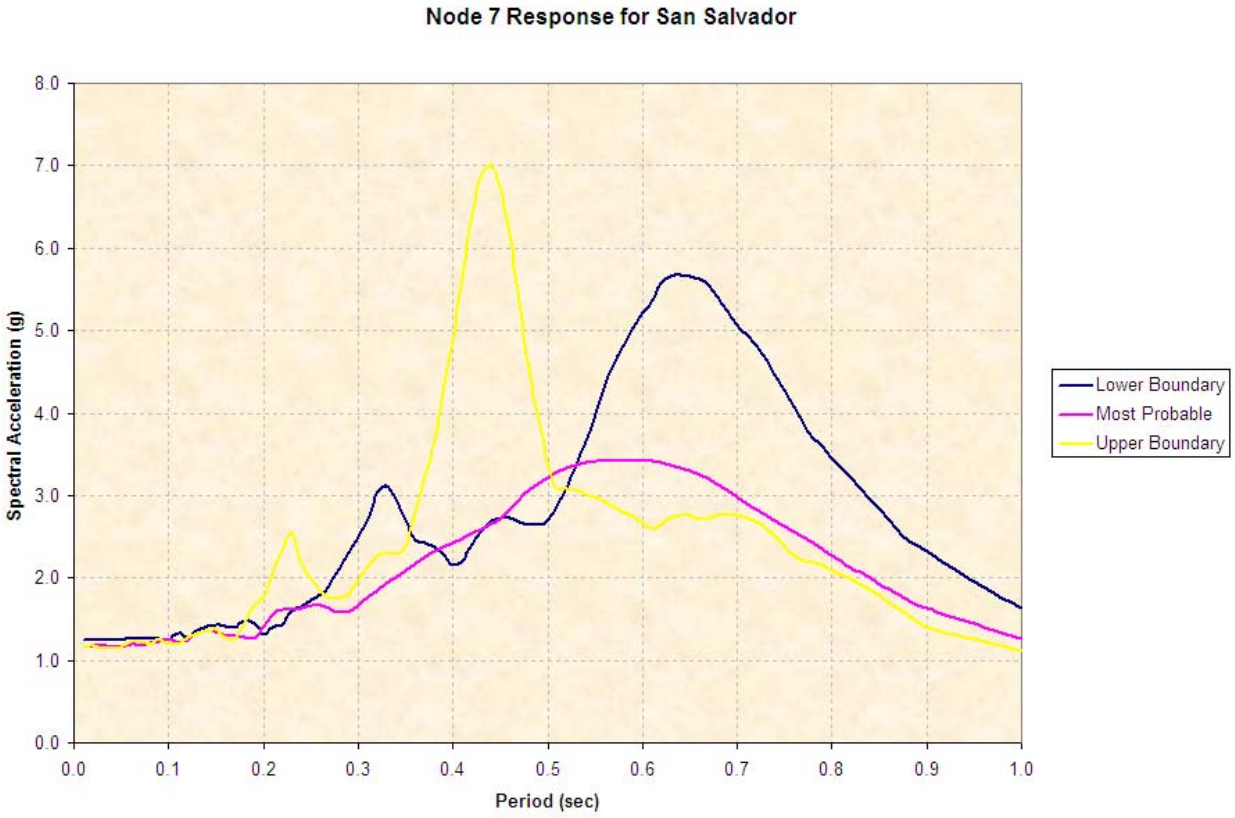

Figure C-24. Node 7 Response for San Salvador Ground Motion

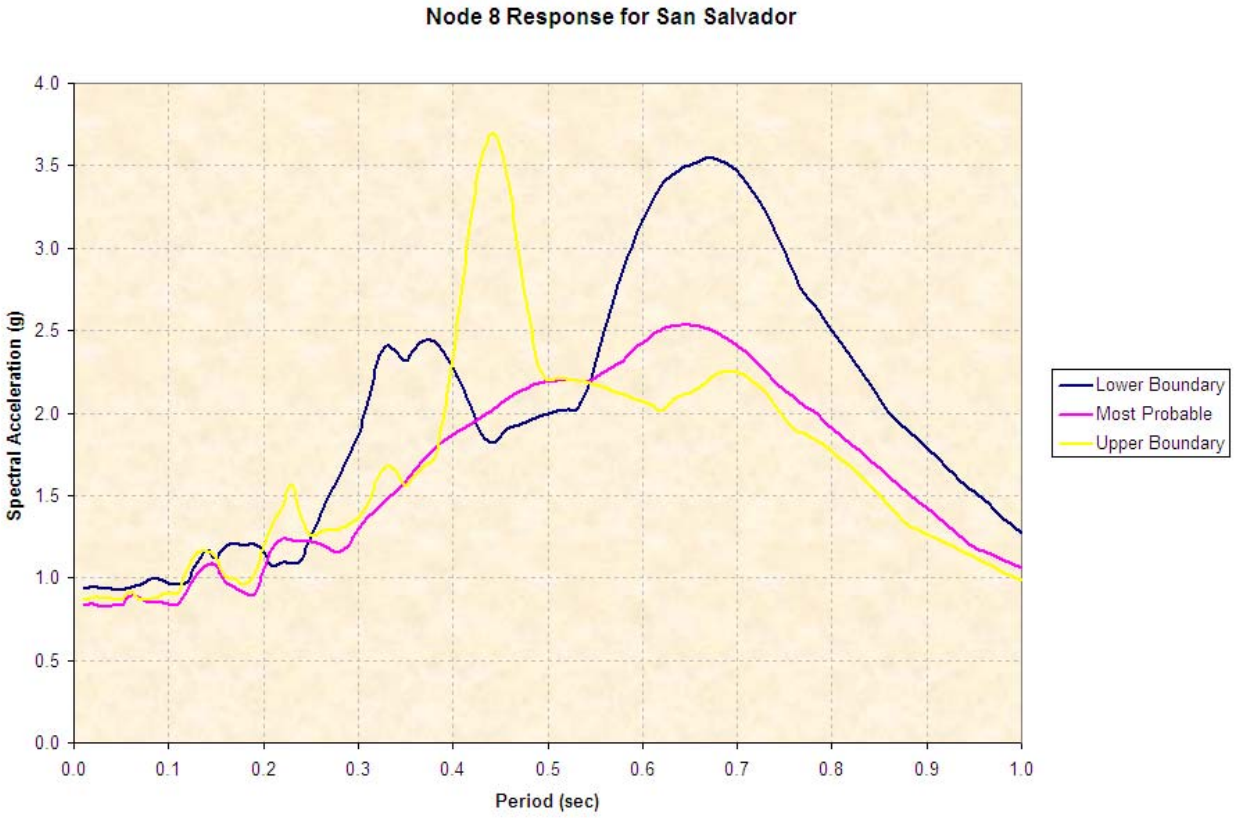

Figure C-25. Node 8 Response for San Salvador Ground Motion

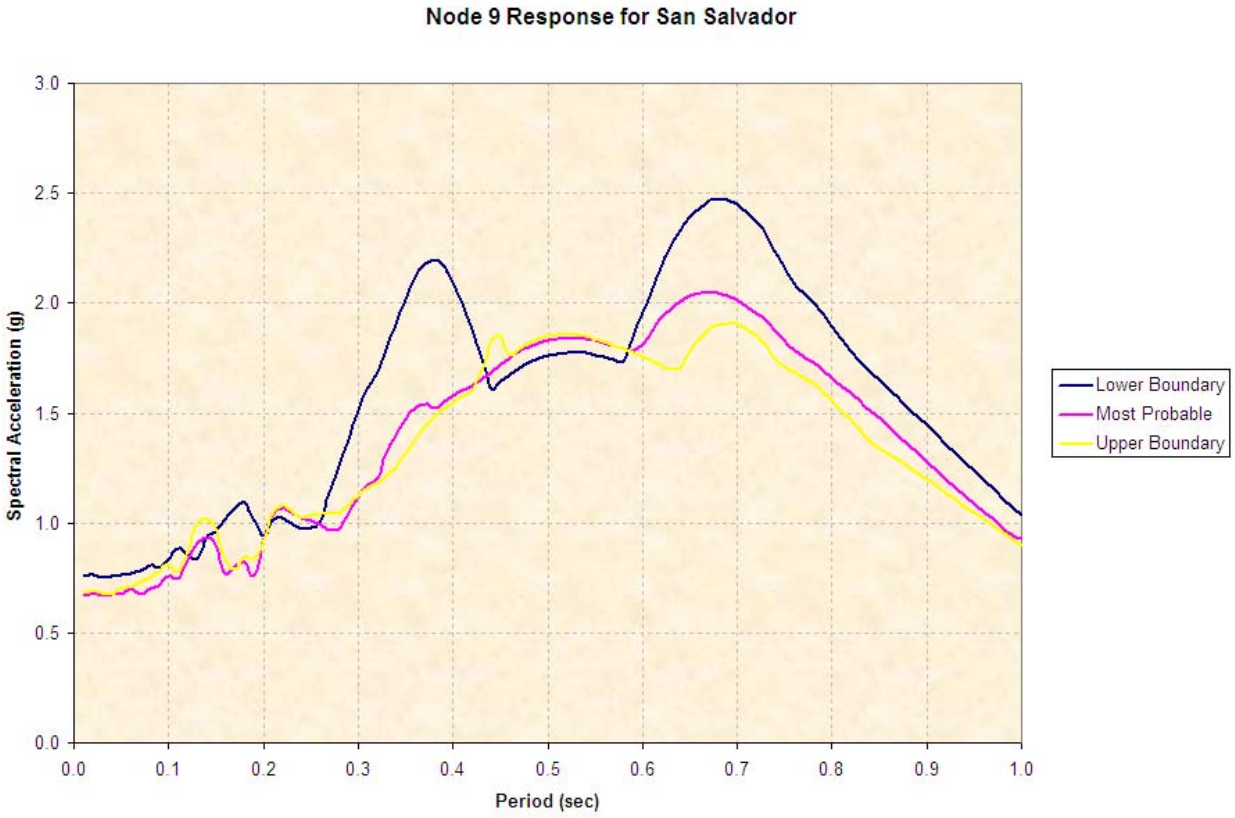

Figure C-26. Node 9 Response for San Salvador Ground Motion

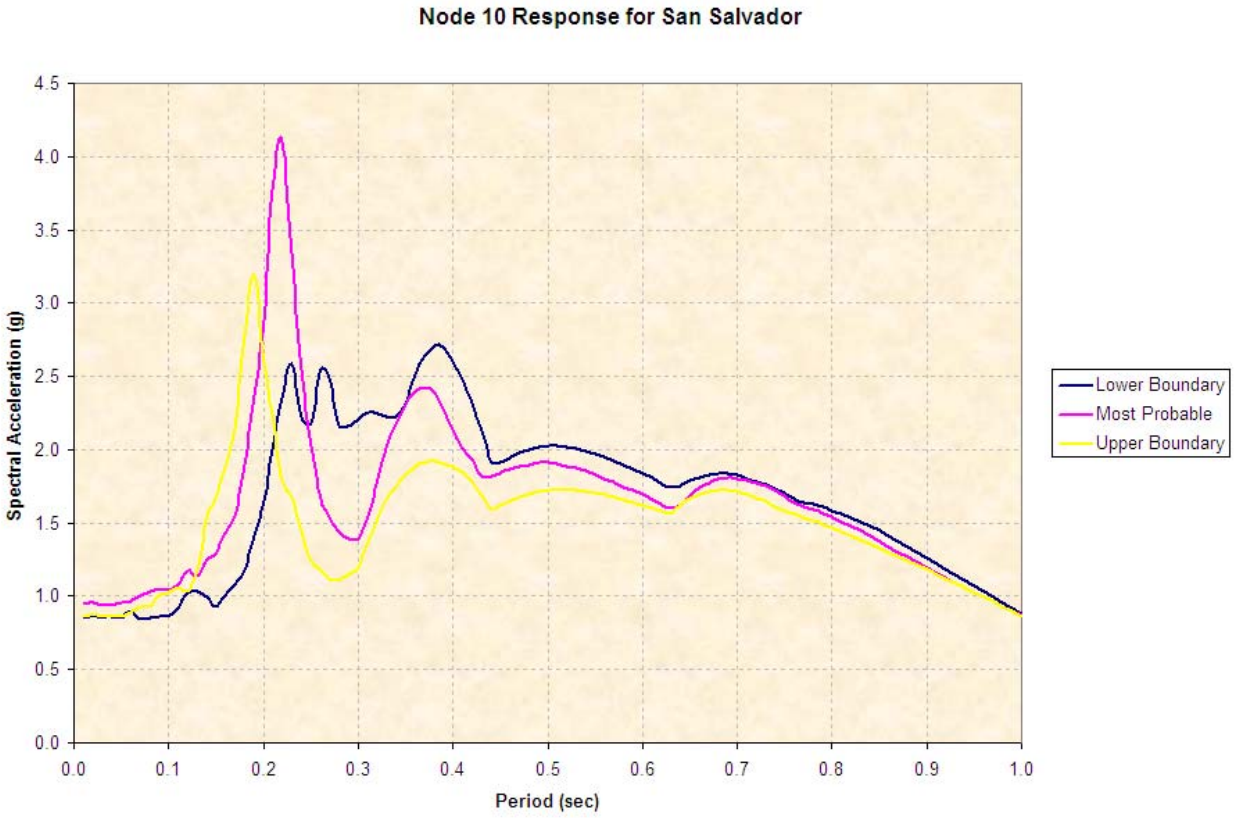

Figure C-27. Node 10 Response for San Salvador Ground Motion

C.3.3. UBC Ground Motion Responses

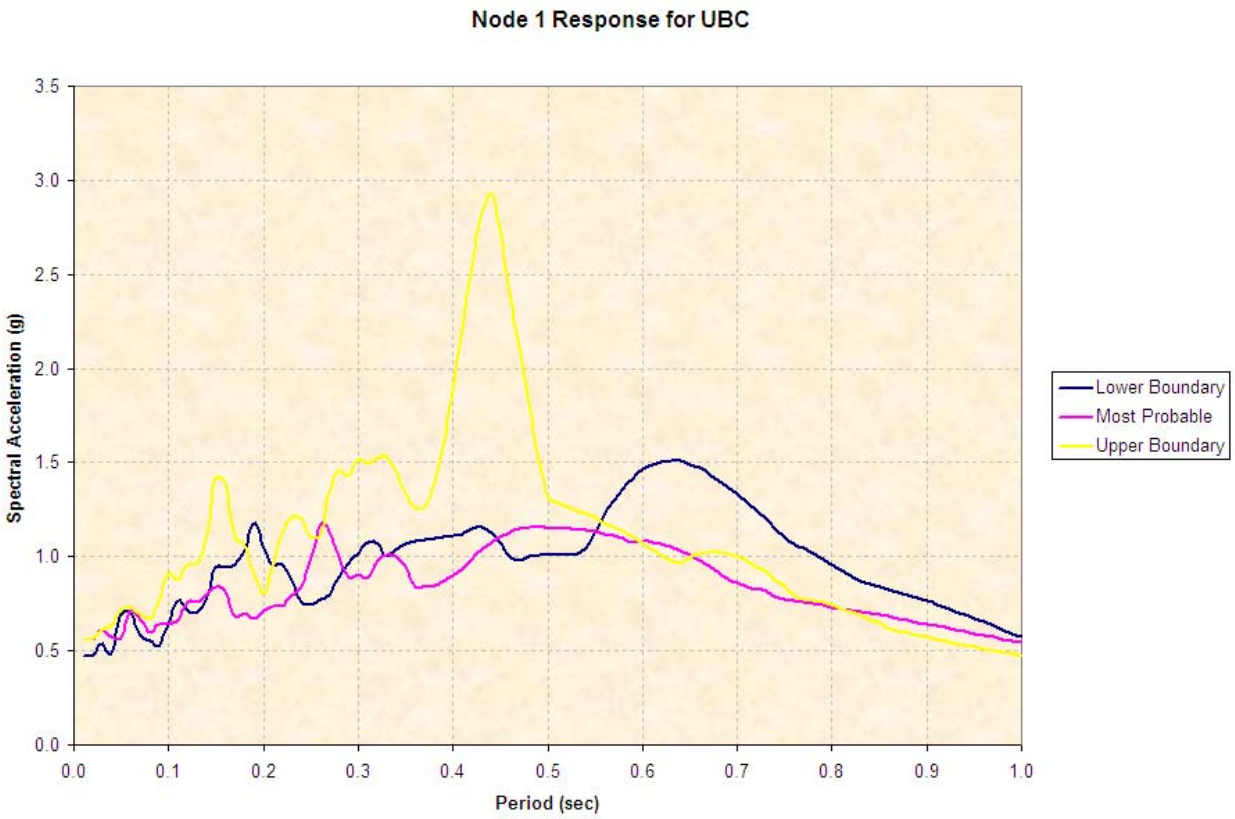

Figure C-28. Node 1 Response for UBC Compatible Ground Motion

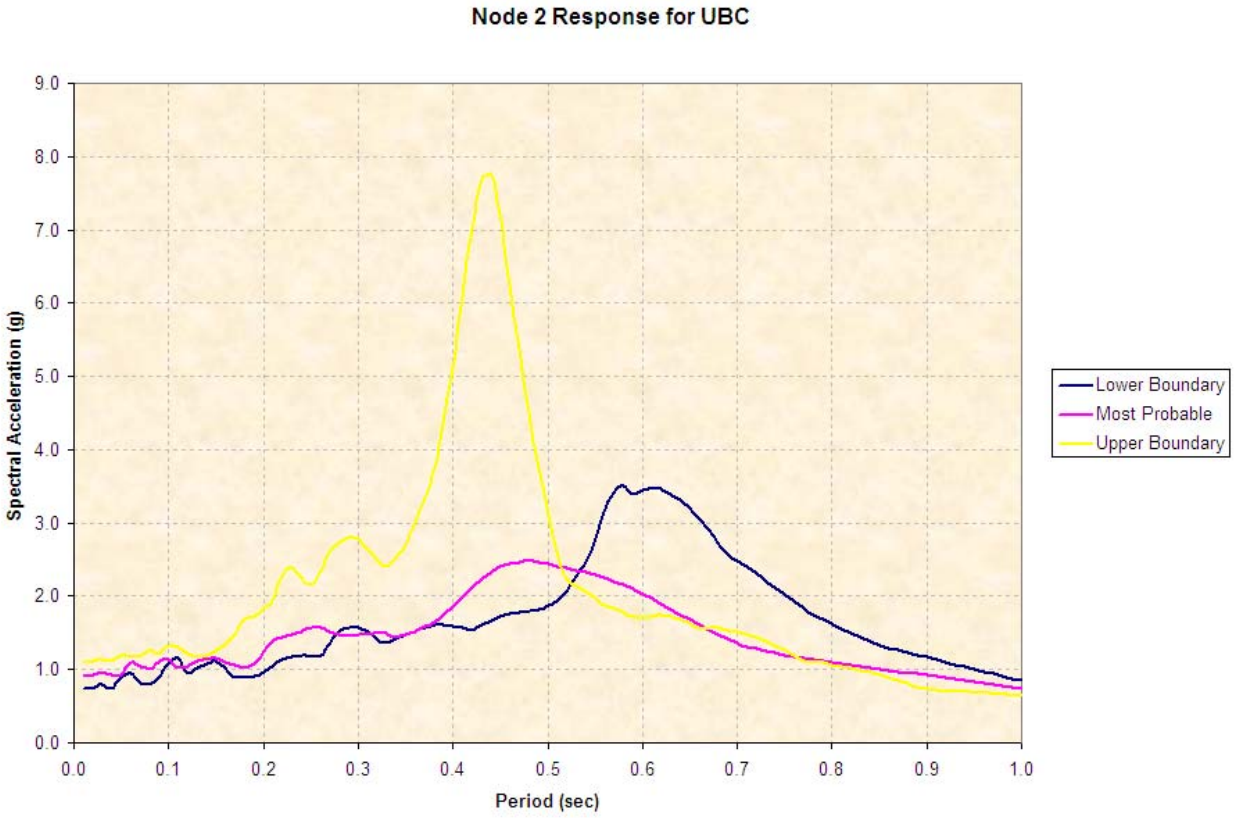

Figure C-29. Node 2 Response for UBC Compatible Ground Motion

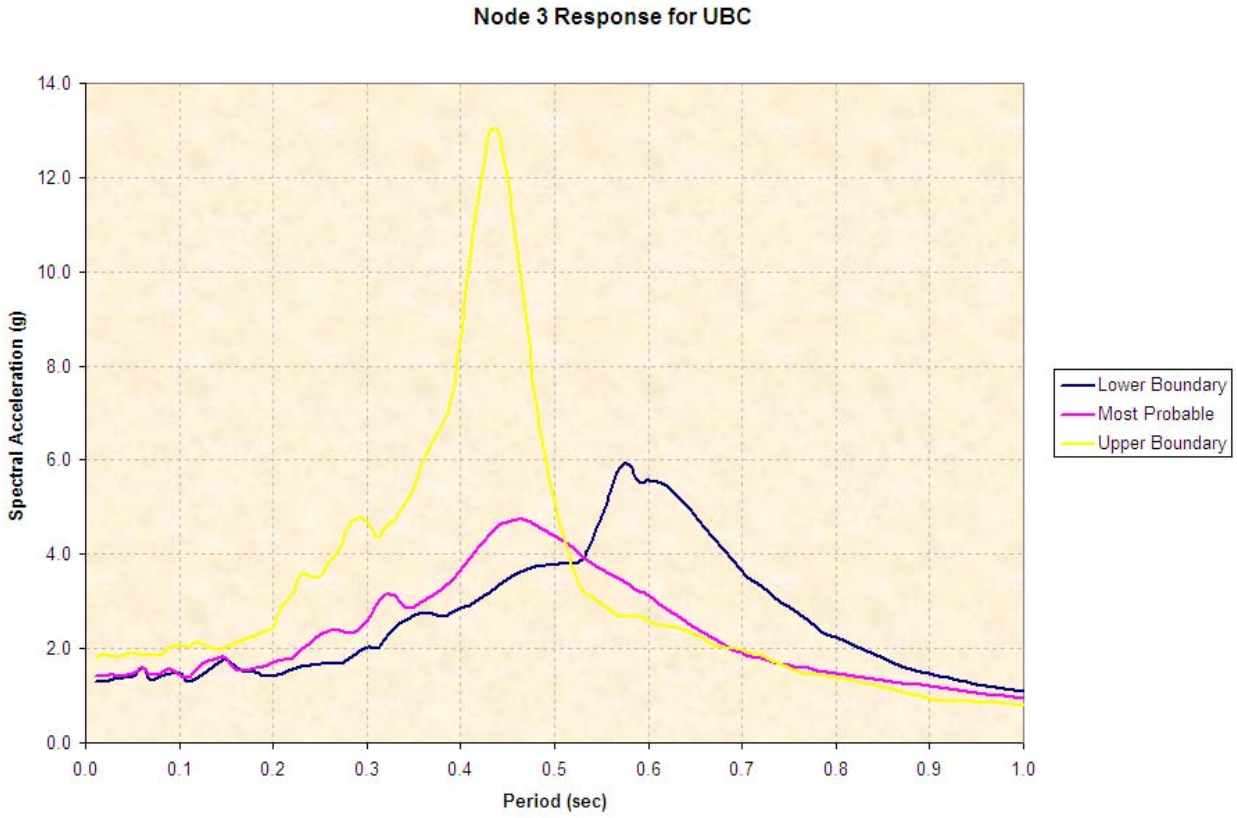

Figure C-30. Node 3 Response for UBC Compatible Ground Motion

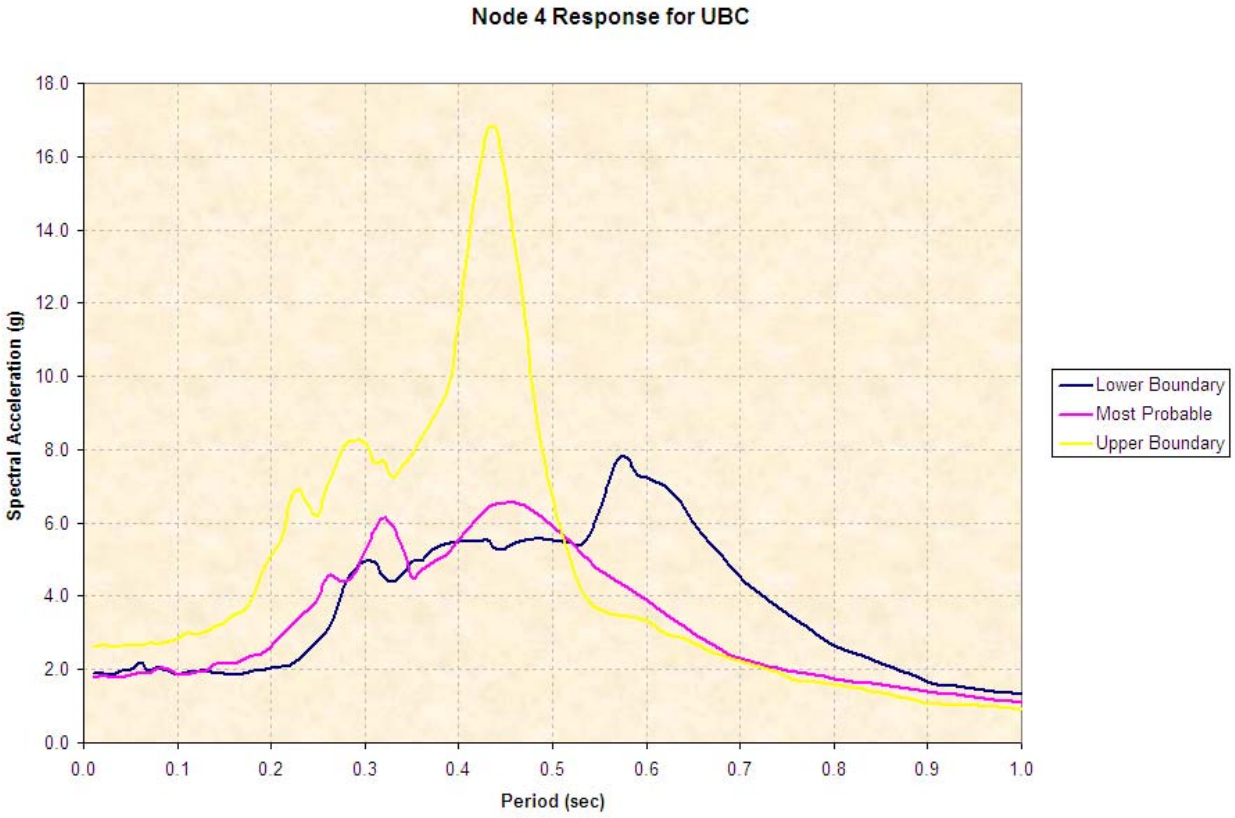

Figure C-31. Node 4 Response for UBC Compatible Ground Motion

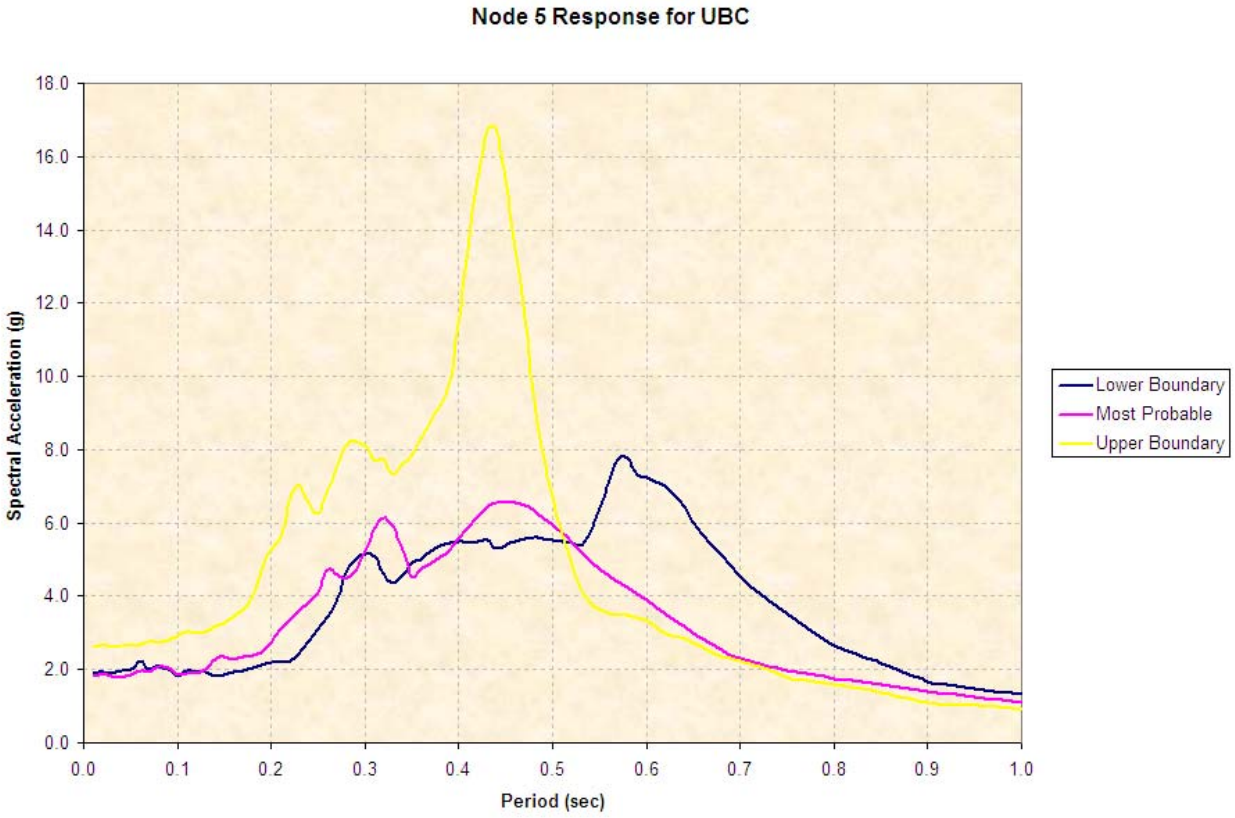

Figure C-32. Node 5 Response for UBC Compatible Ground Motion

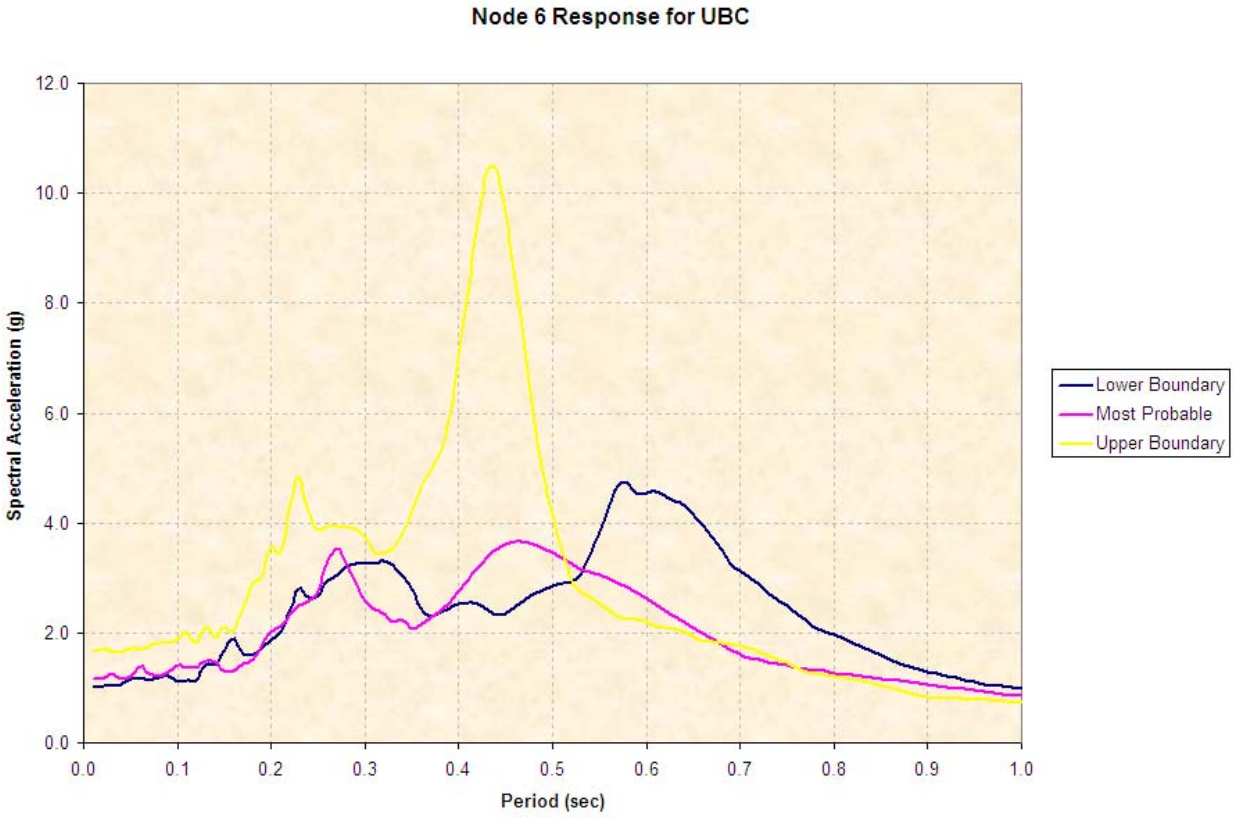

Figure C-33. Node 6 Response for UBC Compatible Ground Motion

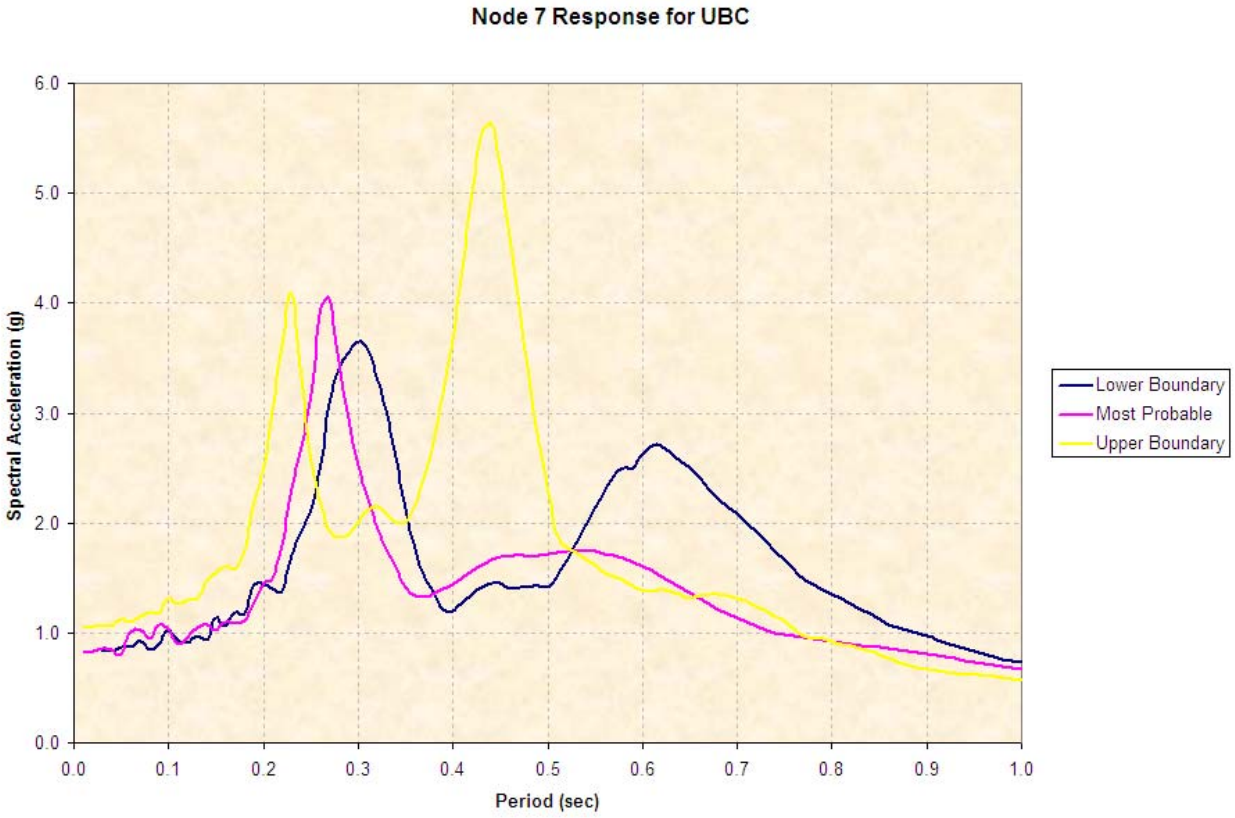

Figure C-34. Node 7 Response for UBC Compatible Ground Motion

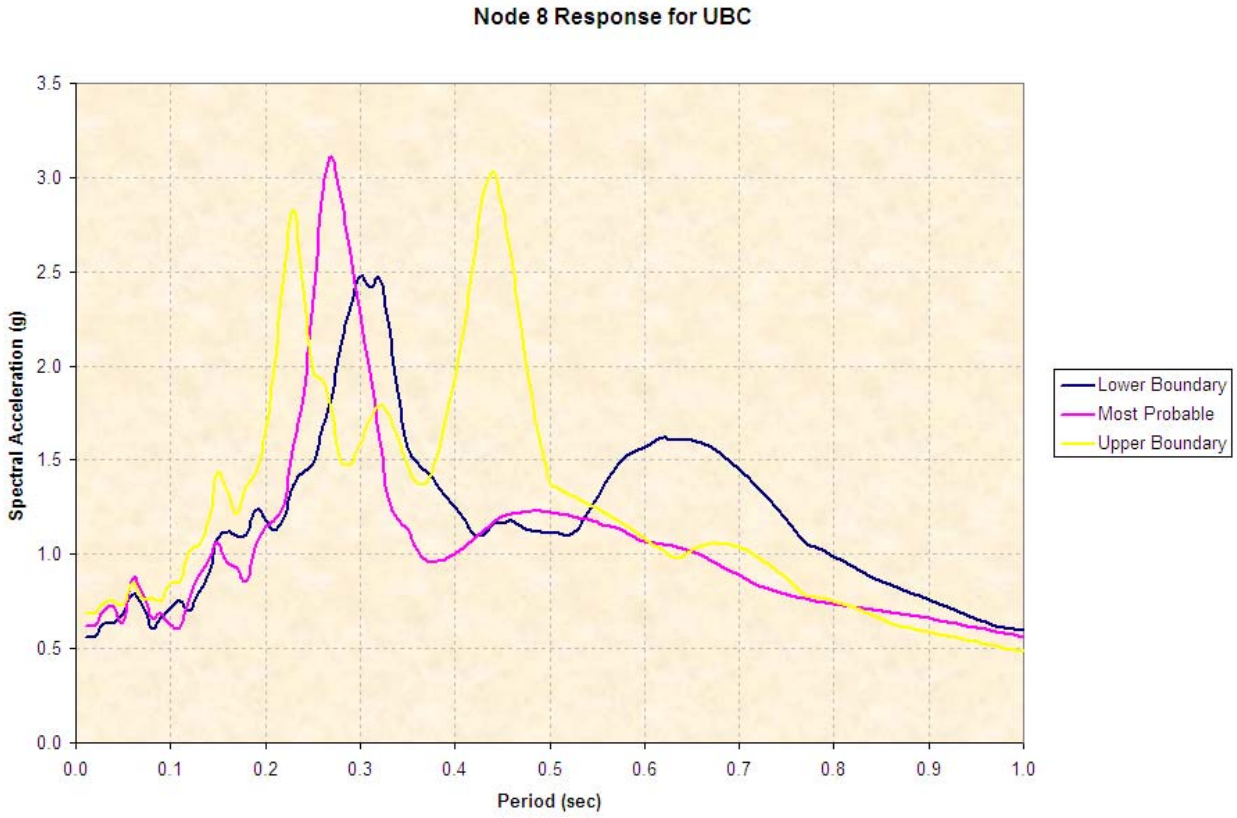

Figure C-35. Node 8 Response for UBC Compatible Ground Motion

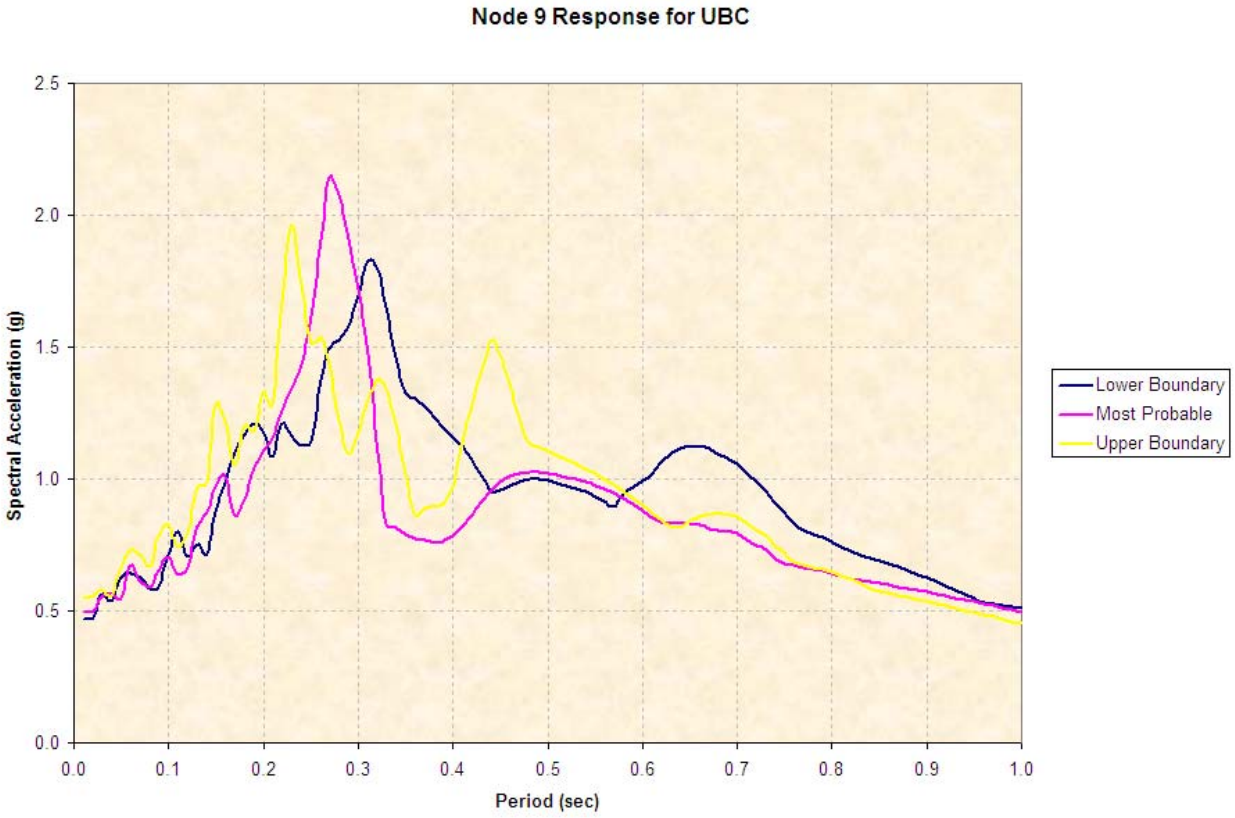

Figure C-36. Node 9 Response for UBC Compatible Ground Motion

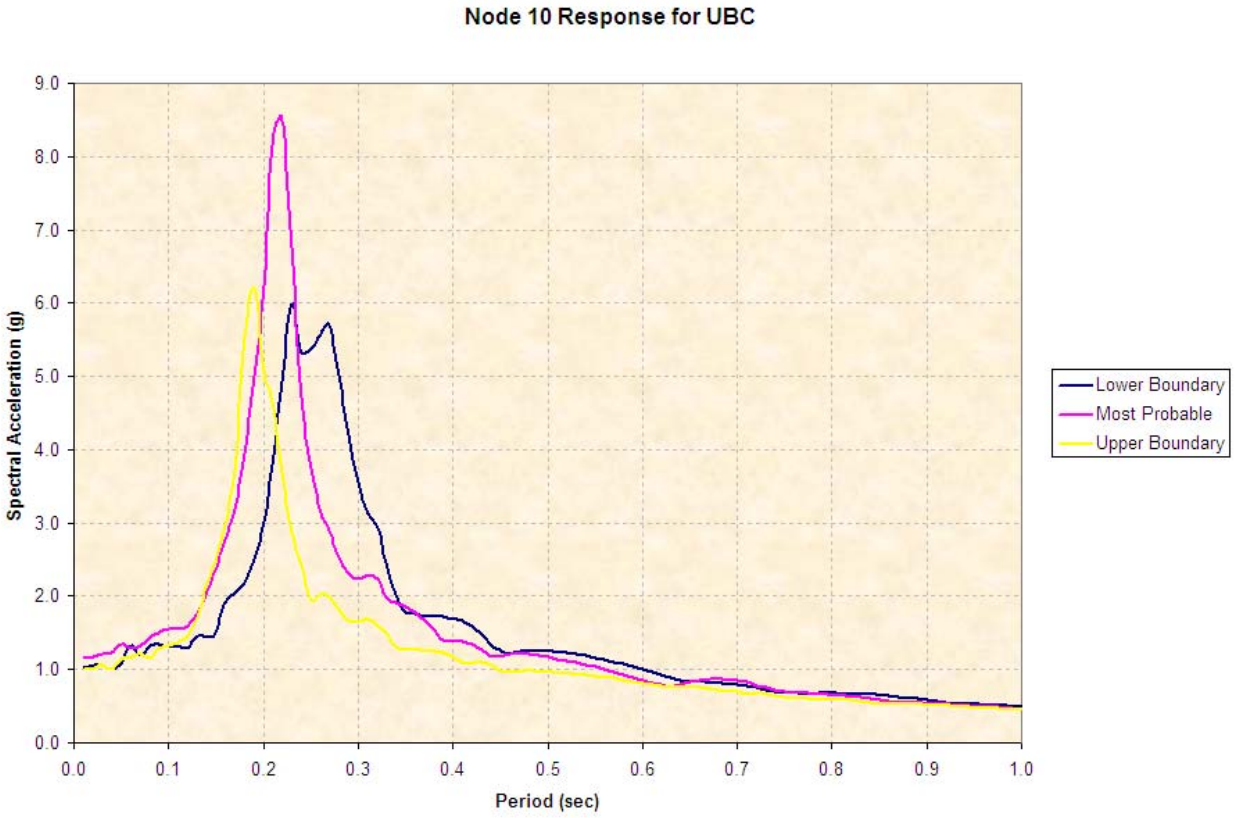

Figure C-37. Node 10 Response for UBC Compatible Ground Motion